NEW PERSPECTIVE ON THE ROLE OF CONCEPTUS ESTROGENS IN CONCEPTUS DEVELOPMENT, MATERNAL RECOGNITION, AND THE ESTABLISHMENT OF PREGNANCY IN PIGS.

A Thesis presented to

the Faculty of the Graduate School

at the University of Missouri – Columbia

In Partial Fulfillment

of the Requirements for the Degree

Master of Science

By

ASHLEY ELIZABETH MEYER

Dr. Rodney Geisert, Thesis Supervisor

JULY 2018

The undersigned, appointed by the Dean of the Graduate School, have examined the thesis entitled

NEW PERSPECTIVE ON THE ROLE OF CONCEPTUS ESTROGENS IN CONCEPTUS DEVELOPMENT, MATERNAL RECOGNITION, AND THE ESTABLISHMENT OF PREGNANCY IN PIGS

Presented by Ashley E. Meyer
A candidate for the degree MASTER OF SCIENCE
We hereby certify that in our opinion it is worthy of acceptance

---

_____
Dr. Rodney Geisert – Thesis Advisor

_____
Dr. Thomas Spencer

_____
Dr. Randall Prather

_____
Dr. Laura Schulz

ACKNOWLEDGEMENTS

The students and professors at the University of Missouri and the Department of Animal Sciences will forever hold a place in my heart. I would like to thank them for their continuous support and the friendships that will last a life time. I would like to thank my thesis advisor Dr. Rod Geisert for always having faith in me and pushing me to be my best self. Without his guidance and priceless lessons, I would not be the scientist I am today. He took an interest in me, not just as a student, but as a future colleague and friend. Dr. Geisert really is the best academic dad. I would like to thank Dr. Prather, Dr. Spencer, and everyone in their labs for teaching me everything I know about working in a lab, especially Kelsey Brooks. I would like to thank Dr. Smith for sparking my interest in reproductive biology. Taking his class and exposing me to repro is what set me on the path I am on today.

I would like to thank Eric Walters and my undergraduate advisor Chip Kemp, who lead me to graduate school after I had decided not to pursue vet school. I would like to thank my high school anatomy teacher Ms. Betty Hoeing for exposing me to how exciting science could be and igniting my passion for it. I owe a great deal of thanks to anyone who helped make this project possible and was always willing to offer a helping hand: Lee Spate, Josh Benne, Raissa Cecil, Stephanie Murphy, Dr. Murphy, Melissa Samuel, Caitlyn Duff, Sabrina Hammond, and Elizabeth Blackstock. I would like to thank my fellow graduate students and officemates Caroline Pfeiffer, Eleanore O'Neil, Paula Chen, Megan McLean, Lauren Ciernia, Jenna Monnig, Jessica Foster, and Fayth Kumro. Their

friendship and the memories made while at MU made my time here one of the best experiences of my life.

Finally, I would like to thank my friends and family. My mom and dad always supported my curiosity and helped me grow into a successful, independent woman. I will never be able to fully express the level of gratitude for everything they have done for me. I would like to thank my brother Ethan, for being my best friend and sharing a love for science. I need to thank my husband, Robbie, for loving me for who I am and always being so understanding of the time commitment graduate school requires. My love and appreciation for everyone who has been a part of my life will be eternal.

TABLE OF CONTENTS

LIST OF TABLES

LIST OF FIGURES

LIST OF ABBREVIATIONS

17β-HSD: 17-betahydroxysteroid dehydrogenase

3β-HSD: 3-betahydroxysteroid dehydrogenase

4-OHA: 4-hydroxyandrostenedione

BMP4: bone morphogenetic protein 4

CL: corpus luteum

CPM: counts per million

CRISPR: Cluster Regularly Interspaced Short Palindromic Repeats

CT: cycle threshold

CYP19A1: aromatase

DE: differentially expressed

ER: estrogen receptor

ERα: estrogen receptor-α

ERβ: estrogen receptor-β

FDR: false discovery rate

FGF4: fibroblast growth factor 4

GE: glandular epithelium

GFP: green fluorescent protein

gRNA: guide RNA

HDR: homology directed repair

IFND: interferon-δ

IFNG: interferon-γ

IL18: interleukin 18

IL1B: interleukin 1β

IL1B2: interleukin 1β2

IL1Rant: Interleukin 1 receptor antagonist

IL1RAP: Interleukin 1 receptor accessory protein

IL1RT1: Interleukin 1 receptor 1

IL1RT2: Interleukin 1 receptor 2

IVF: *in vitro* fertilization

LE: luminal epithelium

LH: luteinizing hormone

NFKB: nuclear factor-kappa B

NHEJ: non-homologous end joining

P_4: progesterone

P450scc: cholesterol side-chain cleavage enzyme

PAM: protospacer adjacent motif

PG: prostaglandins

PGE_2: Prostaglandin E

PGES: prostaglandin E synthase

PGF2α: prostaglandin $F_{2\alpha}$

PLA2: phospholipase A2

PR: progesterone receptor

PR: progesterone receptor

PRRS: Porcine Reproductive and Respiratory Syndrome

PTGS2: prostaglandin endoperoxide synthase 2

SAL1: salivary lipocalin

SCNT: somatic cell nuclear transfer

SPP1: secreted phosphoprotein 1 (osteopontin)

STAR: steroidogenic acute regulatory protein

TNFAIP6: tumor necrosis factor-inducible protein 6 precursor

ULF: uterine luminal flush

ABSTRACT

NEW PERSPECTIVE ON THE ROLE OF CONCEPTUS ESTROGENS IN CONCEPTUS DEVELOPMENT, MATERNAL RECOGNITION, AND THE ESTABLISHMENT OF PREGNANCY IN PIGS

Ashley Meyer

Rodney Geisert, Thesis Advisor

The proposed signal for maternal recognition of pregnancy in pigs is estrogen, produced by the elongating conceptus. To understand the role of estrogen in porcine conceptus elongation and pregnancy establishment, a loss-of-function study was conducted by biallelically editing pig aromatase (*CYP19A1*) gene by using CRISPR/Cas9 technology. *CYP19A1*$^{+/+}$ and *CYP19A1*$^{-/-}$ blastocysts were transferred into synchronized recipient gilts and the reproductive tract was collected on days 14 or 17 post-estrus. Elongated and attaching conceptuses were recovered from gilts receiving either *CYP19A1*$^{+/+}$ or *CYP19A1*$^{-/-}$ embryos on both day 14 and 17. Conceptus estrogen production was inhibited as estrogen concentrations in the uterine luminal flush (ULF) of gilts with *CYP19A1*$^{-/-}$ conceptuses was significantly lower ($P<0.01$) than those with *CYP19A1*$^{+/+}$ conceptuses on day 14 and day 17. Despite the loss of conceptus estrogen production, *CYP19A1*$^{-/-}$ conceptuses were capable of maintaining the corpora lutea (CL). However, gilts containing *CYP19A1*$^{-/-}$ embryos all aborted between days 27 and 31 of gestation. Attempts to rescue the pregnancy of *CYP19A1*$^{-/-}$ embryos with exogenous estrogen failed to maintain pregnancy. However, co-transfer of *in vitro* fertilized (IVF) *CYP19A1*$^{+/+}$ and *CYP19A1*$^{-/-}$

embryos successfully maintained pregnancy. Furthermore, conceptus estrogen production is not essential for pre-implantation development, conceptus elongation, and the early maintenance of CL. However, conceptus estrogen is essential for programming endometrial function for maintenance of pregnancy beyond 25 days.

CHAPTER ONE

1. INTRODUCTION

As of March 2018, the USDA National Agricultural Statistical Service reports the United States inventory of all hogs and pigs was estimated to be at 72.9 million head, of which 6.2 million are gilts and sows utilized for breeding. The breeding inventory has steadily increased since 2014, as consumer demand for pork has increased. The United States average pigs weaned per litter is 10.58, the highest number on record since the first inventory was conducted in 1866 (http://www.nass.usda.gov/). However, the average ovulation rate of female pigs is approximately 20-24 follicles in the modern commercial herds today (Da Silva et al., 2017), indicating a significant amount of early embryonic and fetal loss occurs between ovulation and parturition. In a previous breeding program, early genetic studies attempted to increase litter size through selection of gilts with higher ovulation rates, resulting in a slight improvement on litter size. These results indicated that embryonic survival and/or uterine capacity play a major role in the capability to increase litter size in the pig (Gama and Johnson, 1993).

Previous research has demonstrated how critical events during embryonic development and implantation play a role for subsequent fetal survival to term. Prenatal embryonic mortality ranges from 20-45%, which predominantly occurs during early embryonic development at days 10 to 30 of gestation. This is the time period that the developing conceptuses and the uterus communicate via a

complicated series of cohesive signaling pathways needed to stimulate maternal recognition (maintenance of the corpora lutea) and establishment of pregnancy. Failure or improper timing of conceptus/uterine signaling contributes to embryonic mortality. The period of greatest early embryonic mortality in the pig encompasses the time in which the conceptus undergoes a drastic morphological change to initiate placental attachment and establish the uterine surface area to provide nutrient flow to the fetus during pregnancy. Expansion across the uterine lumen is also essential to deliver the conceptus signal for maternal recognition of pregnancy and maintain progesterone production from the corpora lutea. Porcine conceptuses rapidly elongate from a tubular (10 mm) form into a long, thread-like filamentous form on approximately day 12 of pregnancy, reaching about 1 meter in length by day 16 of pregnancy (Perry and Rowlands, 1962). Conceptus elongation and placental expansion allow the conceptus to acquire an adequate amount of placenta-to-uterine surface area to survive to term.

Swine have an epitheliochorial type of placentation (Fig 1.1). The diffuse placenta (attachment is through loose adhesion between the epithelium microvilli of the trophoblast and uterine endometrial surface) provides a mechanism for fetal/endometrial communication through numerous signaling pathways, attachment factors, and nutrient transfer from the mother to the developing fetus (Geisert and Schmitt, 2001). Prior to and during attachment of the conceptus to the uterine surface, the pig conceptuses must relay a signal to establish

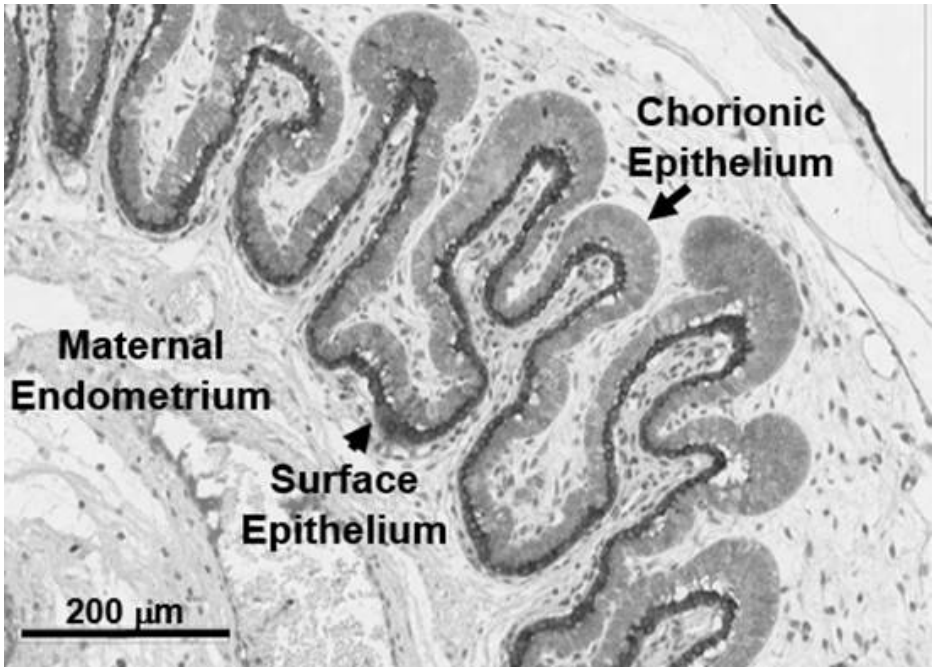

Figure 1.1 Epitheliochorial Placentation. The porcine placenta attaches through loose adhesion, allowing adequate placental to endometrial surface area.

pregnancy by preventing luteolysis (regression of the corpora lutea) which normally occurs after day 15 of the estrous cycle (Bazer et al., 1984). The presumed signal for maternal recognition in the pig is conceptus-derived estrogen, which is secreted on days 11 to 12 and 15 to 25 of pregnancy (Geisert et al., 1990). Conceptus estrogen synthesis is proposed to block luteolysis by moving transport of prostaglandin F2α (PGF2α) away from the uterine vasculature and sequestering it in the uterine lumen during early pregnancy. The altered transport of PGF2α away from, rather than towards the uterine vasculature, occurs during luteolysis in the estrous cycle has been termed the endocrine/exocrine hypothesis for maternal recognition in the pig (Bazer and Thatcher, 1977; Bazer et al., 1984). Estrogen is secreted into the uterine lumen from the elongating conceptus, along with a variety of factors including cytokines, interleukin-1β2 (IL1B2), interferons (IFN), and prostaglandins (PG) (Jaeger et al., 2001; Bazer and Johnson, 2014; Mathew et al., 2015). During this period, there is a significantly complex fetal-maternal interaction. Consequently, any failure of the conceptus to properly signal, mistiming of the conceptus development with uterine development and secretion, genetic factors, immunological rejection, or competition of embryos for sufficient uterine space can lead to either early embryonic or later fetal mortality. Therefore, despite the average number of pigs weaned per litter being the highest on record, litter size has only increased by 0.08 pigs in the past 18 years (USDA 2001; USDA 2018). However, there is potential to increase average litter size if we take advantage of the total uterine space available in the pig. Overall profitability increases as the number of pigs

born per sow increases (Tomes and Nielsen, 1982; Rothschild, 1996). Improving litter size could have a substantial impact on the efficiency of swine production; however, larger litter sizes can result in smaller piglets born. Therefore, improving intrauterine fetal development and survival is an important focus to increase overall efficiency in the swine industry. Fully understanding the role of conceptus estrogen during maternal recognition of pregnancy, placental attachment, and early embryonic development is critical to develop selection programs and/or therapies to improve piglet survival. The following review will provide insight into regulation of sow reproduction, conceptus development, and estrogen in the establishment of pregnancy in the pig.

CHAPTER TWO

2. LITERATURE REVIEW

2.1 The Pig Estrous Cycle

The normal length of the pig estrous cycle is 18-22 days, consisting of a luteal (d3 to d16) and a follicular (d17 to d2) phase (Flowers et al., 2001). The estrous cycle can be further divided into proestrus, estrus, metestrus, and diestrus. Proestrus is defined as the time in which a significant increase in plasma estradiol-17β occurs as the result of active steroidogenesis by the developing follicles. The increase in estrogen secretion begins approximately 48 hours before a surge release of luteinizing hormone (LH). In the pig, the first expression of behavioral estrus (standing heat) is considered day 0 of the estrous cycle. Behavioral estrus in gilts and sows can last for 24-72 hours, with ovulation occurring about 36-48 hours after the start of estrus. About 20-24 follicles ovulate and release an oocyte during estrus (Da Silva et al., 2017). Following ovulation, granulosa and theca cells undergo luteinization to form the corpora lutea (CL) during metestrus. The CL are well formed and fully functional by day 4 or 5 of the estrous cycle (Henricks et al., 1972). Diestrus, which lasts 10 to 14 days, is the period of the estrous cycle in which CL progesterone production plateaus and remains elevated until the CL begins regression (Senger, 2003). Secretion of the endometrial prostaglandin F2α (PGF2α) is responsible for luteolysis of the CL beginning on day 15 in cyclic female pigs. The concentration of progesterone rapidly declines to basal levels by days 17 or

18, resulting in the end of diestrus (Patten and Carlson, 1974). Regression of the CL and decline of progesterone allow recruitment of the next set of mature follicles to drive the female back into estrus (Bazer et al., 1982).

Physiological events during the estrous cycle and early pregnancy are dependent on progesterone and estrogen acting on their corresponding nuclear receptors. Progesterone receptor (PR) is found in the uterine luminal epithelium (LE), glandular epithelium (GE), and the stroma until day 10 of the estrous cycle. Uterine stroma and myometrium maintain PR throughout the duration of the estrous cycle and pregnancy. However, PR (especially PR-A) in the endometrial LE and GE rapidly declines from days 12-18 of the estrous cycle and early pregnancy (Geisert et al., 1994). The production of progesterone by the CL induces down-regulation of epithelial PR after about 10 days of increased plasma progesterone exposure. The loss of endometrial epithelial PR occurs before the first pulse of PGF2α release, suggesting PR initially has an inhibitory effect on the synthesis and/or release of endometrial PGF2α (Bazer et al., 1984). While epithelial PR is being down-regulated during the luteal phase, concentration of estrogen receptor (ER) in the uterine epithelium increases on day 12. Estrogen has two receptors, ERα and ERβ, both present at this time but ERα is predominantly present (Knapczyk-Stwora et al., 2011). The increase of ER in the endometrial surface and glandular epithelium allows the uterus to be responsive to conceptus estrogen signaling during the critical period of maternal recognition of pregnancy, thus preventing luteolysis (Geisert et al., 1994).

2.2 Early Pregnancy in the Pig

After ovulation, fertilization occurs in the ampulla-isthmic junction of the oviduct. The zygote undergoes its first cleavage within 24 hours of fertilization. After development to the morula stage, the embryo will move from the oviduct into the uterine horns, where the embryos develop to blastocysts by day 5 post-estrus. The blastocyst is initially comprised of two cell types: the inner cell mass and the surrounding trophectoderm, which give rise to embryonic tissues and placental tissues, respectively. Blastocyst hatching from the zona pellucida occurs on days 6 and 7 of pregnancy. After hatching, the conceptus will grow in size reaching 2-6 mm in diameter by day 10 of pregnancy (Perry and Rowlands, 1962).

Pigs have a diffuse, epitheliochorial type of placenta; therefore, the embryos must acquire adequate placental-to-uterine surface area for embryo survival throughout pregnancy. Between days 7 to 11 of pregnancy, the preimplantation conceptus uses peristaltic movements of the uterine wall and long slender microvilli on its outer surface to migrate throughout the uterine horns until evenly spaced. Porcine conceptuses increase estrogen production during the period of embryo migration and increased myometrial activity. Pope and others (1982) performed an experiment to investigate estrogen contribution to migration by using silastic beads infused with cholesterol or estradiol-17β to simulate embryos in the uterus. They observed that the beads with estradiol-17β migrated further along the uterine horn, indicating estrogen aids in embryo migration and spacing. Despite the migration seen with the estradiol-17β beads, it was noted that the presence of the embryos or estrogen did not directly

stimulate myometrial contractions, which help with embryo migration throughout the horn. Histamine release increases uterine blood flow and myometrial contractions (Ford et al., 1982) contributing to the movement and even spacing of porcine embryos (Pope et al., 1982). In some species (guinea pigs and humans), the embryos would now begin interstitial implantation and embed into the uterine wall through penetrating the luminal epithelium. However, in pigs, implantation is superficial, and the blastocysts expand and fill the uterine lumen before the trophoblast attaches or adheres to the luminal epithelium (Perry, 1981).

2.3 Conceptus Elongation

Heuser and Streeter (1929) were some of the first anatomists to truly explore the developmental stages of porcine embryos throughout early pregnancy by collecting the reproductive tracts from an abattoir. After the blastocyst stage, Heuser and Streeter observed that the porcine conceptus goes through a morphological change from spherical, to tubular, and finally a filamentous morphology (Fig. 2.1 A, B). After day 10 of pregnancy, the 2-6 mm spherical conceptus will grow in diameter by increased cellular proliferation until it reaches an approximate spherical diameter of 9-10 mm. At this point, the conceptus rapidly transforms to a tubular and then filamentous shape, elongating at a rate greater than 30-40 mm/h until it is greater than 100 mm (Geisert et al., 1982b). The rapid elongation from tubular to filamentous morphology takes just about 1 hr (Geisert et al., 2015). The porcine conceptus will continue

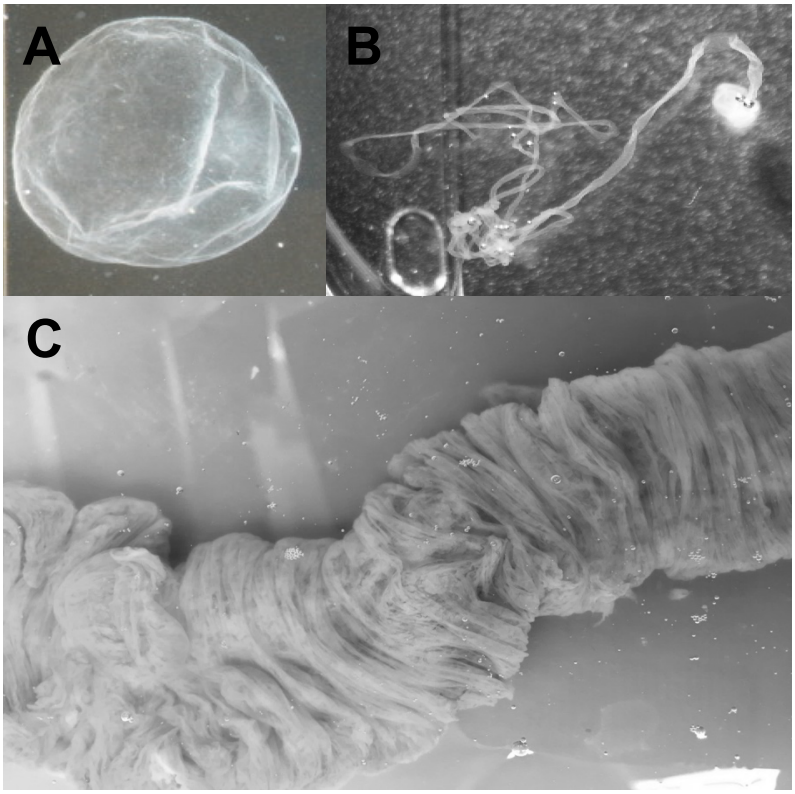

Figure 2.1 Conceptus Elongation

A) Spherical pig conceptus. **B)** The porcine conceptus rapidly elongates into a thread-like, filamentous morphology on day 12 of pregnancy. **C)** Pig conceptuses interlace themselves into the folds of the endometrium to expand their placenta across the uterine luminal surface without overlapping.

to grow and expand until day 16, where it can reach a meter in length (Perry and Rowlands, 1962). The conceptuses elongate along the mesometrial side of the uterine horn, where placental attachment occurs shortly following elongation. Despite the competition among the conceptuses to elongate and expand their placenta across the uterine luminal surface, the conceptuses rarely overlap because of their ability to take up only 20-30 cm of the uterine horn by interlacing themselves into the endometrial folds (Fig. 2.1 C) (Perry, 1981). Since the conceptuses do not overlap, they must compete for adequate uterine space for survival. Therefore, some early embryonic loss can be contributed to competition for uterine space during rapid elongation, especially in females with high ovulation rates (Pope, 1994). The rapid nature of the remodeling process of conceptuses suggests that elongation occurs through cell migration and deformation, rather than by cell division (Geisert et al., 1982b). Rapid remodeling of the endoderm and trophectoderm occurs during the period of differentiation of the epiblast mesoderm (Geisert et al., 1982b). Migration of the underlying endoderm and alterations to the junctional complexes of the trophectoderm to increase fluidity for rapid remodeling may be activated though cellular pathways initiated by bone morphogenetic protein 4 (BMP4) and fibroblast growth factor 4 (FGF4) (Valdez Magana et al., 2014). Conceptus expression of interleukin 1β (*IL1B*) is greatly enhanced at the time of rapid elongation and could be a factor in stimulating the rapid morphological change (Tuo and Bazer, 1996; Ross et al., 2009).

2.4 Placentation

After completing elongation, the conceptus begins to develop placental membranes (extraembryonic membranes) which are responsible for securing nutrients from the maternal blood and acting as a form of protection from maternal immunological recognition as a foreign tissue. The pig extraembryonic membranes consist of the yolk sac, amnion, chorion and allantois (Patten and Carlson, 1974). The first functional placental membrane to develop from the conceptus is the yolk sac (Vallet et al., 2009). The conceptus first consists of the embryo and the trophectoderm. The primitive endoderm layer forms beneath the embryo, growing downwards and forming the inner surface of the trophoblast. The primitive endoderm continues to grow until it forms a cavity called the yolk sac (Senger, 2003). The yolk sac serves as a temporary absorptive tissue that can act as a reservoir for nutritive material because the yolk sac's abundant blood vessels are only separated from the uterine endometrial surface by a thin layer. The close proximity of the maternal and the fetal blood supply makes absorption readily possible (Patten and Carlson, 1974). The extraembryonic mesoderm layer (originating between the endoderm and the developing embryo) begins to grow and surround the yolk sac, while pushing against the trophectoderm to form "wings" called amniotic folds. The combined layers of the mesoderm and the trophectoderm become the chorion, while the amniotic folds grow until they envelop the embryo forming the amnion (Senger, 2003). The amnion sac will with a water-like fluid in which the embryo is suspended. This provides an environment for the embryo, in which pressure is equalized and the

embryo is protected from injury. The allantois develops while the chorion and amnion form. The allantois forms from the primitive gut of the embryo, it takes over the function of the yolk sac (Patten and Carlson, 1974). The yolk sac rapidly decreases in size as the allantois grows outward into the chorion between days 14-20 of pregnancy (Vallet et al., 2009). The portions of the allantois and chorion that fuse becomes vascularized and are the functional fetal placenta. The portion not vascularized because the chorion and allantois do not meet, is called necrotic tips (Friess et al., 1980). Similar to the development of fetal cotyledons that interlock with the maternal caruncle in the ewe and cow, the pig placenta has many chorionic villi on the surface of the placenta that penetrate into the endometrium to form the fetal-maternal interface (Senger, 2003). Beginning around day 15 of pregnancy, the placenta forms ‘areolae’ at the opening of the uterine glands during attachment that are responsible for the uptake of products from uterine gland secretions (Vallet et al., 2009). The chorioallantois expands and presses against the uterine wall as it fills with allantoic fluid. The allantoic fluid accumulation peaks around day 30 of pregnancy. This development of the membranes and accumulation of fluid likely aids in the process of implantation (Vallet et al., 2009). The volume of allantoic fluid declines to day 45 (Knight et al., 1977), peaks again at day 60 of pregnancy, then recedes to a minimal volume until the end of gestation (Vallet et al., 2009). Development and the formation of the placenta is dependent on the elongation of the conceptus and attachment to the surface of the uterine epithelium. One of the factors important for the success

of elongation has recently been discovered and its role in elongation is discussed in the section below.

2.5 Conceptus Expression and Secretion of IL1B2 During Elongation

The analysis of the transcriptome during rapid trophoblast elongation identified *IL1B* as one of the most abundantly expressed transcripts during conceptus transition from tubular to filamentous morphology (Tuo and Bazer, 1996; Ross et al., 2009) IL1B is a pro-inflammatory cytokine, which is an important mediator of the inflammatory response, and is involved in a variety of cellular activities, including cell proliferation, differentiation, and apoptosis (Dinarello, 2009). The expression of *IL1B* rapidly increases on day 12 of pregnancy as the conceptuses initiate rapid elongation and is immediately followed by the loss of transcription upon completion of the remodeling process (Ross et al., 2003). Although conceptus IL1B secretion rapidly increases at the time of elongation on day 12, the presence of IL1B declines in the uterine lumen by day 18 (Ross et al., 2003). As a result of gene duplication, the pig conceptus is unique in that it expresses a novel *IL1B* isoform, *IL1B2*, which has not been reported in other mammals or in other tissues of the pig. *IL1B2* is only highly expressed from the porcine conceptus during the morphological transition from spherical to tubular to filamentous form (Mathew et al., 2015). Therefore, IL1B2 has been proposed to initiate cell signaling pathways for the cellular remodeling that occurs during rapid conceptus elongation in the pig. IL1B stimulates phospholipase A2 (PLA2) (Kol et al., 2002). PLA2 releases arachidonic acid from the phospholipid bilayer of the cell membrane, which increases membrane fluidity

needed for remodeling, further supporting the hypothesis that IL1B2 is the possible initiator of elongation. Using genomic editing technologies, (Whyte et al., 2018) knocked out *IL1B2* in pig conceptuses to determine the role it plays in conceptus elongation. *IL1B2* null embryos fail to elongate and developed an abnormal oblong morphology, despite being transcriptionally active and viable. Thus, conceptus *IL1B2* expression is necessary for the successful elongation of porcine conceptus due to its role in stimulating multiple signaling pathways.

2.5.1 Endometrial Stimulation by IL1B2

Along with IL1B2 role in conceptus elongation, IL1 signaling activates a variety of genes in the endometrium during the establishment of pregnancy. The IL-1 system consists of two receptors, IL1RT1 (functional) and IL1RT2 (pseudo-receptor), an IL1 receptor accessory protein (IL1RAP), and an IL1 receptor antagonist (IL1Rant) (Mantovani et al., 1998). At various time points during the estrous cycle and pregnancy, the porcine endometrium expresses *IL1RT1*, *IL1RAP*, and *IL1Rant* (Ross et al., 2003). During elongation and the onset of implantation, high concentrations of conceptus IL1B2 stimulate *IL1RT1*, and *IL1RAP*, while *IL1Rant* is low. This indicates that the endometrial expression of *IL1R1* and *IL1RAP* is regulated by conceptus factors. During elongation, IL1B2 induces an increase of salivary lipocalin (*SAL1*) expression in in the glandular epithelium and SAL1 protein to be secreted from the uterine glands (Seo et al., 2011). SAL1 is present in the uterine lumen on day 12 of the estrous cycle but the concentrations are much greater during day 12 of pregnancy when the conceptuses elongate and secrete IL1B2. SAL1 is a transporter of hydrophobic

compounds and may play an important role in binding to lipids and prostaglandins (PG) during implantation and the establishment of pregnancy but is not fully understood (Seo et al., 2008). As a member of the cytokine family, IL1B2 signaling results in many pro-inflammatory effects (Dinarello, 2009). Mathew and colleagues (2015) demonstrated that treating endometrial tissue with IL1B activates the nuclear factor-kappa B (NFKB) signaling pathway in epithelial cells. IL1B2 stimulation of NFKB activation is localized to the uterine LE directly in contact with the attaching conceptus (Mathew et al., 2015). Activation of NFKB results in immune responses by the stimulation of transcription pathways for inflammation, cytokine release, cell adhesion, anti-apoptotic factors and immune receptors, all of which must be tightly regulated (Hayden and Ghosh, 2012). If these inflammatory pathways are not kept in check, it could possibly result in immunological rejection of the conceptus. Quaedackers et al. (2007) and King et al. (2010), indicated that estrogen can act as either an antagonist or agonist of NFKB activity. During conceptus elongation in the pig, IL1B2 secretion from the conceptus is mirrored by secretion and release of estrogen which may be acting as a mediator of the NFKB pathway to regulate the localized pro-inflammatory response (Geisert et al., 2015). There is a biphasic increase in uterine luminal estrogen content during the establishment of pregnancy in the pig (Geisert et al., 2017). Estrogen plays a major role in the establishment and maintenance of pregnancy in the pig. Therefore, to provide background, the history for the discovery of estrogens and their role in the reproduction of pigs is reviewed in the following sections.

2.6 Estrogen

It has been well established that specific hormones have significant roles during pregnancy across all mammalian species. Early in pregnancy, though exact timing varies from species to species, a systemic increase of progesterone and estrogen occurs from the presence of CL and conceptuses (embryo and placental membranes). Progesterone, secreted from the CL, is needed to stimulate the endometrium transformation into an environment accommodating to early embryo development and attachment. Estrogen is a hormone that some could argue is the most important hormone secreted during the gestational period of the pig as well as other mammals. To fully appreciate the significance of estrogen and the necessity of its production, one must understand estrogen biosynthesis and its biological roles during pregnancy in pigs.

2.6.1 Discovery of Estrogen

The long and established history of estrogen began with two investigators, Edward Doisy and Edgar Allen (Simpson and Santen, 2015). Allen was a biologist who utilized a mouse model to study the components of the estrous cycle and how the uterus changed with each specific phase of the cycle (Watkins, 2007). It was observed that ovarian follicles changed in size and appearance as the uterine appearance was altered during the estrous cycle. It was hypothesized that the ovary secreted a hormone, which at the time had not been determined. For his efforts to identify the hormone being secreted by the ovary, Allen needed a large quantity of samples. Ovaries were acquired from sows at a meat packaging plant and Allen recruited his wife to help collect the

fluid from the follicles in their own kitchen (Doisy, 1976). Allen then injected the follicular fluid into pre-pubertal mice and rats, which stimulated changes in the uteri, mimicking changes seen during the estrous cycle. The follicular fluid needed to be purified in order to isolate the possible ovarian hormone responsible for the changes observed in the mice/rat uterus (Doisy, 1976). Edgar Allen met Edward Doisy at Washington University School of Medicine where they both worked. Doisy was a biochemist who had trained at Harvard (Watkins, 2007) and worked on purifying insulin. Allen approached Doisy with the proposed task of purifying the mystery hormone. Because follicular fluid from sow ovaries was hard to acquire and isolate, the two investigators had to find a new source of the ovarian hormone. It was at this time Allen and Doisy became aware of research being done by German scientists Selmar Aschheim and Bernhard Zondek, who in 1927 found urine from pregnant women contained estrogenic material and would later become known for developing the “Aschheim-Zondek pregnancy test” which was accomplished by taking urine from a woman and injecting it into immature female mice to observe ovarian maturation, as a result of the presence of human chorionic gonadotropin (Schneck, 1997; Simpson and Santen, 2015). After finding a more abundant source of the ovarian hormone using the urine from pregnant women, Doisy spent the next 5 years working on a purification method. In 1929, the Doisy lab isolated pure estrone crystals. Years later, Doisy and his colleges isolated a compound they termed dihydrotheelin, which is now known as estradiol (Huffman et al., 1940). Around the same time Doisy purified estrone, Adolf Butenandt had also purified estrone and later

received the Nobel Prize with Leopold Ruzincka for the purification of estrogens and testosterone (Butenandt, 1929). After estrogens were isolated and identified, the next question became whether the structure of estrogens had three or four rings. The similarity of the structure of testosterone and estradiol led to the hypothesis of the conversion of androgens to estrogens (Zondek, 1934; Simpson and Santen, 2015). Steinach and Kun (1937) first tested this theory in male rats and then in five men. They injected the five men with 50 mg of testosterone propionate three times per week, ending with a total of 20 injections. They collected urinary samples before and after the injections to measure levels of urinary estrogens. Before the injections, the estrogen levels of the men were between 0-36 rat units (unit corresponding to the minimum amount of a substance required to produce a biological response in a rat) and after the testosterone propionate injections had a maximum of 1200 rat units. The administration of additional testosterone increased the production of estrogen, essentially the first documented demonstration of aromatase and the biosynthesis of estrogens (Steinach and Kun, 1937).

2.6.2 Conceptus Estrogens

It wasn't until almost 50 years after the identification of estrogen that Perry and colleagues (1973) first reported the ability for the early stage porcine conceptuses to synthesize and secrete estrogens, specifically estradiol-17β and estrone. Later studies confirmed and expanded the steroidogenic capabilities of the early pig conceptus utilizing techniques such as gas and high-pressure liquid chromatography and recrystallization (Gadsby et al., 1980; Fischer et al., 1985).

Since then, researchers have identified the pattern of estrogen production from the conceptus and characterized two waves of secretion (Geisert et al., 2015). The uterine luminal content of estrogen increases on day 12 of pregnancy as the pig conceptuses rapidly elongate (Zavy et al., 1980; Geisert et al., 1982a). The increase in conceptus estrogen synthesis and secretion closely mirrors the increase in production of IL1B2 from the elongating conceptus (Ross et al., 2003). After the increase of conceptus estrogen on day 12, the uterine luminal estrogen content declines between day 13 to 14 and then is followed by the prolonged second wave with an increase of conceptus production from day 15 to about day 25 of pregnancy (Zavy et al., 1980; Geisert et al., 1982a; Stone and Seamark, 1985). Measurements of estrogen from the uterine lumen, utero-ovarian vein, and peripheral circulation from a pregnant gilt reflect the biphasic change in conceptus estrogen synthesis and release (Robertson and King, 1974; Zavy et al., 1980; Stoner et al., 1986).

2.6.3 Conceptus Steroidogenesis

The pig conceptus and other steroidogenic tissues, such as the gonads and adrenal glands, are capable of the biosynthesis of estrogen and other steroid hormones. Steroid hormones are cholesterol-derived and synthesized through conversion by specific enzymes during steroidogenesis (Fig 2.2). The steroidogenic acute regulatory (STAR) protein is the rate-limiting factor in

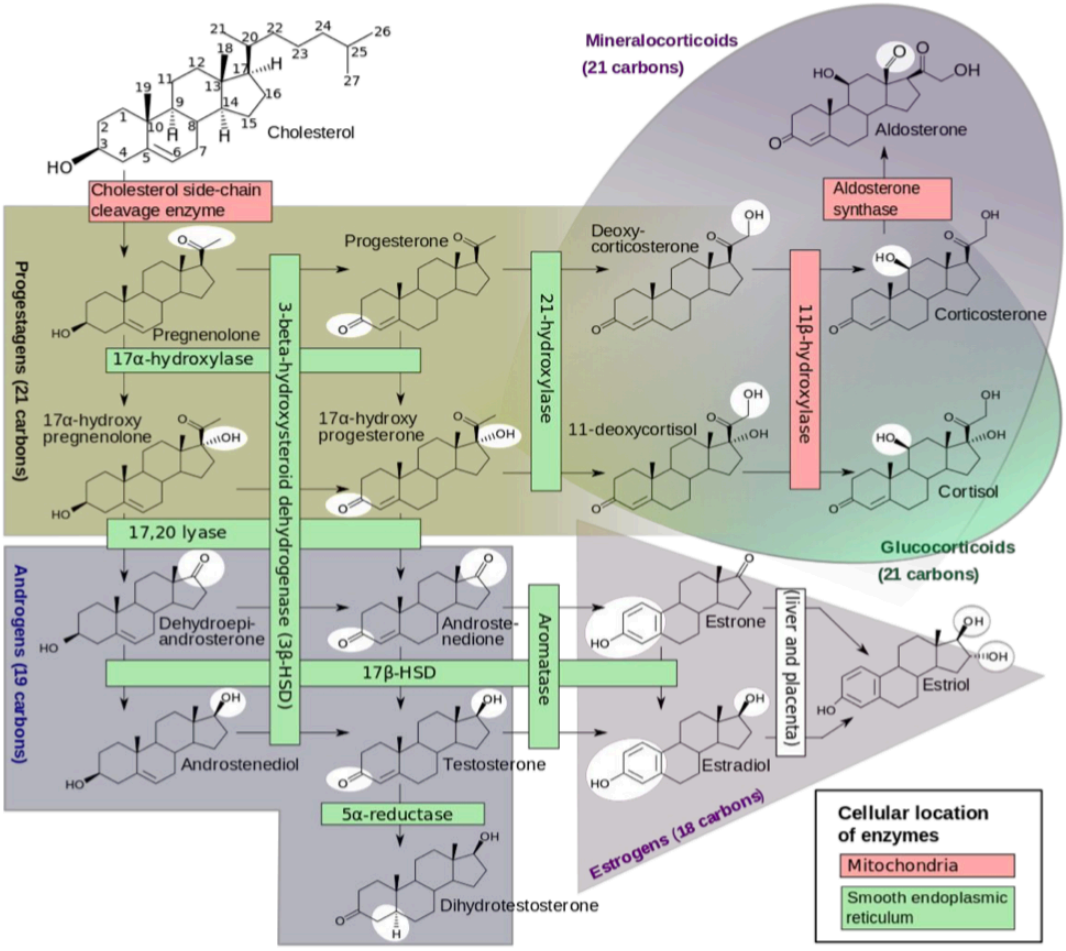

Figure 2.2: Diagram of the Steroidogenesis Pathway

Häggström M, Richfield D (2014). All steroid hormones are derived from cholesterol. The action of aromatase converts androstenedione and testosterone into estrone and estradiol, respectively.

steroidogenesis as it mediates transfer of cholesterol into the inner mitochondrial membrane for processing by cholesterol side-chain cleavage (P450scc) enzyme (Stocco, 2000). Enzymes involved with the steroidogenic pathway are divided into two major classes of proteins: the cytochrome P450 heme-containing proteins and the hydroxysteroid dehydrogenases (Payne and Hales, 2004). These enzymes are responsible converting pregnenolone (the result of the cholesterol being cleaved by the P450scc enzyme) to various products such as progestagens, mineralocorticoids, androgens, and estrogens (Payne and Hales, 2004). Progestagens are a result of pregnenolone being converted into progesterone by 3-betahydroxysteroid dehydrogenase (3β-HSD), into 17α-hydroxy pregnenolone, or progesterone to 17α-hydroxy progesterone by the enzyme 17α-hydroxylase. The enzyme 3β-HSD can also synthesize 17α-progesterone directly from 17α- hydroxy pregnenolone. Mineralocorticoids are derived from progesterone and 17α-hydroxy progesterone via 21-hydroxylase. Androgens are a result of the enzyme 17,20 lyase converting 17α- pregnenolone and 17α-progesterone into dehydroepiandrosterone and androstenedione, respectively. 17-betahydroxysteroid dehydrogenase (17β-HSD) uses dehydroepiandrosterone to synthesize androstenediol and androstenedione to make testosterone. The last androgen is a result of 5α-reductase changing testosterone into dihydrotestosterone. The cytochrome P450 enzyme aromatase (CYP19), is the enzyme that converts androgens, androstenedione and testosterone, into estrogens, estrone and estradiol, respectively (Payne and Hales, 2004). The aromatase reaction involves three consecutive hydroxylations

of the C19 methyl group of the steroid structure and the aromatization of the steroid A ring (Conley and Hinshelwood, 2001). The liver and placenta are both capable of the biosynthesis of a third estrogen, estriol, through conversion of either estrone or estradiol. Estradiol can be reversibly produced from estrone via 17β-hydroxysteroid dehydrogenase, and vice versa (Payne and Hales, 2004). During steroidogenesis, aromatase is required for production of all three estrogens.

2.6.4 Aromatase

Original publications indicated that humans, rats, mice, ruminants, and most mammals express only a single aromatase gene (*CYP19A1*) (Payne and Hales, 2004). However, there are species that were reported to express more than one aromatase gene that appear to occur through gene duplication. Conley et al. (2009) indicated that the pig is one of the rare species that had at least three separate aromatase genes. The sites of gene expression are tissue specific to each of the three aromatase genes and gave rise to nomenclature for the gonadal, placental, and embryonic aromatase enzymes. However, the most recent pig genome annotation (Ensembl: ENSSSCG00000030168.2) establishes that the pig genome contains a single aromatase gene (*CYP19A1*) that spans approximately 219 kb of chromosome 1 (120,477,197-120,696,877 forward strand) with 10 exons and can express 8 different transcripts through alternate splicing (Fig 2.3). The *CYP19A1* gene in mice and humans is encoded by a single gene with coding region encompassing

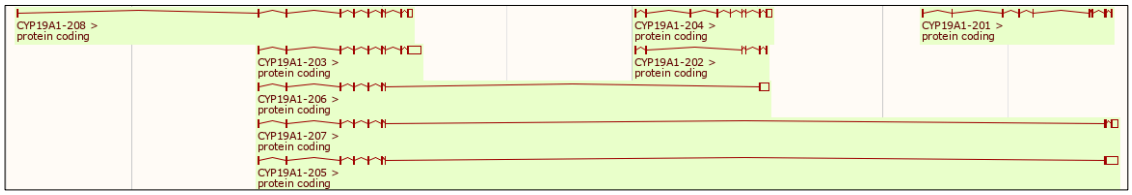

Figure 2.3: *CYP19A1* Splice Structure

Porcine Aromatase *CYP19A1* has 8 transcripts (splice variants) on Chromosome 1. Ensembl gene annotation ENSSSCG00000030168 produced by the Ensembl genebuild. (ensemble.org)

exon 2-10. The single gene has alternative untranslated first exons that are regulated by tissue-specific promoters, while the ATG translation start site is exon 2 (Zhao et al., 2016). Based on the new genome annotation of the pig, it would appear that the pig *CYP19A1* gene is similar to the human and mouse than previously believed. Therefore, a single aromatase gene can be alternatively spliced to express different isoforms during specific conceptus physiological events, such as maternal recognition and the establishment of pregnancy in pigs.

2.7 Maternal Recognition of Pregnancy

Maternal recognition of pregnancy is a process by which a chemical signal from the developing conceptuses result in the protection of the CL from luteolysis and the continued production of progesterone (P_4) throughout pregnancy. The luminal and glandular epithelium of the uterus has the capacity to secrete PGF2α in pulses into the uterine vasculature where it is carried to the ovaries on day 15 of the estrous cycle, causing luteolysis. In a pregnant gilt/sow, PGF2α production is not altered or inhibited, but sequestered away from the uterine vasculature within the uterine lumen through the conceptus secretion of estrogen which is the proposed maternal recognition of pregnancy signal in the pig (Bazer et al., 1982). The endocrine/exocrine hypothesis has been proposed as the biological mechanism for the maternal recognition of pregnancy in the pig. The hypothesis suggests that the CL of the pig is maintained as the production of PGF2α changes from an endocrine (towards and into the vasculature) during the estrous cycle to exocrine (released into the uterine lumen) secretion at the time of

maternal recognition of pregnancy (Bazer et al., 1982). During the estrous cycle, endometrial release of PGF2α into the uterine vein draining the uterine horn can be locally transferred to the ipsilateral ovary through countercurrent exchange with the ovarian artery, which directly wraps around it. However, the pig also has a systemic pathway of luteolysis as only 40% of the PGF2α in the blood is metabolized to 13,14-dihydro-15-keto prostaglandin F2α by single passage through the lungs. Thus, PGF2α can have a local and systemic effect on luteolysis of both ovaries. By moving the PGF2α into the uterine lumen and metabolism by the conceptus and endometrium, it ensures protection from the luteolytic effects allowing continued CL production of P_4, which is necessary for conceptus development and survival during pregnancy (Spencer and Bazer, 2002). Because the extensive length of the uterine horns of the pig, at least two embryos per uterine horn must be present to maintain pregnancy by protecting against both the local and systemic sources of PGF2α delivery during luteolysis (Dziuk, 1968).

As previously indicated, conceptus estrogen production has been proposed to be the maternal recognition signal of pregnancy in the pig for 40 years. The production of estrogen from the conceptus during rapid elongation and the initiation of attachment correlates with the timing of PGF2α being moved into the uterine lumen (Bazer and Thatcher, 1977). A pseudopregnancy model was utilized to explore the importance of the timing of the biphasic production of conceptus estrogen that occurs during the establishment of pregnancy. Geisert and others (1987) performed a study to mimic the production of estrogen from

conceptuses by administering estradiol-benzoate to gilts on days 11 through 15; days 14 to 16; and on days 9.5, 11, 12.5, 14 or 15.5 of the estrous cycle. Injections of estradiol-benzoate on day 11 or day 14-16 lengthen the estrous cycle to about 28 days. However, when treated with estradiol-benzoate on day 11 and day 14-16 or daily from day 11-15, the pseudopregnancy was extended beyond 60 days. The single injections on days 9.5, 11, 12.5, 14, or 15.5, the gilts fail to extend their estrous cycle beyond 30 days. This study demonstrated that both phases of estrogen production are needed to extend maintenance of the CL and progesterone production

As stated earlier in the review of literature, during elongation and the first wave of conceptus estrogen production, IL1B2 is secreted by the elongating conceptus (Ross et al., 2003). In human pregnancies, IL1B may initiate communication between the fetus and the uterus (Lindhard et al., 2002) which might play a role in successful establishment of pregnancy. It should be noted that IL1B stimulates aromatase activity in human cytotrophoblasts (Nestler, 1993), as well as increases transcription of aromatase in many different human cell types (Yang et al., 2002). Production of IL1B2 may be a regulatory factor for aromatase expression and activity during conceptus rapid elongation and estrogen synthesis possibly aiding in the increase of estrogen during maternal recognition of pregnancy.

2.7.1 Prostaglandin E Role in Maternal Recognition

There have been alternate hypotheses proposed for maternal recognition of pregnancy that suggest that estrogen is either not the only factor involved with

maintenance of CL function or acts upstream to stimulate other uterine factors that serve to protect the CL from luteolysis. It has been proposed that the sequestering of PGF2α into the uterine lumen may not fully explain the maintenance of CL function and it has been suggested that conceptus and/or endometrium prostaglandin E (PGE_2) plays a role in protecting the CL against the PGF2α luteolytic effect (Waclawik et al., 2009a). Inhibiting PG synthesis during the pre-implantation period of pregnancy results in the loss of pregnancy in multiple species ruminants (Dorniak et al., 2011), rodents (Kennedy et al., 2007), and pigs (Kraeling et al., 1985). However blocking production of PG synthesis with prostaglandin synthetase inhibitors did not prevent porcine conceptuses from undergoing rapid elongation (Geisert et al., 1986), indicating PG plays a role in the establishment of pregnancy but not in rapid remodeling of the conceptus prior to attachment to the uterine lumen.

Ford and Christenson (1991) demonstrated that intraluteal injections of PGE_2 into individual CL could protect against luteolysis from PGF2α during the estrous cycle. In addition, constant intrauterine fusion of PGE_2 from day 7 of the estrous cycle to day 23 demonstrated that PGE_2 was capable of extending the lifespan of the CL (Akinlosotu et al., 1986). During the period of maternal recognition of pregnancy, production of prostaglandins from the endometrium and conceptuses increases the PGE_2/PGF2α ratio in the uterine vasculature and uterine lumen indicating the increase in PGE_2 is aiding in the protection against luteolysis (Waclawik et al., 2009a). In humans, cells from endometrioma stimulated with PGE_2 increase expression of aromatase (Yang et al., 2002).

Therefore, PGE_2 may have an indirect effect on the maternal recognition of pregnancy through a localized stimulation of endometrial aromatase expression to increase estrogen content at the placental-maternal interface during early pregnancy.

2.7.2 Immune Function of Estrogen

During rapid elongation, the pig conceptus synthesizes IL1B2 on day 12 of pregnancy. As explained previously, IL1B2 stimulates the nuclear translocation of NFKB into the epithelial cells and activates the NFKB signaling pathway (Mathew et al., 2015). NFKB signaling results in the transcription of genes and pathways involved in inflammation and must be tightly regulated to prevent immunological rejection of the conceptuses (Geisert et al., 2015). Work done by Quaedackers et al. (2007) demonstrated that estrogen acted as an antagonist of NFKB activity. Conversely, King et al. (2010) observed estrogen also can serve as an agonist for NFKB activity. This data and the correlation with IL1B2 and estrogen production during rapid elongation and the maternal recognition of pregnancy indicates that estrogen may have a regulatory role in the immune responses related to the NFKB signaling pathway. Estrogen works to protect against immune response by activating estrogen receptors to regulate transcription and reducing the production of pro-inflammatory cytokines by inhibiting NFKB activation and apoptosis (Enninga et al., 2014). Thus, conceptus estrogen production is not only responsible for maternal recognition of pregnancy but may also have a function in preventing immunological rejection.

In all placental mammalian species, the conceptus must protect itself from the maternal immune system to successfully establish and maintain pregnancy. Interestingly, trophoblast and cancer cells can have similar biological activities based on how they are both a form of malignant cell growth and express cell surface antigens foreign to the host body (Enninga et al., 2014). Therefore, the shared pathways and immunologic regulators have been studied to obtain a better understanding of maternal immune responses to the placenta and tumors. Estrogen has been proposed to play a role in regulating the maternal immune system by acting as a negative regulator of the NFKB pathway, which is stimulated by proinflammatory cytokines. Certain tumors utilize estrogen to inhibit and protect the malignant cells from immunological recognition and rejection by directly inhibiting NFKB activation (Zang et al., 2002). Mak and others (2015) indicated that loss of ERβ is linked to chronic inflammation in patients with prostate cancer. These authors suggest that estrogen can act through ERβ to prevent NFKB activation leading to lack of immunological reaction which allows the unchecked growth of prostatic cancer cells. Therefore, it is possible that one of the major functions of placental estrogen production is to regulate the endometrial NFKB pathway to protect it from negative maternal immunological responses which could lead to abortion of the pregnancy.

2.8 Estrogen and Aromatase Inhibition

To clearly establish the role of conceptus estrogen production for the establishment and maintenance of pregnancy in the pig, a method for inhibiting conceptus estrogen synthesis or receptor activity is needed. The importance of

estrogen production during early pregnancy in the pig was first explored by the utilization of inhibitors to block or antagonize conceptus estrogen synthesis or action during elongation and establishment of pregnancy. O'Neill et al. (1991) designed a study to block conceptus estrogen action and determine the role of estrogen during early pregnancy in the pig. Two estrogen antagonists, keoxifene and clomiphene, were either infused via a uterine arterial catheter or injected alongside the arterial vasculature of the mesometrium during days 10 to 16 of pregnancy. The estrogen antagonists had no effect on the ability for the porcine conceptuses to elongate. The same result was observed when using an aromatase inhibitor, 4-OHA (4-hydroxyandrostenedione). Estrogen content in the uterine lumen was only decreased by 57% when gilts were treated with the aromatase inhibitor. Although estrogen production was significantly decreased, the quantity of estrogen available in the uterine lumen was more than sufficient for pregnancy to continue (O'Neill et al., 1991). Thus, estrogen antagonists or aromatase inhibitors were not an effective method of blocking estrogen synthesis in utero during elongation and the establishment of pregnancy. Antagonists and inhibitors are also not very specific and will target maternal and conceptus estrogen synthesis, which makes it difficult to evaluate the direct role of conceptus produced estrogen on maternal recognition. Recently, new genetic editing technologies have become available that allow a new approach to studying and understanding the role conceptus derived estrogen.

2.9 CRISPR/Cas9 Genomic Editing Technology

The CRISPR/Cas9 nuclease gene editing system allows a researcher to create targeted changes to the genome of a living cell. This technology was developed by utilizing the adaptive immunity of some bacteria and archaea that results in the elimination of foreign DNA. The initial action of the immune response is to incorporate a portion of the foreign DNA into the loci of Cluster Regularly Interspaced Short Palindromic Repeats, or CRISPRs. The CRISPR loci is followed by CRISPR-associated (Cas) genes, specifically the endonuclease Cas9, which cleaves the foreign DNA (Jinek et al., 2012). The function of CRISPR and CRISPR-associated protein-9 nuclease (Cas9) was observed in 2007 by Barrangou and others. They observed how bacteria could develop specific resistance against bacteriophages. The Doudna and Charpentier labs discovered the potential of this bacterial immune system to be manipulated into a gene editing technology. They developed a simplified component of the bacterial CRIPSR/Cas9 system, called guide RNA (gRNA). The CRISPR/Cas9 system use of the gRNA allows researchers to specifically target any gene in a variety of cell types. In CRISPR/Cas9 system, the targeted loci are cleaved by Cas9 resulting in a double stranded break and undergoes two major forms of repair: non-homologous end joining (NHEJ) and homologous directed repair (HDR) (Fig 2.4). In the absence of a donor DNA template that would be used for HDR, the error prone repair system NHEJ is used, resulting in base pair deletions or insertions (Reis et al., 2014). Different software programs have been created to design and optimize CRISPR gRNA to a region of

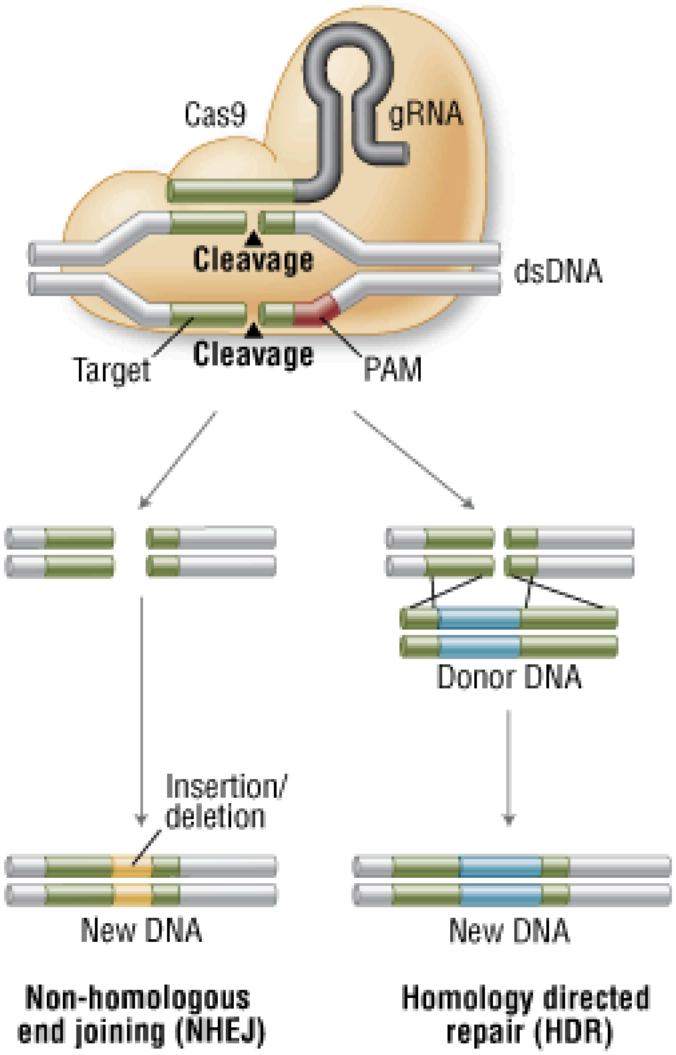

Figure 2.4: Genome Engineering with Cas9 Nuclease

Cas9 nuclease, guided to a specific location by the gRNA, makes a double stranded break resulting in an insertion or deletion from non-homologous end joining (NHEJ) or a donor DNA template is provided for homology directed repair (HDR) (Reis et al., 2014).

interest. The only requirement for this system is the target DNA must be followed by a protospacer adjacent motif (PAM), the sequence 5′-NGG-3’ (Sorek et al., 2013). The CRISPR/Cas9 system can be used in two ways: CRISPR mRNA injected into zygotes or in vitro transfections of a CRISPR gRNA and Cas9 protein complex followed by nuclear transfer cloning techniques (Sorek et al., 2013). These two techniques have been successfully used in multiple species. For example, CRISPR/Cas 9 technology was used in pigs to knock out the conceptus IL1B2, to determine if it was necessary for rapid conceptus elongation. Conceptuses IL1B2$^{-/-}$ failed to properly elongate, demonstrating its importance for proper conceptus elongation (Whyte et al., 2018). CRISPR/Cas9 has been used to create disease resistant models that could be used in the industry. In pigs, the CRISPR/Cas9 system was used to edit the CD163 gene which prevented the infection of Porcine Reproductive and Respiratory Syndrome (PRRS) virus, which would normally cause severe reproductive failure in sows (Whitworth and Prather, 2017). Zhengxing and others (2014) successfully created a myostatin knockout sheep using CRISPR/Cas9 gene editing system. The CRISPR/Cas9 system can be utilized on multiple mammalian species, providing an efficient way to generate animal models that can be used to understand gene function.

2.10 Utilizing CRISPRs for the Generation of Pig Conceptus Aromatase Null Research Model

Embryonic loss in mammals occurs predominantly during the preimplantation period. In the pig, this embryonic mortality occurs from days 10 to 30 of gestation (Pope, 1994), encompassing rapid conceptus elongation,

maternal recognition of pregnancy, placental attachment, and the establishment of pregnancy. Previous research has explored the concept of conceptus estrogen production as the signal for maternal recognition of pregnancy in the pig. In the past, studies that attempted to utilize inhibitors directed at estrogen receptor and aromatase to investigate the biological role of conceptus estrogen on conceptus development and the communication between the conceptus and maternal interface, were not efficient enough to totally block conceptus estrogen synthesis or action (O'Neill et al., 1991). Development of CRISPR technology allows for the generation of genetically modified animal models to study specific gene functions. The present research will utilize CRISPR/Cas9 gene editing to specifically target and edit the porcine conceptus aromatase gene to perform a loss-of-function study to establish the role of conceptus estrogen production during early pregnancy.

CHAPTER THREE

NEW PERSPECTIVE ON THE ROLE OF CONCEPTUS ESTROGENS IN CONCEPTUS DEVELOPMENT, MATERNAL RECOGNITION, AND THE ESTABLISHMENT OF PREGNANCY IN PIGS.

3.1 INTRODUCTION

Roger Short (1969) first coined the term 'maternal recognition of pregnancy,' which in its simple definition is the process by which a chemical signal from the conceptus prevents luteolysis of the corpora lutea (CL) by prostaglandin F2α (PGF2α), sustaining progesterone secretion beyond the length of a normal estrous cycle (Geisert et al., 1990). Although the intricate communication and activation of biological pathways between the developing conceptus and uterine endometrium during the establishment of pregnancy extends beyond CL maintenance, preventing luteolysis is critical in domestic farm species. Porcine conceptuses synthesize and release estrogen, the proposed signal for maternal recognition of pregnancy in the pig (Bazer et al., 1982), as they rapidly elongate and expand across the endometrial surface to prevent regression of the CL (Dhindsa and Dziuk, 1968). Because the pig has both a local and systemic vascular pathway for delivery of PGF2α to the ovaries for initiation of CL regression during the estrous cycle (Anderson et al., 1966), at least two conceptuses must be present initially in each uterine horn to establish and maintain pregnancy (Dziuk, 1968). Rapid elongation of the conceptuses

across the uterine surface is not only essential for the delivery of estrogen to prevent CL regression but also provides adequate uterine surface area for epitheliochorial pig placenta to uptake nutrients and establish the essential fetal-maternal communication needed for fetal survival to term (Geisert et al., 2017).

Historically, conceptus production of estrogen has been the proposed and accepted signal for maternal recognition of pregnancy in the pig (Bazer et al., 1982). In addition, estrogen has been suggested to assist with the uterine migration and equidistant spacing of blastocysts (day 8 to 12) within the uterine horns prior to the time of conceptus rapid elongation and attachment to the endometrial surface (Pope et al., 1982). Bazer and Thatcher (1977) first proposed the endocrine/exocrine hypothesis for maternal recognition of pregnancy in the pig. In this model, conceptus estrogen secretion during the period of rapid elongation and placentation results in the secretion of endometrial PGF2α being directed away from the uterine vasculature (endocrine secretion) and sequestered into the uterine lumen (exocrine secretion) where it is metabolized to its inactive 13,14-dihydro-15-keto prostaglandin $F_{2\alpha}$ metabolite. Thus, conceptus estrogen production and rapid elongation have been accepted as two of the major critical events for the establishment of pregnancy in the pig.

There is a biphasic production and release of estrogen into the uterine lumen by porcine conceptuses during the establishment of pregnancy and placentation in the pig (Geisert et al., 2017). The first increase in conceptus estrogen release into the uterine lumen occurs on days 11 to 12, during the period of rapid elongation as tubular (10 mm) conceptuses transform into a thin,

thread-like filamentous morphology greater than 200 mm in length in 1 hr (Geisert et al., 1982a). During rapid elongation, the increase in conceptus estrogen release directly mirrors production of conceptus interleukin 1β2 (IL1B2), a proinflammatory cytokine involved in pig conceptus elongation (Ross et al., 2003; Whyte et al., 2018). Conceptus IL1B2 not only is essential for initiating conceptus remodeling during its rapid morphological transformation but stimulates activation of the nuclear factor-kappa B (NFKB) signaling pathway in the underlying endometrial epithelial cells (Mathew et al., 2015). NFKB signaling results in the transcription of pathways involved with inflammation, cytokine release, and cell adhesion which must be closely regulated to prevent a full proinflammatory response and immunological reaction to the conceptuses during pregnancy (Hayden and Ghosh, 2012). Estrogen has been proposed to act as an immune regulator based on its ability to be an antagonist (Quaedackers et al., 2007) or agonist (King et al., 2010) of NFKB activity. A second sustained increase of conceptus estrogen production occurs during the period of uterine attachment and placental development from day 15 through 25 of pregnancy (Geisert et al., 1990). Using a pig pseudopregnancy model, Geisert et al. (1987) demonstrated that both phases of conceptus estrogen production are necessary for the maintenance of the CL beyond 60 days in the pig.

To more fully understand and establish the role(s) of conceptus estrogen production during pregnancy in the pig, previous studies have attempted to utilize aromatase inhibitors and estrogen antagonists to block estrogen synthesis or estrogen receptors during the period of conceptus elongation and placental

attachment. Estrogen antagonists, keoxifene and clomiphene, were not effective in inhibiting estrogen receptor activation *in vivo* (O'Neill et al., 1991). Although the aromatase inhibitor, 4-hydroxyandrostenedione (4-OHA), effectively inhibited conceptus estrogen production in vitro, the inhibitor proved to be much less sufficient in vivo (O'Neill et al., 1991). The development of CRISPR/Cas9 genomic editing technology provides a specific and efficient method to generate animal models to perform loss of function studies (Whitworth et al., 2014). Previously our laboratory has utilized CRISPR/Cas9 genomic editing to establish that porcine conceptus *IL1B2* expression is involved with rapid conceptus elongation (Whyte et al., 2018). The ability to inhibit the pig conceptus estrogen synthesis provides a more direct and specific way to analyze the biological role of conceptus estrogen in the establishment and maintenance of pregnancy. The present study utilizes CRISPR/Cas9 genomic editing technology to create *CYP19A1*$^{-/-}$ (aromatase) pig conceptuses to evaluate the role of estrogen in blastocyst migration, conceptus elongation, uterine attachment, placentation, and maintenance of pregnancy.

3.2 MATERIALS AND METHODS

All procedures used in this study were approved by the University of Missouri-Columbia Institutional Animal Care and Use Committee under Protocol 8813.

Animals. Recipient gilts utilized for embryo transfer were large white crossbred gilts of similar age (8-10 months) and weight (100-130 kg). Gilts were observed for estrus behavior twice daily with the onset of estrus designated Day 0 of the estrous cycle.

CRISPR/Cas 9 Design and Transfection of Porcine Fibroblast Cells Two pairs of guide RNAs (gRNA) were designed by using Broad Institute design tool (http://www.broadinstitute.org/rnai/public/analysis-tools/sgrna-design) to specifically target exon 2 of *CYP19A1* in the *Sus scrofa* genome. To minimize off targeting events, each gRNA was tested by using NCBI's Nucleotide BLAST Tool (https://blast.ncbi.nlm.nih.gov/Blast.cgi). Annealed gRNA oligonucleotides were cloned into the pX330 vector (Addgene) that contains expression cassettes for human codon-optimized Cas9 and the chimeric gRNA. The ability of the gRNA pairs to cleave was tested in vitro. The two pairs of guides were transfected together to optimize cutting efficiency. To determine optimal concentration of gRNAs, porcine fetal fibroblasts were transfected with the gRNA pairs at various concentrations (2 μg, 4 μg, or 8 μg total) and cultured for 2-3 days. Transfected cells were lysed, and DNA was used for PCR amplification by using primers specifically designed to amplify the location of gRNA design. The PCR amplicon was evaluated on a 2% ethidium bromide agarose gel for multiple bands and sequenced to determine which guides were cutting the most efficiently. The optimal guide pair (116 and 215) was determined the most efficient and optimal at a concentration of 4 μg (2 μg per gRNA).

Clonal Expansion and Colony Screening. Transfected fibroblast cells were plated using a dilution curve to promote colony growth from a single cell. Individual colonies were collected, lysed, and used for PCR amplification to determine editing (Fig 3.1). The PCR product was run on a 2% ethidium bromide agarose gel and bands were assessed for insertions or deletions. The PCR

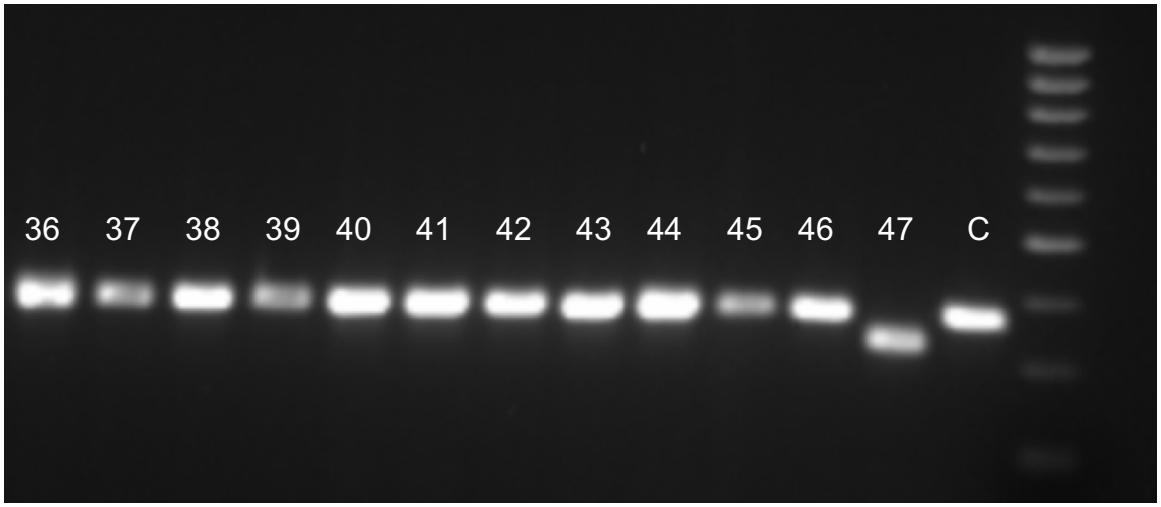

Figure 3.1: Colony Screening for Biallelic Modifications. Individual cell colonies were picked, lysed, and used for PCR amplification. The amplicon was run on an ethidium bromide 2% agarose gel and imaged. Cell colonies identified with a modification were cleaned up and submitted to sequencing (MU DNA Core, University of Missouri-Columbia). Each band represents an individual cell colony or control *CYP19A1*$^{+/+}$cells (labeled C). The image demonstrates the identification of the biallelic edited cell line #47, AM82, used for somatic cell nuclear transfer.

amplicon from individual cell colonies with edits were submitted to the University of Missouri DNA Core Facility for Sanger Sequencing and selected for biallelic edits. Out of 1,135 cell colonies screened, two cell colonies, designated 'AM82' and 'AM37', were identified by PCR and Sanger Sequencing to have a biallelic deletion on exon 2 of *CYP19A1*. TOPOcloning, using the PCR amplicon from each cell line, was used to identify the nature of the modification on each allele. Both cell lines had the same modification, a 40 base pair deletion on one allele and a 39 base pair deletion on the second allele (Fig 3.2).

Somatic Cell Nuclear Transfer (SCNT). Fibroblast colonies (Unedited control, *CYP19A1*$^{+/+}$ or *CYP19A1*$^{-/-}$ biallelic modification) were used as donor cells for SCNT as previously described (Whitworth et al., 2014). Briefly, sow-derived oocytes (Desoto Biosciences) were matured in vitro, cumulus cells were removed from the oocytes, and the polar body and the metaphase II plate were removed. A donor cell (*CYP19A1*$^{+/+}$ or *CYP19A1*$^{-/-}$) was placed in the perivitelline space and electrically fused to the oocyte. Reconstructed zygotes were chemically activated (Machaty et al., 1997) and cultured. Day 6 blastocysts (n=30-50) were surgically transferred into the ampullary–isthmic junction of the oviduct of the surrogate gilts at day 3, 4, or 5 after first standing estrus as previously described (Lee et al., 2013).

Experiment 1. Conceptuses were collected by uterine flushing as previously described (Ross et al., 2003; Mathew et al., 2011). Recipient gilts were euthanized on either day 14 (n=12 *CYP19A1*$^{+/+}$, n=6 *CYP19A1* $^{-/-}$) or day 17 (n=4) *CYP19A1*$^{+/+}$, n=4 *CYP19A1*$^{-/-}$) of pregnancy.

Figure 3.2: Biallelic Modification on Exon 2 of the Porcine *CYP19A1* gene. Sequence shows Exon 2 (highlighted in blue) of the *CYP19A1*$^{-/-}$ has a 40 base pair deletion in one allele (GE1) and a 39 base pair deletion in the second allele (GE2) compared to the *CYP19A1*$^{+/+}$ control sequence (CS). The locations of the gRNAs are underlined. Introns are displayed in lowercase.

The uterus and ovaries were recovered and transferred to the lab for processing. The exterior of the uterus was rinsed, and the broad ligament trimmed away. Conceptuses were recovered from the uterine horns by flushing one random horn twice with 30 mL of PBS as previously described (Ross et al., 2003; Mathew et al., 2015). The second uterine horn was opened along the antimesometrial side and laid flat in a Pyrex dish filled with PBS (~6 liters) to "float" out conceptuses to determine positioning along the uterine horn and collect individual conceptuses for analysis. The collected conceptuses recovered in the uterine flushing (ULF) were examined and the morphology and viability were assessed. Endometrial tissue (~5 g) was removed from six random sections along the mesometrial side of each uterine horn. Conceptuses and endometrial tissue were immediately snap-frozen in liquid nitrogen and stored at −80 °C until RNA isolation. The uterine flushing from the horn was centrifuged at 3,000 × g at 4 °C for 10 min to remove cellular debris and preserved at −80 °C until utilized for interleukin 1β (IL1B), estradiol-17β, testosterone, prostaglandins (PGs), and interleukin 18 (IL18) analysis**.**

An additional group of recipient gilts (n=4) containing *CYP19A1*$^{-/-}$ conceptuses were allowed to continue pregnancy. Blood samples were collected for plasma progesterone analysis via jugular venipuncture every 3 days beginning on day 13 of pregnancy. Blood samples were centrifuged at 2400 x g for 20 min at 4 °C and plasma was stored at -20°C. Gilts were monitored for standing heat every day after day 17. If estrus was not detected, gilts were

ultrasound starting on day 21 to detect the presence of embryos and monitor pregnancy.

Total RNA, Genomic DNA, and Protein Isolation. Total RNA was isolated from endometrial samples using TRIzol-RNA lysis reagent (ThermoFisher Scientific, 15596018). The AllPrep DNA/RNA/Protein Mini kit (Qiagen, 80004) was used for simultaneous purification of DNA, RNA, and protein from conceptus samples. To eliminate genomic DNA contamination, extracted RNA was treated with DNase I and purified using RNeasy MinElute cleanup kit (Qiagen, 74204). The quantity and quality of total RNA were determined by spectrometry and running a 1% agarose, 1% standard bleach RNA integrity gel. RNA from each endometrium sample (25 ul) was submitted for deep-sequencing at a concentration of 100ng/ul. Total RNA from each sample was reverse transcribed in a total reaction volume of 20 µl using iScript RT supermix (BioRad, 1708841). Reverse transcription was performed as follows: 5 min at 25°C; 30 min at 42°C; and 5 min at 85°C. Control reactions in the absence of reverse transcriptase were prepared for each sample to test for genomic DNA contamination. The resulting cDNA was stored at -20°C for further analysis.

Reverse Transcription and RT-PCR Gene Expression Analysis. First-strand cDNA for RT-PCR was synthesized from total RNA, and real-time RT-PCR was performed and quantified on a CFX384 Real-Time System (Bio-Rad). Expression was measured for conceptus genes using primers specific for *CYP19A1, IL1B2, PTGS2, PTGES, STAR, BMP4, IFND* and *IFNG* (primer design and source are listed in Table 3.1).

Table 3.1: Conceptus RT-PCR Primers.

Gene	RefSeq gene	Primers 5'→ 3'	Source
CYP19A1	**NM_214429.1**	GCTAATTGCAGCACCAGACA	**(Ebeling et al., 2011)**
	Provisional	TGTTGGTTCCCTTTTTCACC	
IL1B2	**NM_001302388.1**	GCCAATGGTTTTCTCTGTGATGCC	**(Whyte et al., 2018)**
	Validated	CTCATGCAGAACACCACTTCTCTC	
STAR	**NM_213755.2**	CTCTGGCTGGAAGTCCCTCAA	**(Bolzan et al., 2013)**
	Provisional	CAAAGTCCACCTGGGTCTGTGA	
PTGS2	**NM_214321.1**	GAAAGGCCAAGATTTGTGGA	**(Jeong et al., 2016)**
	Provisional	GGGAGTGGAGTACGTGAAGC	
PTGES	**NM_001038631.1**	ATCAAGATGTACGTAGTGGC	**(Blitek et al., 2010)**
	Provisional	GAGCTGGGCCAGGGTGTAGG	
IFND	**NM_213948.1**	ATGGATTGTCCCCATGTAGG	**(Joyce et al., 2007)**
	Provisional	CTGAGCTACCAGGGTTACCG	
IFNG	**NM_001002832.1**	CCATTCAAAGGAGCATGGAT	**(Joyce et al., 2007)**
	Provisional	TTCAGTTTCCCAGAGCTACCA	
BMP4	**NM_001101031.2**	CGTCATCCCAGATTACAT	**(Hall et al., 2009)**
	Provisional	GAGTCGAAGCTCTGCGGAT	
YWHAG	**XM_003124396.4**	TCCATCACTGAGGAAAACTGCTAA	**(Whitworth and Prather, 2010)**
	Provisional	TTTTTCCAACTCCGTGTTTCTCTA	

The ΔCT was estimated as the difference between the cycle threshold (CT) for the gene of interest and geometric mean of the CT for the reference genes. Fold change was calculated relative to the average of day 14 *CYP19A1*$^{-/-}$ ΔCT. RT-PCR analysis indicated that porcine *YWHAG* (Whitworth and Prather, 2010) gene expression was not statistically different (P > 0.05) in the conceptus RNA, therefore porcine *YWHAG* was used as the endogenous control.

Measurement of ULF IL1B, IL18, Testosterone, Estradiol-17β, and Plasma Progesterone. A pig IL1B ELISA Kit (Abcam, 100754), IL18 ELISA kit (Aviva Systems Biology, OKEH00106), and testosterone ELISA kit (Cayman Chemical Company, 582701) were utilized to detect the uterine luminal content of IL1B, IL18, and testosterone, respectively, in ULF. Samples and standards were added in duplicate to the 96-well ELISA plate and were processed and read on an EL808 Ultra Microplate Reader (Bio-Tek) according to the manufacturer's directions. Uterine luminal flushing concentrations of estradiol-17β were quantified in a single RIA as described previously (Kirby et al., 1997). Sensitivity of the estradiol assay was 0.5 pg/mL. Samples expected to be low were extracted and high were not extracted, using 300 ul or 100 ul of sample, respectively. The intraassay coefficient of variation was 6.04%. Standards and pooled aliquots of ULF were linear and parallel over a mass of 0.25 to 20 pg and ULF volume of 10μl to 100μl, respectively. Plasma concentrations of progesterone were quantified in a single assay using the MP Biomedical. Progesterone RIA kit as described previously (Pohler et al., 2016). Sensitivity of the assay was 0.05 ng/mL. Intraassay coefficient of variation was 1.51%.

Prostaglandins Assay. Prostaglandins in the uterine flushings were analyzed with a Parent Prostaglandin assay by the *Eicosanoid Core Laboratory at Vanderbilt University Medical Center in Nashville, TN*. To quantify eicosanoids in ULF samples, 100uL of fluid was placed in a microcentrifuge tube containing 25% methanol in water (500uL) and internal standard (d_4-PGE_2 and d_4-LTB_4, 1ng each). The sample was vortexed and then extracted on an Oasis MAX uElution plate (Waters Corp., Milford, MA) as follows. Sample wells were first washed methanol (200 uL) followed by 25% methanol in water (200 uL). The sample was then loaded into the well and washed with 600 uL 25% methanol. Eicosanoids were eluted from the plate with 30 uL 2-propanol/acetonitrile (50/50, v/v) containing 5% formic acid into a 96-well elution plate containing 30 uL water in each well. Samples were analyzed on a Waters Xevo TQ-S micro triple quadrupole mass spectrometer connected to a Waters Acquity I-Class UPLC (Waters Corp., Milford, MA USA). Separation of analytes was obtained using an Acquity PFP column (2.1 x 100 mm) with mobile phase A being 0.01% formic acid in water and mobile phase B acetonitrile. Eicosanoids were separated using a gradient elution beginning with 30% B going to 95% B over 8 minutes at a flow rate of 0.250 mL/min.

Analysis of Endometrial Differential Gene Expression. The endometrial RNA samples submitted for deep-sequencing were analyzed as follows: The raw sequences (FASTQ) were subjected to quality check by FastQC (http://www.bioinformatics.babraham.ac.uk/projects/fastqc/). The program fqtrim (https://ccb.jhu.edu/software/fqtrim/) was used to remove adapters, perform

quality trimming (phred score >30) by a sliding window scan (6 nucleotides) and select read length of 30 nucleotides or longer after trimming. The reads obtained from the quality control step were mapped to the Sscrofa11.1 genome assembly by using Hisat2 aligner which is a fast and sensitive alignment program of next-generation sequencing data (Kim et al., 2015). The program FeatureCounts (Liao et al., 2014) was used to quantify read counts by using the sequences alignment files of each sample. The differentially expressed (DE) genes between sample groups, representing the culture treatment, were determined by edgeR-robust (Zhou et al., 2014). The false discovery rate (FDR) < 0.05 was used as threshold for statistical significant differential expression of genes. Top differentially expressed genes, was determined by a FDR of less than 0.05, counts per million (CPM) greater than 1, and a fold change (FC) greater than 2 or less than -2 (Chen et al., 2009).

Cluster and network analysis. To infer gene expression networks within a predicted cluster, an information theory approach (Cover and Thomas, 1991) was adopted. In this method, mutual information (MI) of variation between gene expression was determined. MI measures the information content that two variables share: a numerical value ranging from 0 to 1 depending on, intuitively, how much knowing one variable would predict variability of the other. We calculated MIs in pair-wise manner between each gene (read count data from RNA-seq) to generate a weighted adjacency matrix by the Maximum Relevance Minimum Redundancy (MRMR) method3. The key players were predicted from each network based on measure of ‘degree centrality’ of genes as described

earlier (Behura et al., 2017). The pathway genes were assessed from the pig KEGG (Kyota Encyclopedia of Genes and Genomes) pathway database.

Experiment 2. Results from Experiment 1 indicated that recipient gilts containing *CYP19A1*$^{-/-}$ conceptuses (n=4) either aborted by day 27 to 31 of pregnancy or returned to estrus between days 25-30 of pregnancy. Therefore, recipient gilts containing *CYP19A1*$^{-/-}$ conceptuses were either treated with exogenous estrogen during the period of maternal recognition of pregnancy or *CYP19A1*$^{+/+}$ blastocysts were co-transferred with *CYP19A1*$^{-/-}$ blastocysts to determine if the pregnancy of recipients with *CYP19A1*$^{-/-}$ conceptuses could be rescued.

Estradiol-Benzoate Injections. Recipient gilts containing *CYP19A1*$^{-/-}$ conceptuses (n=4) were treated with estradiol-benzoate injections as described previously (Geisert et al., 1987). Gilts were given a 1 ml intramuscular injection of estradiol-benzoate (5 mg/ml) on days 14, 17, 18, and 19 (n=2) or days 15, 18,19, and 20 (n=2) of pregnancy. Two hundred mg of estradiol-benzoate (Sigma-Aldrich) was dissolved in 4 ml of 100% ethanol in a 50 ml sterile conical tube and vortexed for 3 minutes. Following vortexting, 36 ml of pharmaceutical grade sesame oil was added and vortexed. The solution is rocked overnight at 37 °C.

Co-Embryo Transfer of *CYP19A1*$^{-/-}$ and *CYP19A1*$^{+/+}$ Blastocysts. Fibroblast cell lines *CYP19A1*$^{+/+}$ and *CYP19A1*$^{-/-}$ were used as donor cells for SCNT as previously described. After *in vitro* culture, day 6 blastocysts, half *CYP19A1*$^{-/-}$ and half *CYP19A1*$^{+/+}$ (n=40), were surgically transferred into the ampullary–isthmic junction of the oviduct of the surrogate gilts at day 3, 4, or 5 after first standing

estrus. *CYP19A1*$^{-/-}$ recipient gilts were co-transferred with SCNT *CYP19A1*$^{+/+}$ blastocysts from fibroblast cell line A (n=2), fibroblast cell line B (n=2), and fibroblast cell line C (n=4) fibroblast cell lines. An additional group of recipients (n=4) received *CYP19A1*$^{+/+}$ blastocysts developed from fibroblast cell line C as a positive control to establish pregnancy with SCNT embryos.

Co-Embryo Transfer of *CYP19A1*$^{-/-}$ Clones and *In Vitro* Fertilized (IVF) *CYP19A1*$^{+/+}$ Embryos. The failure of pregnancy to be rescued in recipient gilts containing *CYP19A1*$^{-/-}$ conceptuses through either treatment with exogenous estrogen or co-transfer with SCNT *CYP19A1*$^{+/+}$ conceptuses suggested that *CYP19A1*$^{-/-}$ conceptuses could be inducing a maternal response that prevents maintenance of pregnancy despite continued progesterone production from the CL or in the present of SCNT *CYP19A1*$^{+/+}$ conceptuses that can maintain pregnancy alone. *CYP19A1*$^{-/-}$ blastocysts were co-transferred with *in vitro* fertilized (IVF) blastocysts to determine if pregnancy could be rescued with conceptuses that normally have a great probability of establishing and maintaining pregnancy compared to SCNT embryos. Production of IVF blastocysts has been previously described by (Whitworth et al., 2015). After in vitro culture, day 6 blastocysts, half *CYP19A1*$^{-/-}$ clones and half *CYP19A1*$^{+/+}$ IVF (n=40), were used for embryo transfer into recipient gilts (n=3).

Heat Detection, Ultrasound, and Blood Collection. The recipient gilts were monitored for standing heat every day after day 17. If estrus was not detected, gilts were ultrasound to detect the presence of embryos and monitor pregnancy. Blood samples were collected for plasma progesterone analysis via jugular

venipuncture every 3 days beginning on day 13 of pregnancy. Blood samples were centrifuged at 2400 x g for 20 min at 4 °C and plasma was stored at -20°C. Recipients were euthanized on day 34 of pregnancy to collect embryos and the placenta which were genotyped to determine if they were IVF or *CYP19A1*$^{-/-}$ clones.

Statistical Analysis. All statistical analyses of quantitative data were performed using Sas 9.4 statistical software. Data was analyzed by using the PROC GLM model of the Statistical Analysis System (SAS Institute Inc., Cary, NC). The statistical model used to evaluate uterine flushing content and conceptuses relative gene expression included the conceptus genotype (*CYP19A1*$^{+/+}$ or *CYP19A1*$^{-/-}$), the day collected (day 14 or day 17), and the genotype x day interaction.

3.3 RESULTS

In Vitro Blastocyst Development from *CYP19A1*$^{-/-}$and *CYP19A1*$^{+/+}$ Fibroblasts Following Somatic Cell Nuclear Transfer. The two cell lines identified as *CYP19A1*$^{-/-}$ were used in SCNT to generate *CYP19A1*$^{-/-}$ blastocysts. Fibroblast cells that had been transfected without gRNA/Cas9 complex were used as the *CYP19A1*$^{+/+}$ control. The embryo derived from *CYP19A1*$^{-/-}$ fibroblast cells had an *in vitro* blastocyst development rate of 30-40% during culture which was similar to that of embryos from *CYP19A1*$^{+/+}$fibroblast cells. Blastocysts were genotyped and verified to have *CYP19A1* gene biallelic edit (Fig 3.3).

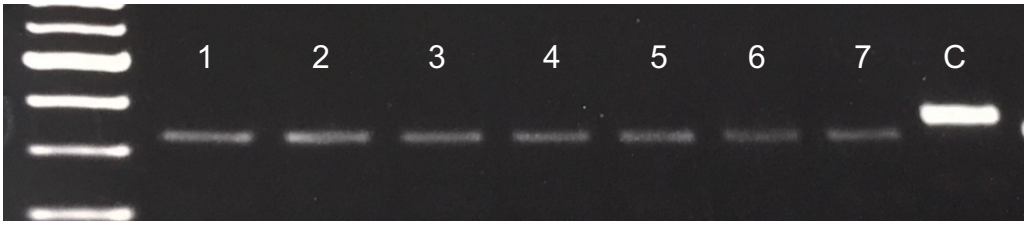

Figure 3.3: Genotyping of *CYP19A1*$^{-/-}$ Blastocysts. Blastocysts derived from SCNT with *CYP19A1*$^{-/-}$ fibroblasts (1-7) were collected from *in vitro* culture on day 7 and genotyped by PCR. Control (C) unedited *CYP19A1*$^{+/+}$ blastocyst.

Experiment 1.

Uterine Flushing of Recipient Gilts Containing Either *CYP19A1*$^{+/+}$ or *CYP19A1*$^{-/-}$ Conceptuses on Days 14 and 17 of Pregnancy. The uterine horns of recipient gilts were flushed on days 14 and 17 of pregnancy to collect the uterine luminal content and *CYP19A1*$^{+/+}$ (n=4, day 14; n=3, day 17) or *CYP19A1*$^{-/-}$ (n=4, day 14; n=3 day 17) conceptuses. Gilts not pregnant (n=5) or yielding only 1 or 2 conceptuses (n=7) were excluded from analysis. On day 14 of pregnancy, both *CYP19A1*$^{+/+}$ and *CYP19A1*$^{-/-}$ recipient gilts contained a variety of conceptus morphologies (ovoid, tubular, and filamentous). However, the majority of *CYP19A1*$^{+/+}$ and *CYP19A1*$^{-/-}$ conceptuses were elongated to the filamentous stage of development (Fig. 3.4). Collected conceptuses were analyzed to confirm the *CYP19A1*$^{-/-}$ genotype (Fig 3.5). Interestingly, large clumps of off-white masses were flushed from the uterine horn of some gilts containing *CYP19A1*$^{-/-}$ conceptuses. These large clumps were also observed when the uterine horn was opened, and conceptuses floated to obtain individual filamentous conceptus (Fig 3.6). When examined under a dissecting microscope, the clumps appeared to be a group of tightly entangled elongated conceptuses. Genotyping verified that the clumps were entangled *CYP19A1*$^{-/-}$ conceptuses. The conceptus clumps were located outside the mesometrial side of the uterine horn, away from where other filamentous conceptuses were attaching to the uterine luminal surface as occurs normally in the pig. Both *CYP19A1*$^{+/+}$ and *CYP19A1*$^{-/-}$ conceptuses had expanded, attached to the mesometrial side of the

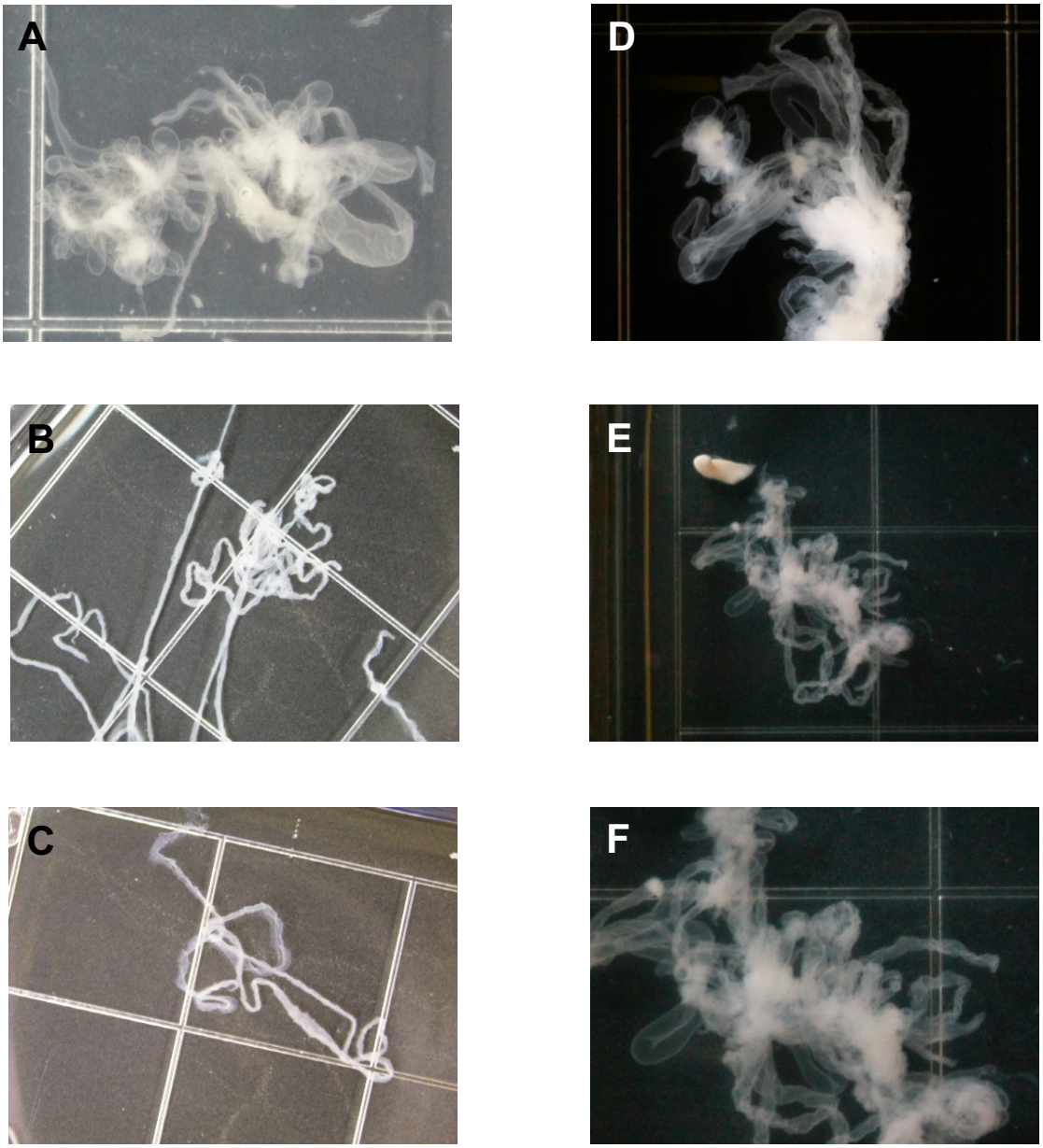

Figure 3.4: Day 14 Elongated Conceptuses. Conceptuses flushed from the uterine horn of recipient gilts containing either *CYP19A1*$^{+/+}$ or *CYP19A1*$^{-/-}$ conceptuses on day 14 of pregnancy. **A, B, C)** *CYP19A1*$^{+/+}$ elongated conceptuses. **D, E, F)** *CYP19A1*$^{-/-}$ elongated conceptuses.

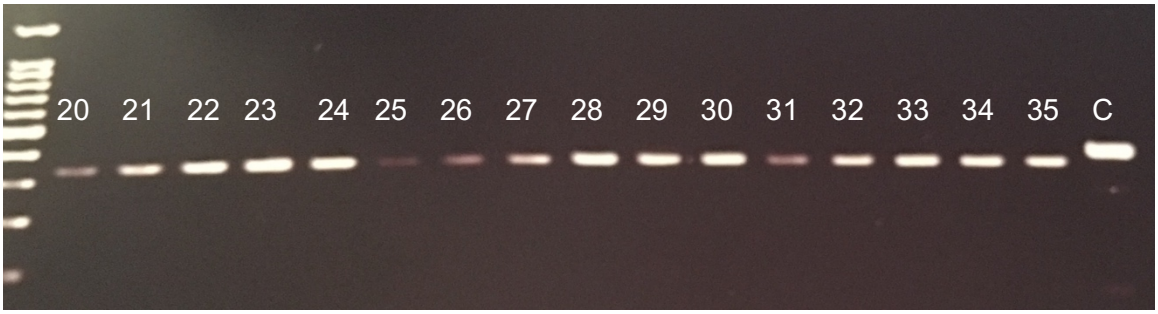

Figure 3.5: Day 14 *CYP19A1*$^{-/-}$ Conceptus Genotyping. Day *CYP19A1*$^{-/-}$ conceptuses (# 20-35) and Control (C) unedited *CYP19A1*$^{+/+}$ conceptuses were analyzed by PCR amplification to confirm genotype.

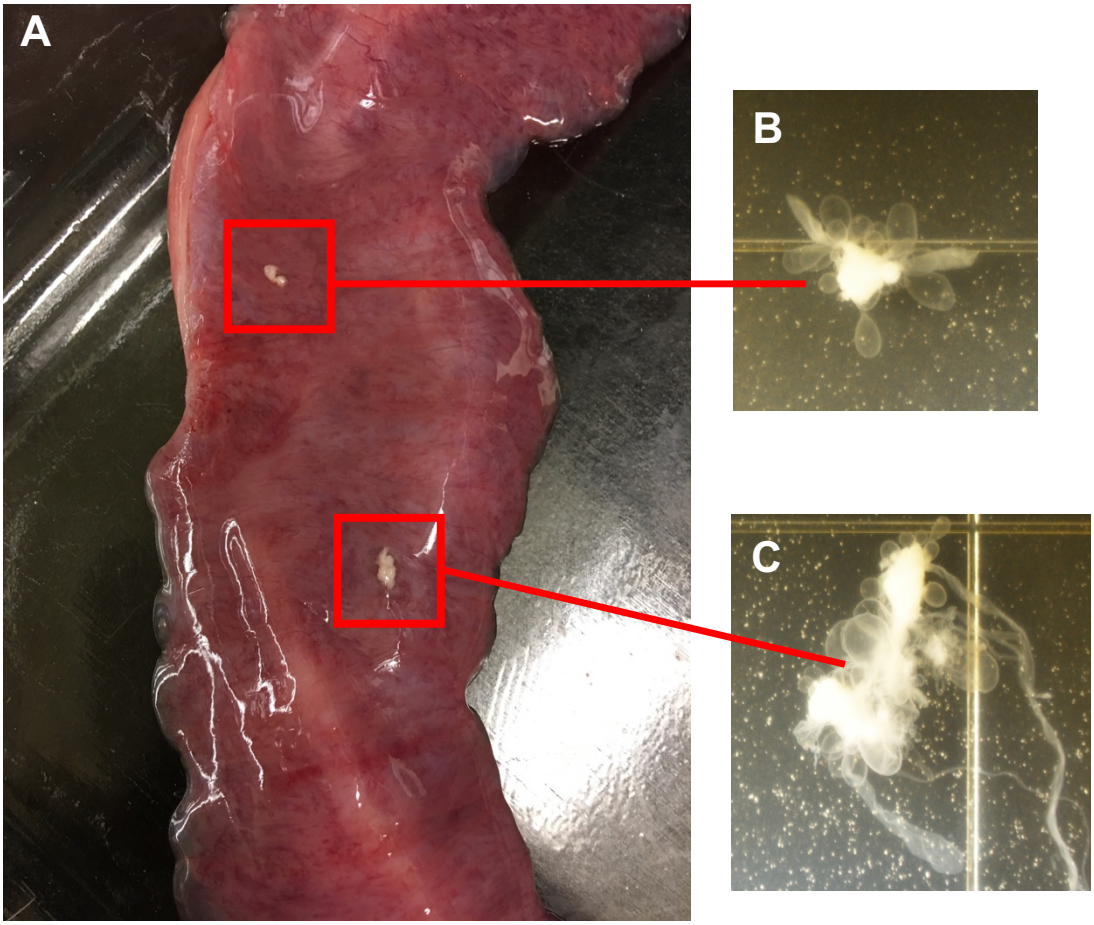

Figure 3.6: Opened Uterine Horn of *CYP19A1*$^{-/-}$ Recipient Gilts. A) The uterine horn was cut open and laid out to float and collect individual conceptuses. The presence of clumps of entangled elongated conceptuses (red boxes) was found outside the mesometrial border of the uterine horn. **B, C)** Images of the clumps of elongated *CYP19A1*$^{-/-}$ conceptuses under a dissecting microscope.

uterine lumen and initiated early placental development on day 17 of pregnancy (Fig 3.7). Ovaries of recipient gilts containing either *CYP19A1*$^{+/+}$ or *CYP19A1*$^{-/-}$ conceptuses had functional CL which was verified by maintenance of high plasma progesterone concentrations. Recipient gilts that did not establish pregnancy regressed the CL on day 15 and had corpora albicantia on day 17. The maintenance of CL in recipient gilts containing *CYP19A1*$^{-/-}$ conceptuses which do not produce estrogen was an unexpected result (Fig 3.8).

Uterine Luminal Flushing Analysis. Total content of estradiol-17β in the ULF was significantly (P=0.0006) decreased in recipient gilts containing *CYP19A1*$^{-/-}$ conceptuses on day 14 and day 17 of pregnancy (Fig 3.9). The estradiol-17β content in ULF from recipients containing *CYP19A1*$^{+/+}$ conceptuses was 3,025 ± 728 pg on day 14 and 2,178 ± 671 pg on day 17 compared to 59.8 ± 16 pg and 60.4 ± 3.5 pg, respectively, from recipients with *CYP19A1*$^{+/+}$ conceptuses. Content of estradiol-17β in ULF of *CYP19A1*$^{-/-}$ conceptuses was similar to ULF of recipient gilts that did not contain conceptuses at the time of flushing (day 14: 79.7 ± 7 pg; day 17: 65.6 ± 7 pg). Although estradiol-17β production by *CYP19A1*$^{-/-}$ conceptuses was greatly suppressed, conceptus steroidogenesis was not inhibited as the uterine luminal content of testosterone was not different across genotype or day (Fig 3.10). However, the total ULF content of IL1B2, which is involved with rapid conceptus elongation on day 14, was significantly lower (P=0.003) in ULF from recipient gilts with *CYP19A1*$^{-/-}$ compared to *CYP19A1*$^{+/+}$ conceptuses (Fig 3.11). Analyses of prostaglandins in the uterine lumen represents both endometrial and conceptus production during Day 14 and

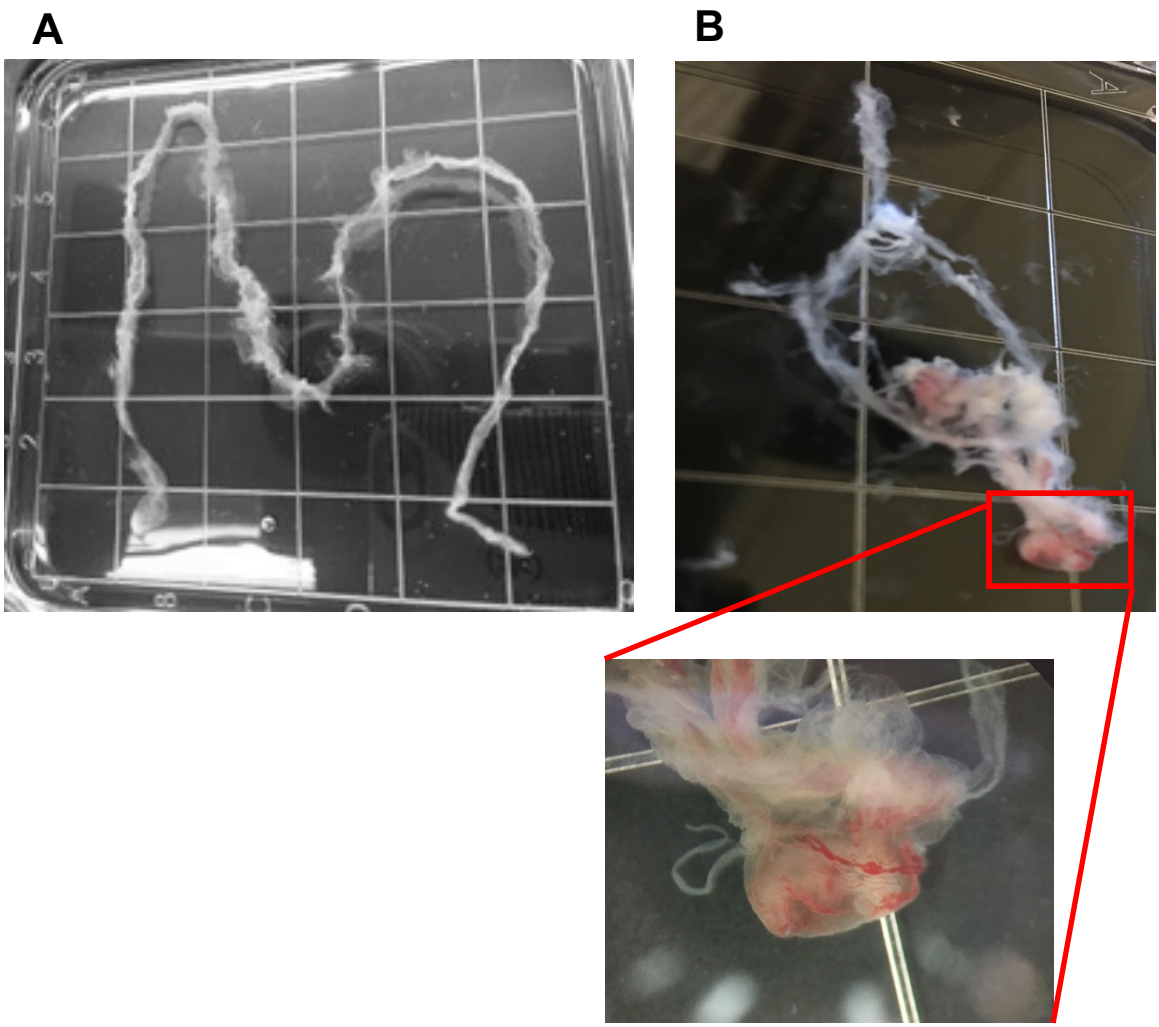

Figure 3.7: *CYP19A1*$^{-/-}$ Day 17 Conceptus. On day 17 of pregnancy, fully elongated *CYP19A1*$^{-/-}$ conceptuses were collected. **A)** An individual day 17 *CYP19A1*$^{-/-}$ conceptus collected by the floating. **B)** Day 17 conceptuses had begun embryo and placental development (insert).

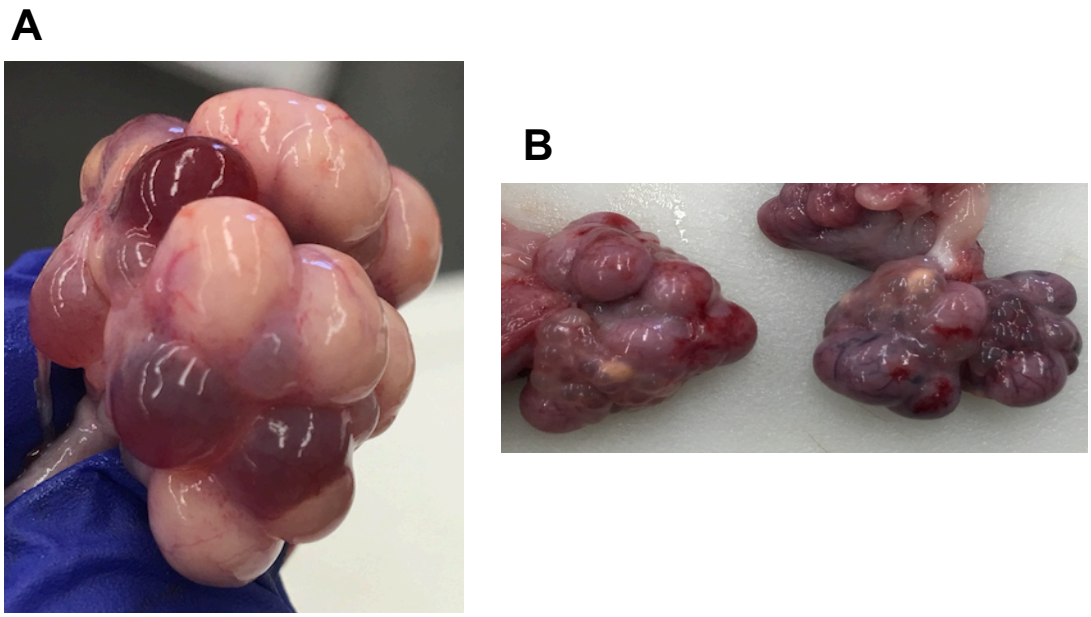

Figure 3.8: Ovaries of Nonpregnant or *CYP19A1*$^{-/-}$ Pregnant Gilts Collected on Day 17. A) Ovary with corpora albicantia from a non-pregnant gilt. **B)** Ovaries containing functional corpora lutea from recipient gilts carrying *CYP19A1*$^{-/-}$ conceptuses.

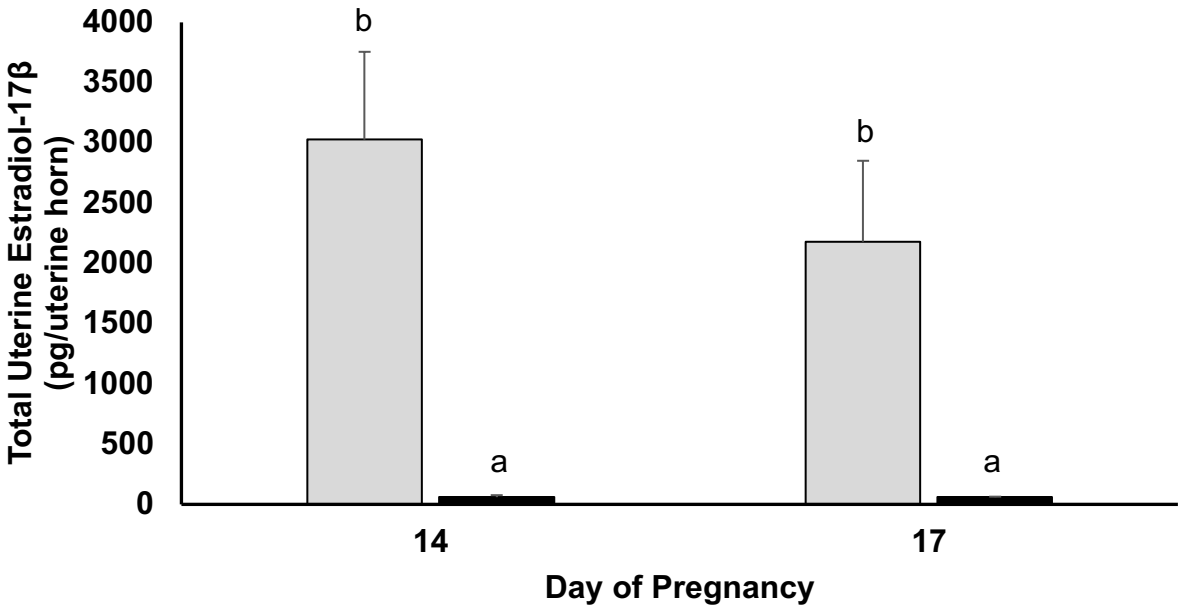

Figure 3.9: Total content estradiol-17β (pg/uterine horn) in uterine flushings collected from recipient gilts containing either *CYP19A1*$^{+/+}$ (Grey bar) or *CYP19A1*$^{-/-}$ (Black bar) conceptuses on days 14 or 17 of pregnancy. A genotype effect ($P < 0.01$) was detected for total estradiol-17β. Bars without a common superscript represent a statistical difference.

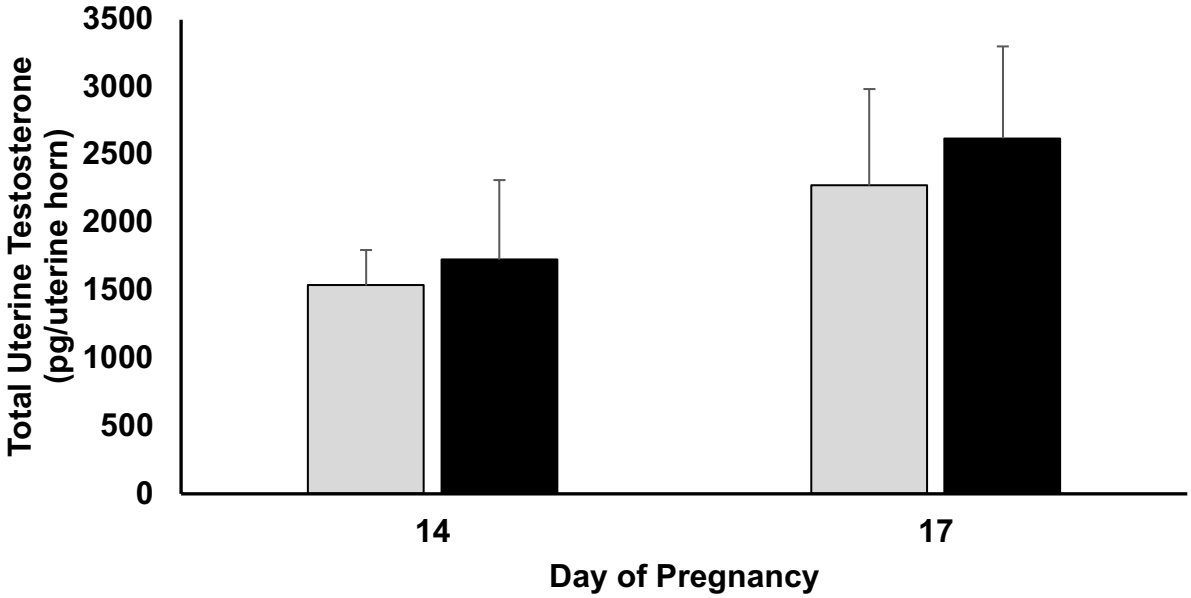

Figure 3.10: Total content Testosterone (pg/uterine horn) in uterine flushings collected from recipient gilts containing either *CYP19A1*$^{+/+}$ (Grey bar) or *CYP19A1*$^{-/-}$ (Black bar) conceptuses on day 14 or 17 of pregnancy.

No statistical difference.

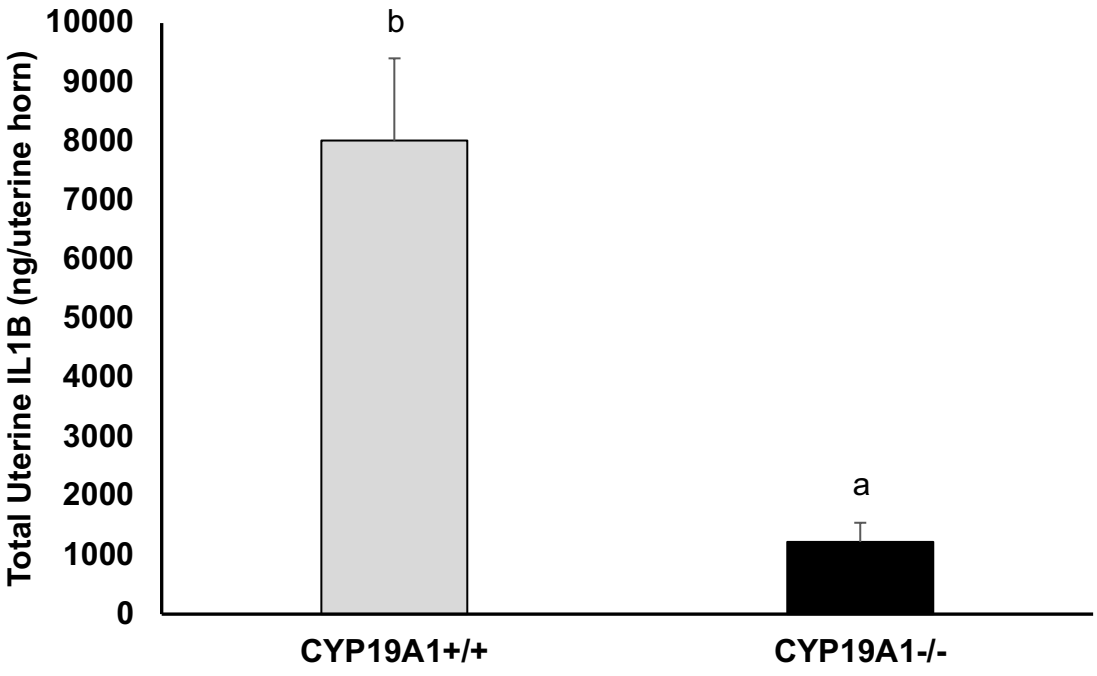

Figure 3.11: Total content IL1B (ng/uterine horn) in uterine flushings collected from recipient gilts containing either *CYP19A1*$^{+/+}$ (Grey bar) or *CYP19A1*$^{-/-}$ (Black bar) conceptuses on day 14 of pregnancy. ^{a,b} Genotype effect (P=0.0032). Bars without a common superscript are different.

17 of pregnancy. The ULF content of PGF2α increased (P<0.0001) from Day 14 to 17 of pregnancy, but there was no effect of the conceptus genotype (Fig 3.12). Although the uterine content of PGF2α was not affected by conceptus genotype, there was a genotype x day interaction (P=0.0087) for total content of PGE_2 in ULF (Fig 3.13). The ULF PGE_2 content between recipient gilts carrying *CYP19A1*$^{+/+}$ or *CYP19A1*$^{-/-}$ was not different on day 14 but the day 17 ULF PGE_2 content was 50% less in recipients containing *CYP19A1*$^{-/-}$ conceptuses. Content of 13, 14-dihydro-15-keto-PGE2 in ULF was similar in recipient gilts containing *CYP19A1*$^{+/+}$ or *CYP19A1*$^{-/-}$ conceptuses. However, there was a significant day effect (P<0.05) as the content of 13, 14-dihydro-15-keto-PGE2 in ULF on day 14 was below the sensitivity of the assay (Fig 3.14). During pregnancy, there is a pregnancy specific estrogen stimulated increase release of IL18 from the endometrium after day 15 (Ashworth et al., 2010). Although content of IL18 in ULF of recipient gilts increased from day 14 to 17 (Day; P<0.05), conceptus genotype did not affect IL18 ULF content (Fig 3.15).

Conceptus Gene Expression Analysis. Relative gene expression (ΔCT) of conceptus genes are listed in Table 3.2. Gene editing of pig conceptus *CYP19A1* did not inhibit *CYP19A1* mRNA expression which was significantly decreased (P<0.0001) in *CYP19A1*$^{-/-}$ compared with *CYP19A1*$^{+/+}$ conceptuses (Fig 3.16 A). Expression of *CYP19A1* was ~5-fold less on day 14 and ~26-fold less on day 17 in *CYP19A1*$^{-/-}$ relative to *CYP19A1*$^{+/+}$ conceptuses. Conceptus mRNA expression of steroidogenic acute regulatory protein (*STAR*) increased (Day; P<0.0001) ~14 -fold on day 17 compared to day 14 (Fig 3.16 B). *CYP19A1*$^{-/-}$ and *CYP19A1*$^{+/+}$

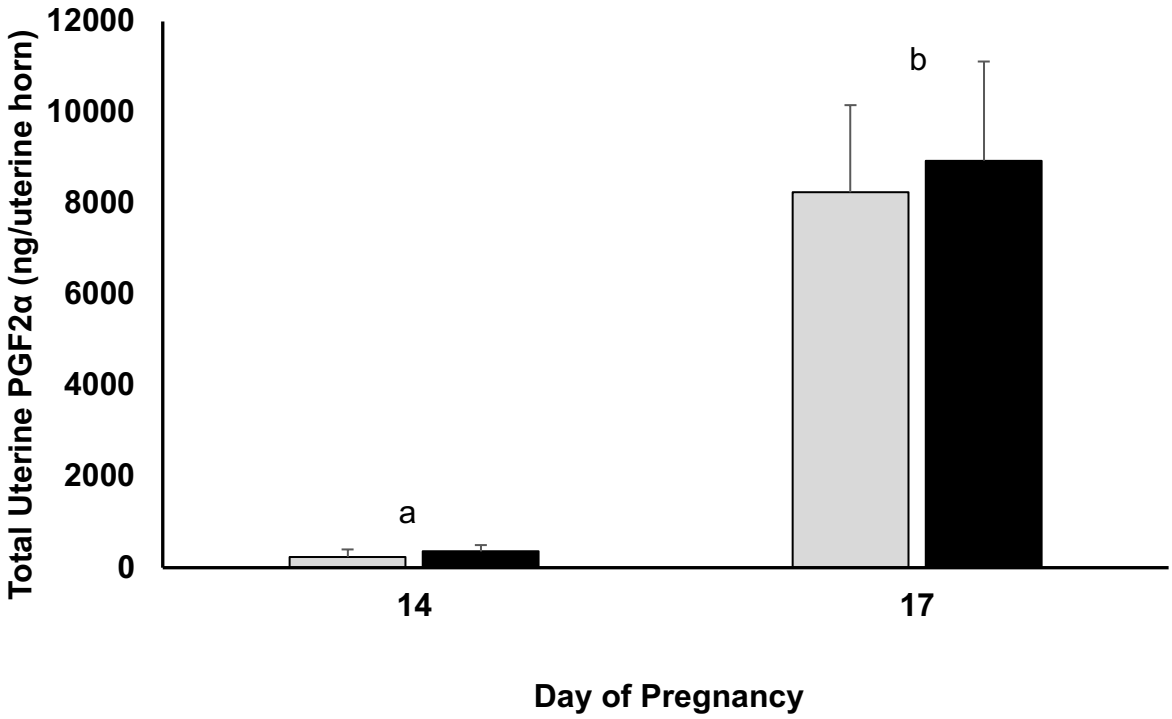

Figure 3.12: Total content PGF2α (ng/uterine horn) in uterine flushings collected from recipient gilts containing either *CYP19A1*$^{+/+}$ (Grey bar) or *CYP19A1*$^{-/-}$ (Black bar) conceptuses on days 14 or 17 of pregnancy. ^{a,b} Day effect ($P < 0.01$). Bars without a common superscript are different.

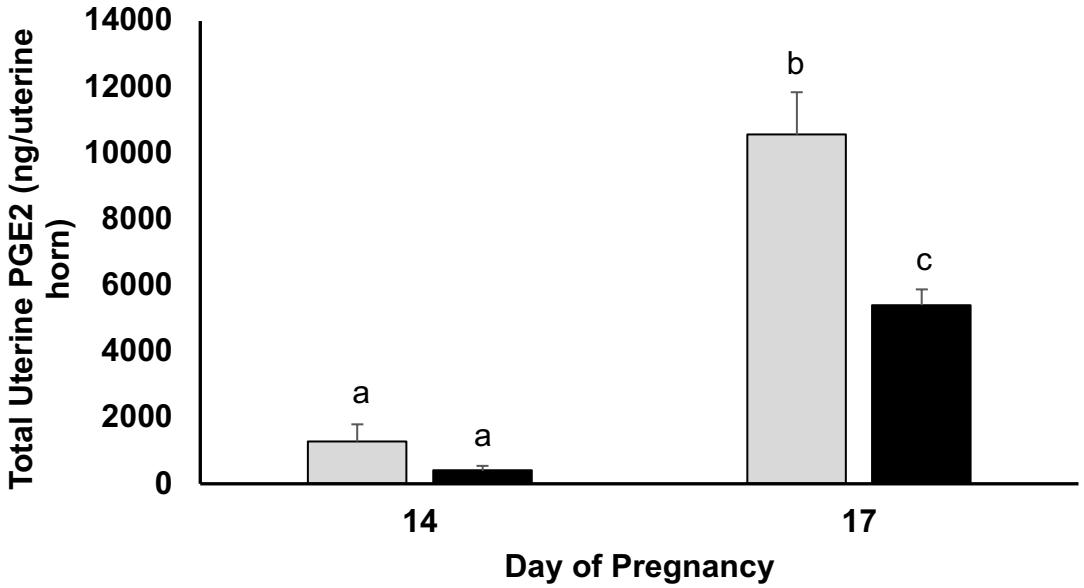

Figure 3.13: Total content PGE2 (ng/uterine horn) in uterine flushings collected from recipient gilts containing either *CYP19A1*$^{+/+}$ (Grey bar) or *CYP19A1*$^{-/-}$ (Black bar) conceptuses on days 14 or 17 of pregnancy. A genotype x day interaction (P=0.0087) was detected for total PGE2. Bars without a common superscript are different.

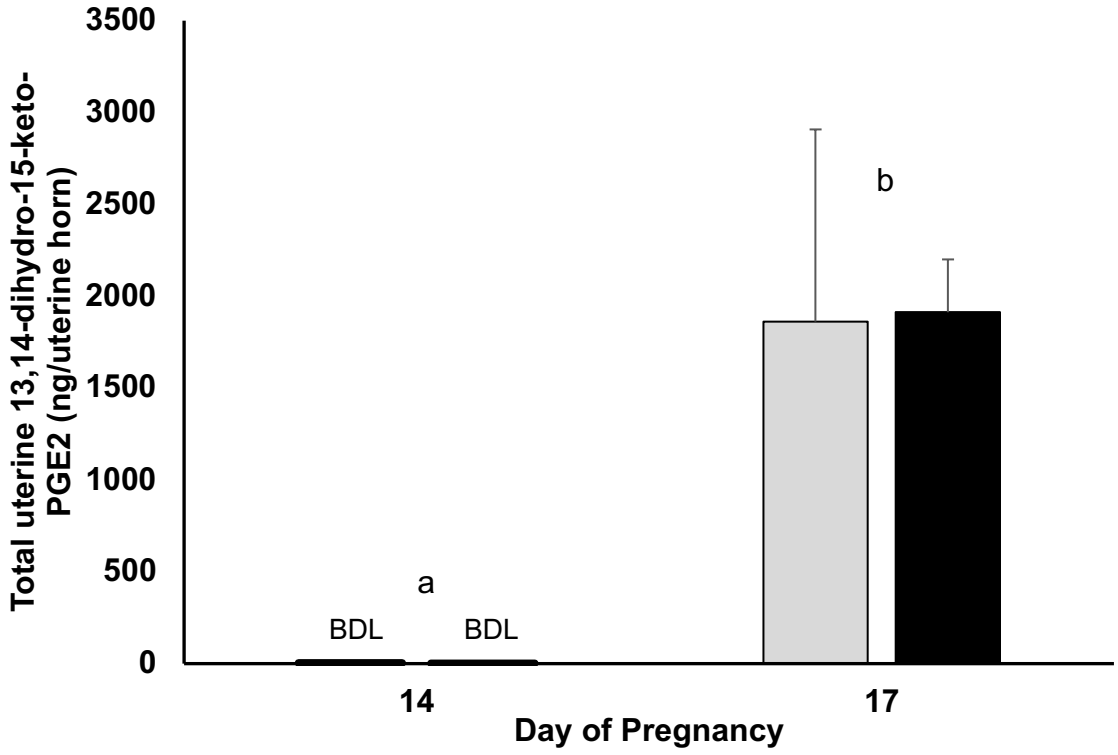

Figure 3.14: Total content 13,14-dihydro-15-keto-PGE2 (ng/uterine horn) in uterine flushings collected from recipient gilts containing either *CYP19A1*$^{+/+}$ (Grey bar) or *CYP19A1*$^{-/-}$ (Black bar) conceptuses on day 14 and 17 of pregnancy. Total uterine 13,14-dihydro-15-keto-PGE2 (ng/uterine horn) on day 14 was below detectable level (BDL). ^{a,b} Day effect ($P<0.05$). Bars without a common superscript are different.

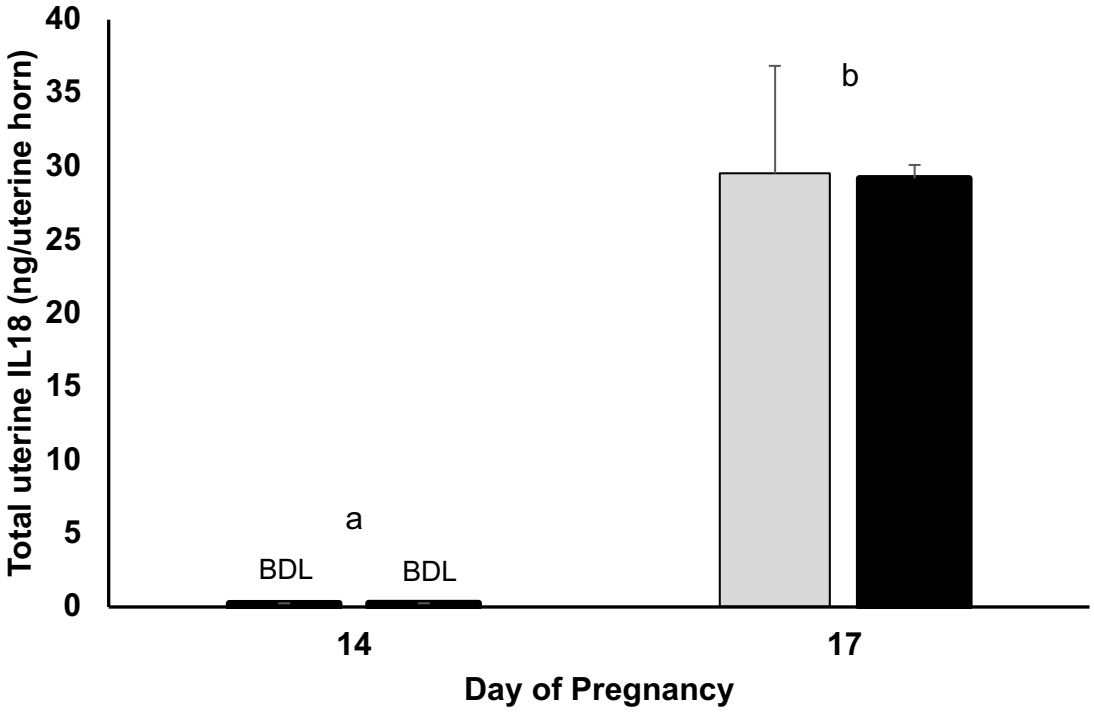

Figure 3.15: Total content IL18 (ng/uterine horn) in uterine flushings collected from recipient gilts containing either *CYP19A1*$^{+/+}$ (Grey bar) or *CYP19A1*$^{-/-}$ (Black bar) conceptuses on day 14 and 17 of pregnancy. Total uterine IL18 (ng/uterine horn) on day 14 was below detectable level (BDL). [a,b] Day effect (P<0.05). Bars without a common superscript are different.

Table 3.2: Conceptus Gene Expression RT-PCR.

Gene	Day 14 of Pregnancy		Day 17 of Pregnancy		Genotype	Day	Genotype x day
	CYP19A1$^{+/+}$	CYP19A1$^{-/-}$	CYP19A1$^{+/+}$	CYP19A1$^{-/-}$			
CYP19A1	4.07 ± 0.36	7.72 ± 0.72	3.44 ± 0.63	8.97 ± 0.56	P<0.0001	NS	NS
StAR	7.79 ± 0.28	7.62 ± 0.62	3.68 ± 0.44	5.12 ± 0.4	NS	P<0.0001	NS
IL1B2	2.76 ± 0.51	1.94 ± 0.8	10.53 ± 0.35	9.97 ± 0.5	NS	P<0.0001	NS
BMP4	8.85 ± 0.51	7.58 ± 0.59	3.79 ± 0.54	5.07 ± 0.89	NS	P<0.0001	NS
PTGS2	8.36 ± 0.43	8.53 ± 0.79	6.5 ± 0.32	6.76 ± 0.33	NS	P=0.0025	NS
PGES	6.79 ± 0.26	5.37 ± 0.59	5.55 ± 0.22	6.6 ± 0.34	NS	NS	P=0.005
IFNG	-7.48 ± 0.23	-6.93 ± 0.14	-5.96 ± 0.24	-5.02 ± 0.3	P=0.002	P<0.0001	NS
IFND	2.69 ± 0.35	4.82 ± 0.6	3.39 ± 0.33	3.66 ± 0.49	P=0.0166	NS	NS

The ΔCT was estimated as the difference between the cycle threshold (CT) for the gene of interest and the CT for the reference gene as previously described in material and methods.

conceptuses did not have a difference in *IL1B2* mRNA expression. However, expression of *IL1B2* from day 14 to 17 was significantly decreased (Day; P<0.0001) ~220-fold (Fig 3.16 C). Expression of bone morphogenetic protein 4 (*BMP4*) was upregulated (Day: P<0.0001) ~22-fold from day 14 relative to day 17 (Fig 3.16 D). The mRNA expression of prostaglandin-endoperoxide synthase 2 (*PTGS2*) increased (Day; P=0.0025) ~3-fold in both *CYP19A1*$^{+/+}$ and *CYP19A1*$^{-/-}$ conceptuses on day 17 relative to day 14 of pregnancy (Fig 3.17 A). A genotype x day interaction (P=0.005) was detected in mRNA expression of prostaglandin E synthase (*PGES*) (Fig 3.17 B). *CYP19A1*$^{-/-}$ expression of *PGES* was up-regulated ~5-fold on day 14 but downregulated on day 17. The mRNA expression of interferon gamma (*IFNG*) was decreased (genotype; P=0.0025) ~1-fold on day 14 and ~5-fold on day 17 of *CYP19A1*$^{-/-}$ conceptuses relative to *CYP19A1*$^{+/+}$ conceptuses (Fig 3.17 C). On day 17, *CYP19A1*$^{+/+}$ had a ~3-fold decrease (day; P<0.0001) in *IFNG* expression relative to day 14 of pregnancy. Expression of interferon delta (*IFND*) decreased (genotype; P=0.0166) ~2 fold on day 14 in *CYP19A1*$^{-/-}$ conceptuses relative to day 14 *CYP19A1*$^{+/+}$ conceptuses, day 17 was not different (Fig 3.17 D).

Pregnancy Loss of Recipient Gilts Containing *CYP19A1*$^{-/-}$. Since results indicated that pregnancy was maintained in recipient gilts with *CYP19A1*$^{-/-}$ conceptuses at day 17 recipient gilts containing *CYP19A1*$^{-/-}$ conceptuses were allowed to continue pregnancy. All of the recipient gilts (n=4) maintained pregnancy beyond 25 days. However, two recipient gilts returned to estrus on day 27, while ultrasonography showed two gilts contained embryos and

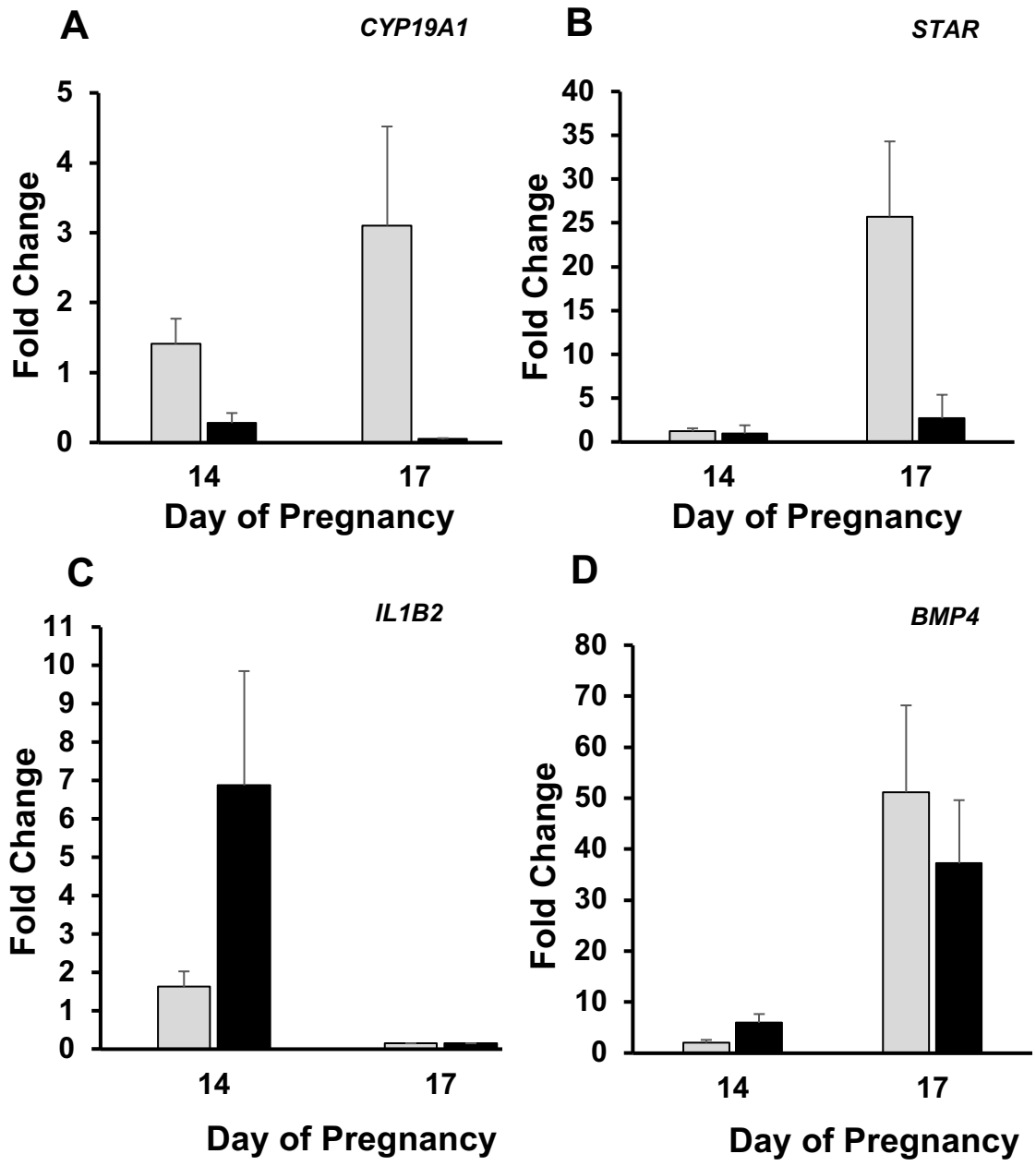

Figure 3.16: Fold Change of Conceptus Gene Expression of *CYP19A1*, *STAR*, *IL1B2*, and *BMP4*. *CYP19A1*$^{+/+}$ (grey bar) and *CYP19A1*$^{-/-}$ (black bar) fold change in gene expression is relative to the average ΔCT of day 14 *CYP19A1*$^{+/+}$. Fold change of **A)** *CYP19A1 (genotype P<0.0001),* **B)** *STAR (day P<0.0001),* **C)** *IL1B2 (day P<0.0001)*, **D)** *BMP4 (day P<0.0001)*.

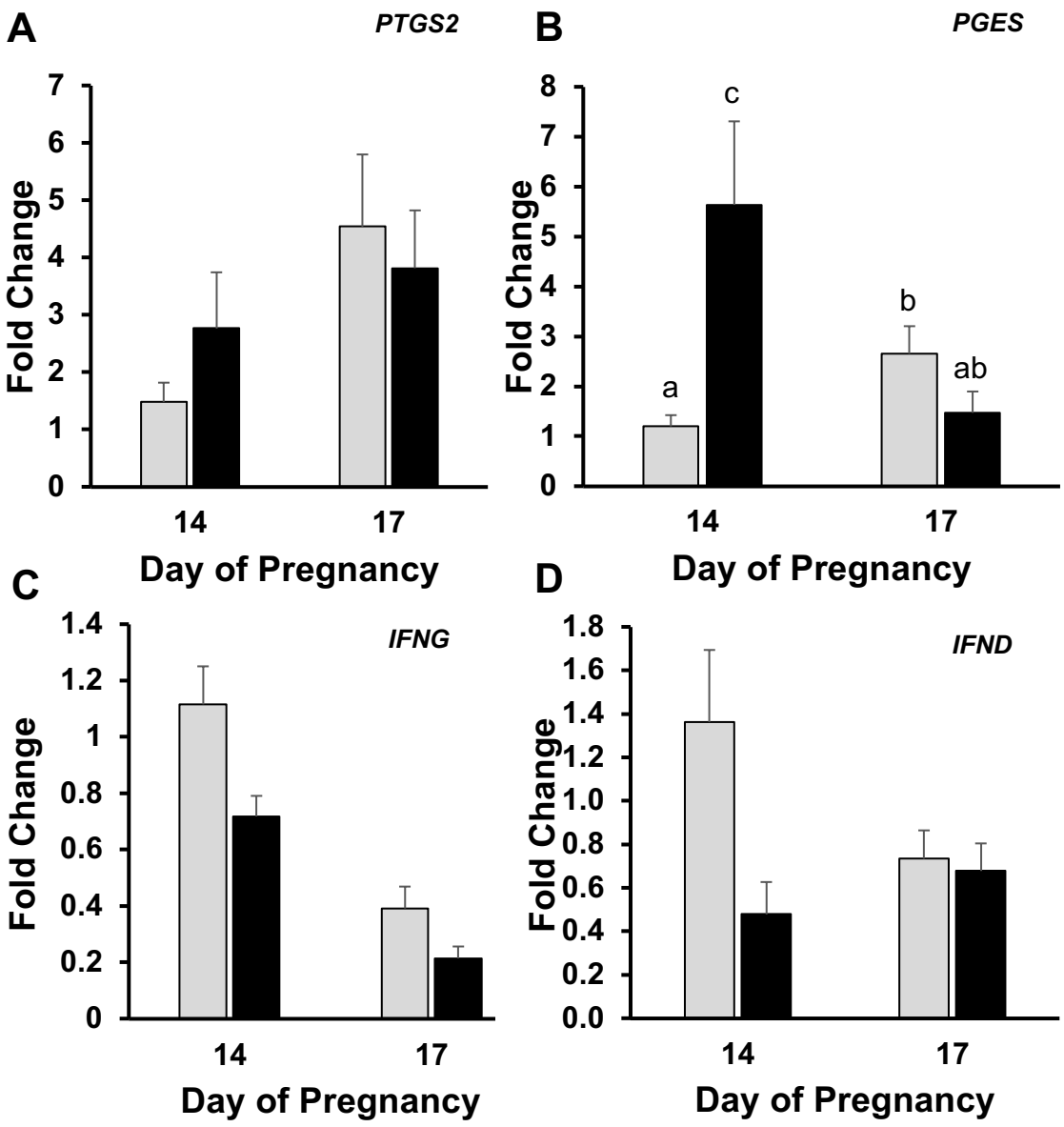

Figure 3.17: Fold Change of Conceptus Gene Expression of *PTGS2, PGES*, *IFNG*, and *IFND.* *CYP19A1*$^{+/+}$ (grey bar) and CYP19A1$^{-/-}$ (black bar) fold change in gene expression is relative to the average ΔCT of day 14 *CYP19A1*$^{+/+}$. Fold change of **A)** *PTGS2* (day; P=0.0025), **B)** *PGES* (day x genotype effect; p=0.005), **C)** *IFNG (genotype P=0.0022; day P<0.0001)*, **D)** *IFND (genotype P=0.016)*.

maintained pregnancy up to day 30 (Table 3.4). However, these gilts both aborted on day 31 of pregnancy. Aborted fetuses were collected and *CYP19A1*$^{-/-}$ genotype. All four gilts were euthanized to observe the ovaries which contained regressed CL (Fig 3.18). Plasma progesterone decreased to less than 1 ng/mL by 2 to 3 days prior to returning gilts returning to estrus or aborting.

Analysis of Endometrial Differential Gene Expression. Endometrial samples from recipient gilts carrying *CYP19A1*$^{-/-}$ conceptuses had 472 differentially expressed genes (Table S5, S6) while recipient gilts carrying *CYP19A1*$^{+/+}$ conceptuses had 416 differentially expressed genes (Table S3, S4) from day 14 to 17 of pregnancy. Of those differentially expressed genes, 321 were expressed by both groups (Fig 3.19). On day 14, 102 endometrial genes were differentially expressed between recipients that carried *CYP19A1*$^{-/-}$ or *CYP19A1*$^{+/+}$ conceptuses (Table S1, S2). However, only 20 differentially expressed genes were detected on day 17 (Table S7, S8) (Table 3.3). Network analysis of NFKB and TNF signaling pathways demonstrated a shift in endometrial gene expression with the presence of *CYP19A1*$^{-/-}$ conceptuses which would alter upstream signaling within the pathways. Alternation of these two key proinflammatory pathways suggest that loss of conceptus estrogen production could lead to down-stream negative responses to the establishment of pregnancy. On day 14, upregulated genes in *CYP19A1*$^{-/-}$ included a number of pro-inflammatory factors such as tumor necrosis factor-inducible protein 6 precursor (*TNFAIP6*), early activation antigen CD69 gamma-glutamyltranspeptidase 1 (*CD69*), ectodysplasin A receptor (*EDAR*),

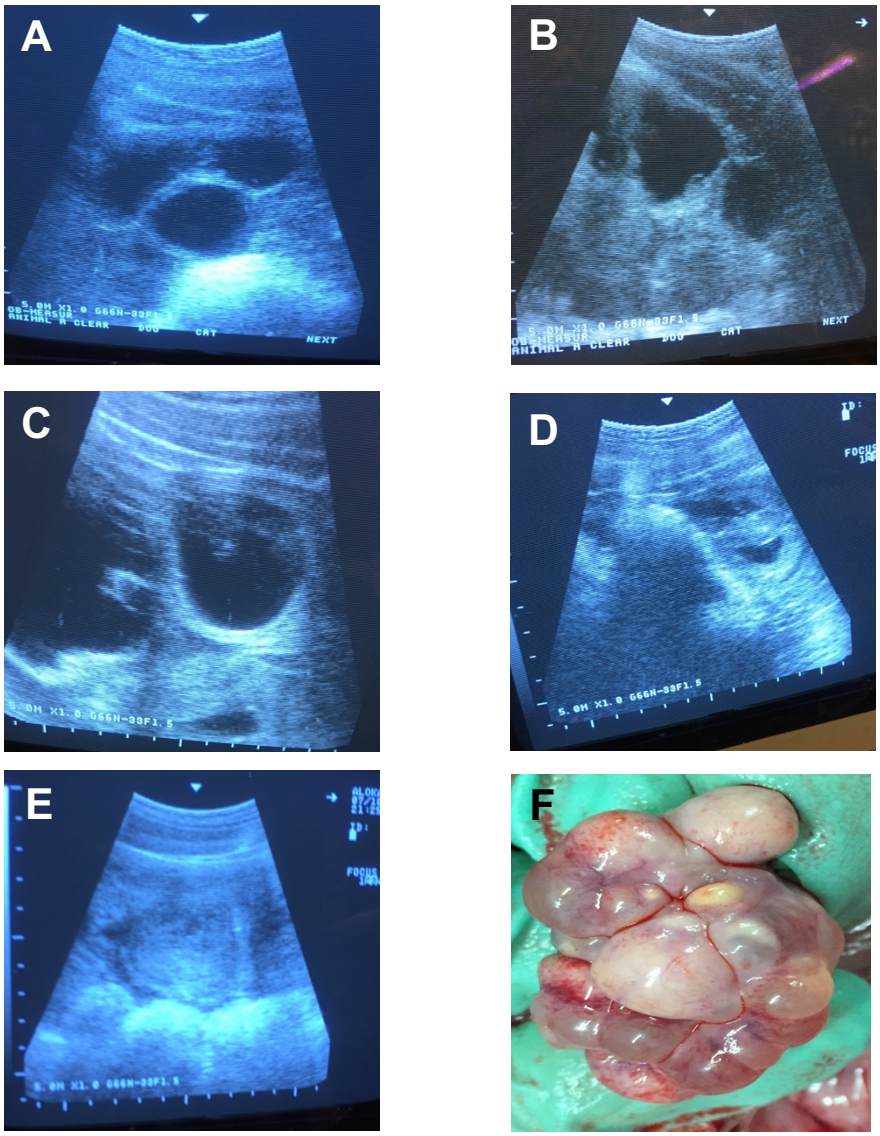

Figure 3.18: Recipient Gilts Containing *CYP19A1*$^{-/-}$ Conceptuses. Ultrasound of recipient gilts containing *CYP19A1*$^{-/-}$ embryos, on day 26 of pregnancy (A,B). Recipient gilts (A,B) ultrasound on day 30 (C) and 31 (D,E) of pregnancy. Both recipient gilts aborted and had regressed CL on their ovaries (F).

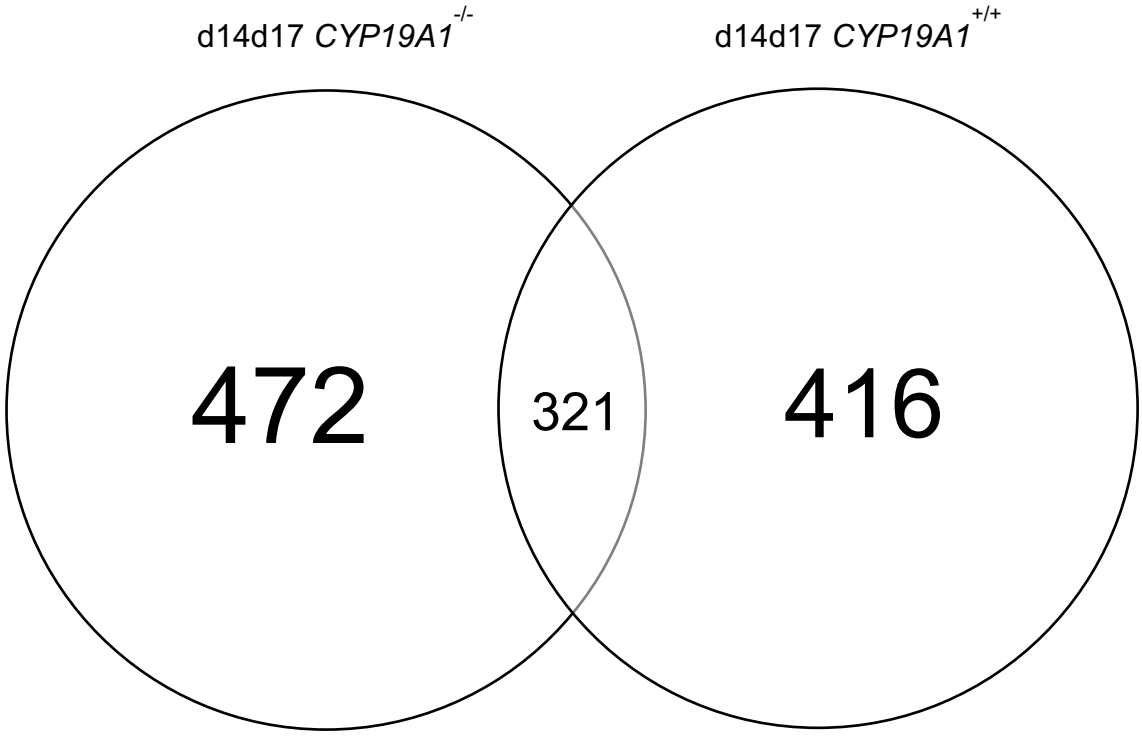

Figure 3.19. Venn Diagram of Endometrial Differentially Expressed Genes. Endometrial samples from recipient gilts carrying *CYP19A1*$^{-/-}$ conceptuses had 472 differentially expressed genes from day 14 to 17 of pregnancy. Recipient gilts carrying *CYP19A1*$^{+/+}$ conceptuses had 416 differentially expressed genes from day 14 to 17 of pregnancy. Of those differentially expressed genes, 321 are the same between both groups.

Table 3.3: Endometrial Differentially Expressed Genes.

Comparison		Number of DEG
Day 14	*CYP19A1*$^{+/+}$ vs *CYP19A1* $^{-/-}$	102
Day 17	*CYP19A1*$^{+/+}$ vs *CYP19A1* $^{-/-}$	20
***CYP19A1*$^{+/+}$**	day 14 vs day 17	416
***CYP19A1*$^{-/-}$**	day 14 vs day 17	472

The number of differentially expressed genes (DEG) in each experimental group.

See supplemental tables S1-S8 for list of DEG.

interleukin17 receptor D (*IL17RD*); solute carriers genes *SLC19A2, SLC6A15, SLC2A8*, and *SLC5A1*; and calcium transport genes *S100A8, S100A2*, and *KCNN4*.

Experiment 2.

Estradiol-Benzoate Injections. In an attempt to rescue the CL and maintain plasma progesterone concentrations, recipient gilts containing *CYP19A1*$^{-/-}$ conceptuses were given estrogen replacement therapy. Treatment of recipients with estradiol-benzoate on days 14, 17, 18, and 19 or 15, 18, 19, and 20 mimics the normal two-phase pattern of conceptus estrogen production during the establishment of pregnancy in the pig. One recipient gilt in which estrogen treated was initiated on day 15, apparently did not have conceptuses on day 14 and was already in the process of regressing the CL as plasma progesterone had declined by day 17 and the gilt return to estrus on day 20. Although estradiol-benzoate administration effectively maintained CL production of progesterone in the other three recipient gilts, no embryos were detectable via ultrasound on days 26-27. Therefore, none of the *CYP19A1*$^{-/-}$ embryos were able to survive beyond day 27 to 30 (Table 3.4) despite the maintenance of CL and continue progesterone support following estradiol-benzoate treatment.

Co-Embryo Transfer of *CYP19A1*$^{-/-}$ and *CYP19A1*$^{+/+}$ Blastocysts. In an attempt to rescue *CYP19A1*$^{-/-}$ embryo development, *CYP19A1*$^{-/-}$ and *CYP19A1*$^{+/+}$ blastocysts were co-transferred into recipient gilts. CYP19A1$^{+/+}$ blastocyst were derived from one of three fibroblast cell lines: cell line A, B, and C. None of the recipient gilts maintained pregnancy beyond day 28 of gestation (Table 3.4).

However, *CYP19A1*$^{+/+}$ SCNT blastocysts were able to maintain pregnancy to term (n=2).

Co-Embryo Transfer of *CYP19A1*$^{-/-}$ Clones and *In Vitro* Fertilized (IVF) *CYP19A1*$^{+/+}$ Embryos. Three recipient gilts were co-transferred with IVF *CYP19A1*$^{+/+}$ and *CYP19A1*$^{-/-}$ cloned blastocysts. In one recipient the plasma progesterone was <1 ng/ml on day 30 and the gilt displayed standing heat on day 27. The remaining two recipient gilts maintained pregnancy beyond day 30 (Table 3.4). Both gilts were euthanized on day 34 of pregnancy and their reproductive tracts removed for embryo collection and genotyping. One recipient gilt contained 4 embryos, one of which was degenerating (Fig 3.20 A). Genotyping indicated that all four were IVF *CYP19A1*$^{+/+}$ embryos (Fig 3.20 B). The second pregnant recipient contained six viable embryos and multiple degenerate embryos (n=13) with small placental membranes (Fig 3.21 A). All of the small degenerate embryos and placentas were *CYP19A1*$^{-/-}$. Of the six viable embryos, 4 were IVF *CYP19A1*$^{+/+}$ (2 in each horn) and two were *CYP19A1*$^{-/-}$ SCNT clones (Fig 3.21 B, C).

Table 3.4: Failed Pregnancy with *CYP19A1*$^{-/-}$ Conceptuses and Rescue Attempt by Estradiol-Benzoate Injections and Co-Embryo Transfers.

Embryo Transfer	Day aborted/displayed estrus
CYP19A1$^{-/-}$	31
CYP19A1$^{-/-}$	30
CYP19A1$^{-/-}$	27
CYP19A1$^{-/-}$	27

Embryo Transfer	Day aborted/displayed estrus
CYP19A1$^{-/-}$ & cell line A *CYP19A1*$^{+/+}$	24
CYP19A1$^{-/-}$ & cell line A *CYP19A1*$^{+/+}$	22
CYP19A1$^{-/-}$ & cell line B *CYP19A1*$^{+/+}$	25
CYP19A1$^{-/-}$ & cell line B *CYP19A1*$^{+/+}$	27
CYP19A1$^{-/-}$ & cell line C *CYP19A1*$^{+/+}$	27
CYP19A1$^{-/-}$ & cell line C *CYP19A1*$^{+/+}$	25
CYP19A1$^{-/-}$ & cell line C *CYP19A1*$^{+/+}$	22
CYP19A1$^{-/-}$ & cell line C *CYP19A1*$^{+/+}$	24

Embryo Transfer	Day aborted/displayed estrus
CYP19A1$^{-/-}$treated gilts with estradiol-benzoate	26
CYP19A1$^{-/-}$treated gilts with estradiol-benzoate	28
CYP19A1$^{-/-}$treated gilts with estradiol-benzoate	27
CYP19A1$^{-/-}$treated gilts with estradiol-benzoate	20

Embryo Transfer	Day aborted/displayed estrus
IVF *CYP19A1*$^{+/+}$	20
CYP19A1$^{-/-}$ & IVF *CYP19A1*$^{+/+}$	27
CYP19A1$^{-/-}$ & IVF *CYP19A1*$^{+/+}$	N/A
CYP19A1$^{-/-}$ & IVF *CYP19A1*$^{+/+}$	N/A

Figure 3.20: Day 34 placenta's (A) and genotyping (B) of Recipient Gilt that was Co-Transferred with *CYP19A1*$^{+/+}$ IVF and *CYP19A1*$^{-/-}$ Clone Embryos. Co-transferred with *CYP19A1*$^{+/+}$ IVF and *CYP19A1*$^{-/-}$ clone embryos. The four embryos were genotyped and determined to be IVF *CYP19A1*$^{+/+}$.

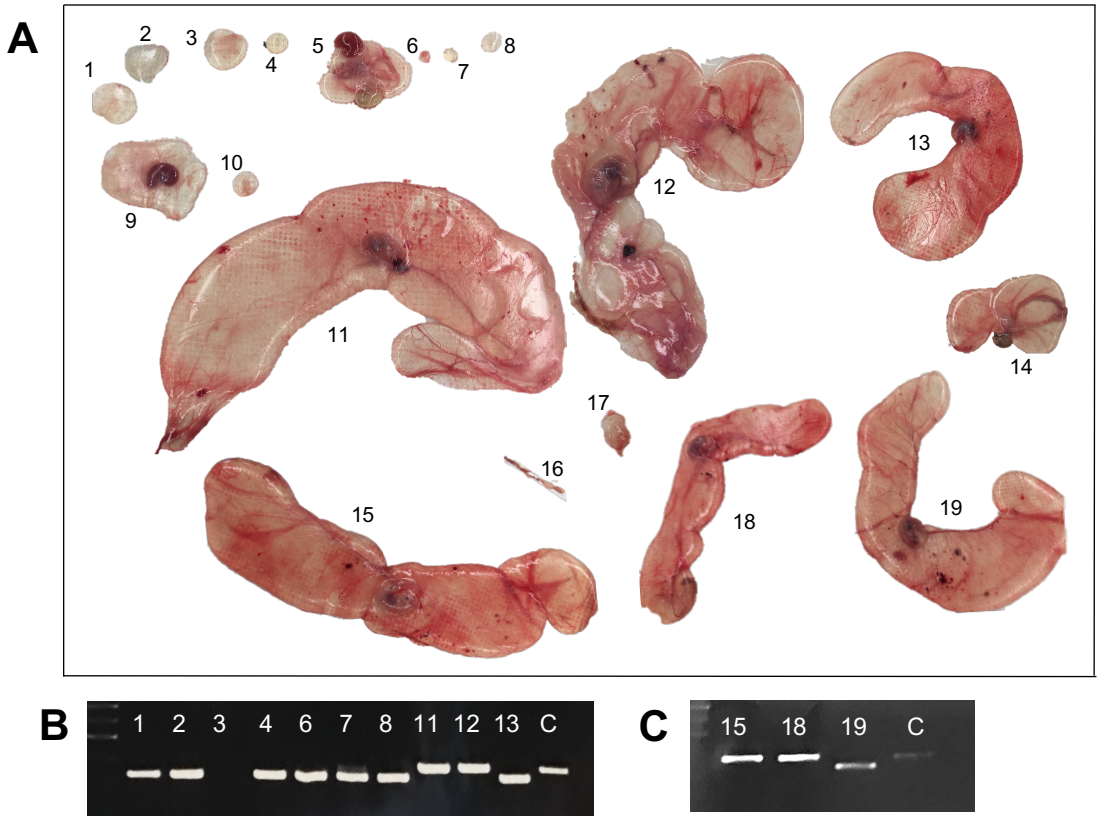

Figure 3.21: Day 34 placentas (A) and genotyping (B, C) of Recipient Gilt that was Co-Transferred with *CYP19A1*$^{+/+}$ IVF and *CYP19A1*$^{-/-}$ Clone Embryos. Recipient gilt contained a mixture of small circle degenerate conceptuses and viable embryo with vascularized placentas, a combination of *CYP19A1*$^{+/+}$ IVF embryos and *CYP19A1*$^{-/-}$ cloned embryos. Degenerate conceptuses 1-9 were crowded in the tip of the same uterine horn. Embryos were genotyped and of the six viable embryos, two were *CYP19A1*$^{-/-}$ clones (embryos 13 and 19) and four were *CYP19A1*$^{+/+}$ IVF (embryos 11, 12, 15, 18). The remainder of the small circular placenta containing degenerating embryos and placental membranes were *CYP19A1*$^{-/-}$.

3.4 DISCUSSION

Porcine conceptus production of IL1B2 initiates a drastic cellular remodeling process to rapidly transform from a tubular to a thin filamentous morphology on day 12 of pregnancy (Whyte et al., 2018). Conceptus elongation is essential, not only to block CL regression for maintenance of progesterone secretion throughout pregnancy, but to acquire adequate uterine space for placental attachment and expansion in the pig. During the period of rapid elongation, conceptuses increase estrogen production, which has long been the proposed signal for maternal recognition of pregnancy in the pig (Geisert et al., 2017). Conceptus estrogen production prevents luteolysis by altering movement of endometrial PGF2α secretion to be sequestered in the uterine lumen rather than being release into the uterine vasculature (Bazer and Thatcher, 1977). Porcine conceptus estrogen production first increases at the time of rapid elongation on day 12 which is followed by a second sustained increase during the initiation of attachment and placental development from days 15 to 25 of pregnancy (Geisert et al., 2015). Geisert et al. (1987) demonstrated that both waves of conceptus estrogen production are necessary for prolonging CL function beyond 30 days in the pig. Attempts to clearly establish the role(s) of conceptus estrogen production during early pregnancy through the use of estrogen receptor and aromatase inhibitors were ineffective *in vivo* (O'Neill et al., 1991) and failed to inhibit conceptus estrogen synthesis or action on the uterine endometrium.

The present study utilized CRISPR/Cas9 genomic editing system to successfully disrupt conceptus aromatase (*CYP19A1*) activity and the ability to synthesize estrogen during maternal recognition, attachment and placentation in the pig. Total content of estradiol-17β in ULF from recipients containing *CYP19A1*$^{-/-}$ conceptuses was significantly reduced to concentrations consistent with ULF of cyclic or nonpregnant gilts on both day 14 and 17 of pregnancy. Total steroidogenesis was not compromised in the *CYP19A1*$^{-/-}$ conceptuses as expression of *STAR* was not different between genotypes and the ULF content of testosterone was not different from recipients with *CYP19A1*$^{+/+}$ conceptuses. The relative gene expression of conceptus *CYP19A1* and lack of estrogen production from *CYP19A1*$^{-/-}$ conceptuses indicates that *CYP19A1* expression was not inhibited but created a functional knockout of *CYP19A1* enzyme activity as would be predicted from the gene edited sequence of *CYP19A1*$^{-/-}$ conceptuses. *CYP19A1*$^{-/-}$ embryos were capable of developing to blastocysts and hatching *in vitro* indicating that estrogen is not essential for the early stages of embryo development. Pope et al. (1982) suggested that estrogen could play a role in final stages of blastocyst migration throughout the uterine horns to acquire equidistant spacing between blastocysts for elongating and attaching to surface epithelium along the mesometrial side of the endometrium. Dissection of *CYP19A1*$^{+/+}$ and *CYP19A1*$^{-/-}$ conceptuses from the uterine horns on day 14 and 17 indicated that inhibition of estrogen synthesis in *CYP19A1*$^{-/-}$ conceptuses did not interfere with uterine migration, rapid elongation, uterine attachment, or placentation. Interestingly, large entangled clumps of conceptuses were observed in some

flushings of day 14 *CYP19A1*$^{-/-}$ conceptuses. When the alternate uterine horn was floated to examine conceptus migration and collect individual conceptuses, the same entangled clumps were observed to be outside the mesometrial border of the uterine horn, indicating the entangled clumps were not the result of entangling filamentous conceptuses through flushing the uterine horn. The clumps of entangled conceptuses were not detected in *CYP19A1*$^{+/+}$ conceptus collections. These cause of entangled conceptuses and abnormal location within the uterus is not known. It is possible that the lack of estrogen production by *CYP19A1*$^{-/-}$ conceptuses may cause some problems with uterine spacing and surface area for elongation when there are an excessively high number of embryos present.

Although conceptus estrogen synthesis was not essential for rapid elongation of the porcine conceptus, IL1B2, a proinflammatory cytokine, has been demonstrated to be essential for inducing the rapid cellular remodeling of the conceptus for elongation (Whyte et al., 2018). The gene editing of *CYP19A1* did not significantly affect the mRNA expression of *IL1B2* of *CYP19A1*$^{-/-}$ conceptuses. However, uterine content of IL1B2 was significantly decreased in recipients with *CYP19A1*$^{-/-}$ on day 14, thus estrogen could be a possible mediator of IL1B2 synthesis and activity. Production of IL1B2 may be a regulatory factor for aromatase expression and activity, or vice versa, during conceptus rapid elongation. In women, IL1B stimulates aromatase activity in human cytotrophoblasts, as well as increases transcription of aromatase in many different cell types (Nestler, 1993). Whyte et al. (2018) indicated that there was a

significant decrease in total estradiol-17β content in the ULF of recipients carrying *IL1B2*$^{-/-}$ compared to *IL1B2*$^{+/+}$ conceptuses. Conceptus IL1B2 secretion activates uterine NFKB which can stimulate many genes and factors need for implantation in the pig (Ross et al., 2009; Mathew et al., 2015). The spatiotemporal release of conceptus IL1B2 and estrogen during elongation would allow estrogen to tightly modulate the IL1B2-induced NFKB uterine inflammatory response(s). Thus, the coupling and interaction of conceptus estrogen synthesis and release with expression of *IL1B2* during conceptus elongation and conceptus attachment implantation could play an important role for the establishment and maintenance of pregnancy in the pig beyond prevent luteolysis (Geisert et al., 2017).

It was hypothesized that the inability of *CYP19A1*$^{-/-}$ conceptuses to produce estrogen and signal maternal recognition of pregnancy, would result in luteolysis on day 15 of pregnancy, similar to non-pregnant females. Unexpectedly, the ovaries from recipient gilts carrying *CYP19A1*$^{-/-}$ conceptuses maintained the CL and progesterone secretion beyond day 24 of pregnancy. The present study indicates that conceptus estrogen production is not necessary for the initial maintenance of the CL up to day 22 to 24 of pregnancy, indicating an additional factor functions to protect the CL from luteolysis.

The endocrine/exocrine hypothesis has been proposed as mechanism for maternal recognition and maintenance of the CL in the pig (Bazer and Thatcher, 1977). This theory was based on the decreased uterine secretion of PGF2α into the uterine vasculature and presence of high concentrations of PGs in the uterine

lumen of pregnant compared to cyclic pigs (Moeljono et al., 1977). In addition, administration of estradiol-valerate on days 11 through 15 of the estrous cycle of gilts resulted in a decrease in plasma PGF2α metabolite, 13,14-dihydro-15-keto prostaglandin F2α and a drastic increase of PGF2α in the uterine lumen comparable to what occurs in pregnant gilts (Frank et al., 1978). Also, Gross et al. (1990) demonstrated that estrogen, in combination with prolactin, acted to reorient the secretion of endometrial PGF2α from an endocrine to exocrine direction *in vitro*. Thus, estrogen has been implicated as the major conceptus factor responsible for inducing the sequestering of PGF2α in the uterine lumen and preventing luteolysis during pregnancy in the pig. However, the results of the current study clearly indicate that luteolysis can be inhibited in the absence of conceptus estrogen synthesis.

Previous research has indicated that PGE_2 plays a role in protecting the pig CL from luteolysis during the establishment of pregnancy. Intrauterine infusions of PGE_2 extend CL function beyond the length of the normal estrous cycle (Akinlosotu et al., 1986) and implanting CL of cyclic gilts with PGE_2 maintained function until day 19 (Ford and Christenson, 1991). The ability for PGE_2 to protect the CL from PGF2α is dose dependent as the higher PGE_2/PGF2α ratio protects luteal cells from luteolysis by PGF2α (Gregoraszczuk and Michas, 1999). The ULF content of PGE_2 in gilts with *CYP19A1*$^{+/+}$ conceptuses was greater than PGF2α, maintaining a PGE_2/PGF2α ratio which is consistent with previous literature (Geisert et al., 1982b; Waclawik et al., 2009a). However, the concentration of PGE_2 is significantly lower than PGF2α in the ULF

from recipient gilts with *CYP19A1*$^{-/-}$ conceptuses. Both pig endometrium and conceptuses express *PGES* and secrete PGE_2 which indicates conceptus and/or endometrial PGE_2 maintains CL function and pregnancy to at least day 25 to 28 (Waclawik et al., 2017). Interestedly, *CYP19A1*$^{-/-}$ conceptus recipients in the present study return to estrus or aborted by day 25 to 30 after luteolysis occurred which is similar to the lengthening CL functionality with PGE_2. There was no significant difference in conceptus *PGES* expression on day 17 in the present study, indicating the decreased in PGE concentration on day 17 in the ULF with *CYP19A1*$^{-/-}$ conceptuses is a result of a decrease in endometrial PGE_2 synthesis. Estradiol-17β stimulates endometrial synthesis of PGE_2 by increasing PTGS2 and the expression of *PGES* mRNA and protein (Waclawik et al., 2009b). Therefore, the lower uterine content of PGE2 in recipients with *CYP19A1*$^{-/-}$ conceptuses would be consistent with the lack of conceptus estrogen stimulation to increase endometrial *PGES* expression and protein for PGE_2 synthesis. It is possible that the decline in PGE2 also contributes to the later luteolysis which occurred in *CYP19A1*$^{-/-}$ recipients allowed to continue pregnancy.

To determine if pregnancy of recipients with *CYP19A1*$^{-/-}$ conceptuses could be maintained with exogenous estrogen therapy, estradiol-benzoate injections were given to mimic to period of conceptus estrogen production. The estradiol-benzoate injections successfully maintained functional CL beyond the length of the estrous cycle, as previously reported (Geisert et al., 1987), but *CYP19A1*$^{-/-}$ embryos still did not survive beyond 28 days. Wilson and Ford (2000) demonstrated that injections of estradiol-17β at the time of elongation of the pig

conceptus stimulated a significant increases in placental growth and placenta efficiency of embryos. Thus, administration of exogenous estradiol to rescue the *CYP19A1*$^{-/-}$ conceptuses should not have been detrimental to the conceptuses and their survival but beneficial for the development and growth. To provide a continuous intrauterine source of estrogen, the *CYP19A1*$^{-/-}$ blastocysts were co-transferred with SCNT *CYP19A1*$^{+/+}$ blastocysts derived from fibroblast cells lines known to result in pregnancies to term. However, these co-transfers were not efficient at maintaining pregnancy beyond day 25. These results indicate the possibility that *CYP19A1*$^{-/-}$ conceptuses' lack of estrogen production contribute to invoking an inflammatory uterine response that causes loss of pregnancy even with competent SCNT *CYP19A1*$^{+/+}$ embryos.

Interleukin 18, also referred to as interferon-γ inducing factor, is a member of the IL-1 family of pro-inflammatory cytokines believed to play a significant role in implantation. Endometrial IL18 secretion has been implicated as a critical cytokine controlling the innate immune system through modulating uterine NK cell cytokine production and cytolytic activity during pregnancy (Laskarin et al., 2005). There is a pregnancy specific release of IL18 from the pig endometrium between days 15 and 18 of pregnancy which has been proposed to be stimulated by conceptus estrogen release (Ashworth et al., 2010). Thus, the abortion of *CYP19A1*$^{-/-}$ embryos might occur through a failure or alteration in endometrial IL18 secretion in the absence of placental estrogen production. However, the content of IL18 in ULF increased on day 17 in recipient gilts containing either *CYP19A1*$^{+/+}$ and *CYP19A1*$^{-/-}$ indicating that conceptuses estrogen secretion is

not essential for endometrial IL18 secretion and therefore, appear to not be a factor leading to pregnancy loss during day 24 to 30 of pregnancy. Endometrial gene expression data was evaluated to explore the signaling events that are occurring during maternal recognition and the establishment of pregnancy to determine the possible cause of pregnancy failure of the *CYP19A1*$^{-/-}$ conceptuses when co-transferred. Interestingly, endometrial osteopontin (*SPP1*) expression which has been shown to be stimulated by estrogen (White et al., 2005), was not affected by conceptus genotype. Many proposed endometrial estrogen stimulated genes that were not altered in recipients with *CYP19A1*$^{-/-}$ conceptuses suggesting that other conceptus secretory factors can stimulate these genes in the absence of conceptus estrogen. The vast majority of the altered endometrial gene expression occurred on day 14 when conceptus production of IL1B2 would initiate conceptus elongation and stimulate the NFKB pathway in the absence of estrogen. A large number of differentially expressed genes are involved in proinflammatory pathways, such as tumor necrosis factor-inducible protein 6 precursor (*TNFAIP6*), early activation antigen CD69 gamma-glutamyltranspeptidase 1 (*CD69*), ectodysplasin A receptor (*EDAR*), interleukin 17 receptor D (*IL17RD*), which are upregulated in the endometrium of *CYP19A1*$^{-/-}$ conceptus recipient gilts. Changes in gene expression of the estrogen receptor pathway result changes of cross talk between genes in the NFKB network, resulting in a shift in NFKB gene signaling. In addition to pro-inflammatory gene expression changes,

a number of differentially expressed genes were solute carriers involved with ion transport and cell vesicle transport.

Endometrial gene expression analysis indicated there was an upregulation of endometrial genes associated with the movement of calcium, such as calcium binding proteins, *S100A8* and *S100A2*, and intermediate conductance calcium activated potassium channel protein 4 (*KCNN4*) in *CYP19A1*$^{-/-}$ conceptus recipients. There is a dramatic increase in the release of calcium into the uterine lumen during the period of rapid conceptus elongation (Geisert et al., 1982a) which is stimulated by estrogen (Geisert et al., 1982b). Gross et al. (1990) suggested that the reorientation of uterine prostaglandin to an exocrine movement during maternal recognition of pregnancy could possibly be aided by the increase in calcium cycling across the uterine epithelium. The upregulation of genes related to calcium movement in recipients with *CYP19A1*$^{-/-}$ suggests that the lack of conceptus estrogen production may alter cellular calcium flow which is involved with downstream effects on prostaglandin transport or synthesis. These results suggest that in the absence of conceptus estrogen production, regulation of pro-inflammatory pathways is altered and the *CYP19A1*$^{-/-}$ conceptuses may not be able to prevent an uterine immune response. Rescue of *CYP19A1*$^{-/-}$ conceptuses only occurred when IVF *CYP19A1*$^{+/+}$ embryos were co-transferred with *CYP19A1*$^{-/-}$ cloned embryos. Out of three embryo transfers into recipient gilts, one gilt was able to maintain and establish pregnancy with both *CYP19A1*$^{+/+}$ IVF conceptuses and *CYP19A1*$^{-/-}$ conceptuses. The ability of IVF derived control embryos to rescue the *CYP19A1*$^{-/-}$ embryos may be due to the

better capacity of IVF embryos to develop, compete, and survive. An accumulation of literature has demonstrated the role high levels of estrogen play a role in mediating immune responses during pregnancy (Trenti et al., 2018). The ability of estrogen to regulate and protect against inflammation and immune responses is also documented in specific cancers. Certain tumors utilize estrogen to inhibit and protect the malignant cells from immunological recognition and rejection by directly inhibiting NFKB activation (Zang et al., 2002). Certainly, the absence of placental estrogen production at the maternal uterine conceptus interface would be detrimental to regulating the proinflammatory response and localized release of cytokines from immune cells trafficking below the endometrial luminal epithelial surface. Development of SCNT conceptuses is delayed as much as 48 hours compared to in vivo pig embryos (Whyte et al., 2018). Therefore, the ability of IVF embryos to develop earlier and secrete high amounts of estrogen during the establishment of pregnancy and placentation could assist in protecting the *CYP19A1*$^{-/-}$ conceptuses which were attached next to them.

The present study establishes that porcine conceptus estrogen production is not essential for early development, conceptus elongation, maternal recognition of pregnancy, placentation and survival to day 24 of pregnancy. However, conceptus estrogen production is clearly necessary for CL maintenance beyond 24 days of pregnancy and continued embryonic survival to term. The *CYP19A1*$^{-/-}$ conceptuses provide an excellent animal model to determine the role of placental estrogen production in directly regulating the

endometrial proinflammatory and immune response to establish and maintain pregnancy.

BIBLIOGRAPHY

Akinlosotu, B. A., J. R. Diehl, and T. Gimenez. 1986. Sparing effects of intrauterine treatment with prostaglandin E2 on luteal function in cycling gilts. Prostaglandins 32(2):291-299.

Anderson, L. L., R. P. Rathmacher, and R. M. Melampy. 1966. The uterus and unilateral regression of corpora lutea in the pig. Am J Physiol 210(3):611-614. doi: 10.1152/ajplegacy.1966.210.3.611

Ashworth, M. D., J. W. Ross, D. R. Stein, F. J. White, U. W. Desilva, and R. D. Geisert. 2010. Endometrial caspase 1 and interleukin-18 expression during the estrous cycle and peri-implantation period of porcine pregnancy and response to early exogenous estrogen administration. Reproductive biology and endocrinology : RB&E 8:33. doi: 10.1186/1477-7827-8-33

Bazer, F. W., R. D. Geisert, W. W. Thatcher, and R. M. Roberts. 1982. The establishment and maintenance of pregnancy. In: D. J. A. Cole and G. R. Foxcroft, editors, Control of Pig Reproduction. Butter-worth Scientific, London. p. 227-252.

Bazer, F. W., and G. A. Johnson. 2014. Pig blastocyst-uterine interactions. Differentiation 87(1-2):52-65. doi: 10.1016/j.diff.2013.11.005

Bazer, F. W., S. R. Marengo, R. D. Geisert, and W. W. Thatcher. 1984. Exocrine versus endocrine secretion of prostaglandin F2α in the control of pregnancy in swine. Animal Reproduction Science 7(1):115-132. doi: https://doi.org/10.1016/0378-4320(84)90031-9

Bazer, F. W., and W. W. Thatcher. 1977. Theory of maternal recognition of pregnancy in swine based on estrogen controlled endocrine versus exocrine secretion of prostaglandin F2alpha by the uterine endometrium. Prostaglandins 14(2):397-400.

Behura, S. K., P. C. Tizioto, J. Kim, N. V. Grupioni, C. M. Seabury, R. D. Schnabel, L. J. Gershwin, A. L. Van Eenennaam, R. Toaff-Rosenstein, H. L. Neibergs, L. C. A. Regitano, and J. F. Taylor. 2017. Tissue Tropism in Host Transcriptional Response to Members of the Bovine Respiratory Disease Complex. Sci Rep 7(1):17938. doi: 10.1038/s41598-017-18205-0

Blitek, A., A. Waclawik, M. M. Kaczmarek, J. Kiewisz, and A. J. Ziecik. 2010. Effect of estrus induction on prostaglandin content and prostaglandin synthesis enzyme expression in the uterus of early pregnant pigs. Theriogenology 73(9):1244-1256. doi: 10.1016/j.theriogenology.2009.12.004

Bolzan, E., A. Andronowska, G. Bodek, E. Morawska-Pucinska, K. Krawczynski, A. Dabrowski, and A. J. Ziecik. 2013. The novel effect of hCG administration on luteal function maintenance during the estrous cycle/pregnancy and early embryo development in the pig. Pol J Vet Sci 16(2):323-332.

Butenandt, A. 1929. Uber progynon ein krytallisiertes weibliches exualhor- mon. Die Naturwissenschaften 17:879.

Chen, J., E. E. Bardes, B. J. Aronow, and A. G. Jegga. 2009. ToppGene Suite for gene list enrichment analysis and candidate gene prioritization. Nucleic acids research 37(Web Server issue):W305-311. doi: 10.1093/nar/gkp427

Conley, A., and M. Hinshelwood. 2001. Mammalian aromatases. Reproduction 121(5):685-695.

Conley, A. J., C. J. Corbin, and A. L. Hughes. 2009. Adaptive evolution of mammalian aromatases: lessons from Suiformes. J Exp Zool A Ecol Genet Physiol 311(5):346-357. doi: 10.1002/jez.451

Cover, T. M., and J. A. Thomas. 1991. Elements of Information Theory. John Wiley & Sons, New York, NY.

Da Silva, C., M. Broekhuijse, B. F. A. Laurenssen, H. Mulder, E. Knol, B. Kemp, and N. M. Soede. 2017. Relationship between ovulation rate and embryonic characteristics in gilts at 35 d of pregnancy.

Dhindsa, D. S., and P. J. Dziuk. 1968. Influence of varying the proportion of uterus occupied by embryos on maintenance of pregnancy in the pig. J Anim Sci 27(3):668-672.

Dinarello, C. A. 2009. Immunological and inflammatory functions of the interleukin-1 family. Annu Rev Immunol 27:519-550. doi: 10.1146/annurev.immunol.021908.132612

Doisy, E. A. 1976. An autobiography. Annu Rev Biochem 45:1-9. doi: 10.1146/annurev.bi.45.070176.000245

Dorniak, P., F. W. Bazer, and T. E. Spencer. 2011. Prostaglandins regulate conceptus elongation and mediate effects of interferon tau on the ovine

uterine endometrium. Biol Reprod 84(6):1119-1127. doi: 10.1095/biolreprod.110.089979

Dziuk, P. J. 1968. Effect of number of embryos and uterine space on embryo survival in the pig. J Anim Sci 27(3):673-676.

Ebeling, S., D. Topfer, J. M. Weitzel, and B. Meinecke. 2011. Bone morphogenetic protein-6 (BMP-6): mRNA expression and effect on steroidogenesis during in vitro maturation of porcine cumulus oocyte complexes. Reprod Fertil Dev 23(8):1034-1042. doi: 10.1071/rd11027

Enninga, E. A., S. G. Holtan, D. J. Creedon, R. S. Dronca, W. K. Nevala, S. Ognjanovic, and S. N. Markovic. 2014. Immunomodulatory effects of sex hormones: requirements for pregnancy and relevance in melanoma. Mayo Clin Proc 89(4):520-535. doi: 10.1016/j.mayocp.2014.01.006

Fischer, H. E., F. W. Bazer, and M. J. Fields. 1985. Steroid metabolism by endometrial and conceptus tissues during early pregnancy and pseudopregnancy in gilts. J Reprod Fertil 75(1):69-78.

Flowers, W. L., S. Webel, and M. Etienne. 2001. Synchronization of estrus in swine. North Carolina State University, Pork Information Gateway:1-8.

Ford, S. P., and L. K. Christenson. 1991. Direct effects of oestradiol-17 beta and prostaglandin E-2 in protecting pig corpora lutea from a luteolytic dose of prostaglandin F-2 alpha. J Reprod Fertil 93(1):203-209.

Ford, S. P., L. P. Reynolds, and R. R. Magness. 1982. Blood flow to the uterine and ovarian vascular beds of gilts during the estrous cycle or early pregnancy. Biol Reprod 27(4):878-885.

Frank, M., F. W. Bazer, W. W. Thatcher, and C. J. Wilcox. 1978. A study of prostaglandin F2alpha as the lutbolysin in swine: IV An explanation for the luteotrophic effect of estradiol. Prostaglandins 15(1):151-160.

Friess, A. E., F. Sinowatz, R. Skolek-Winnisch, and W. Traautner. 1980. The placenta of the pig. I. Finestructural changes of the placental barrier during pregnancy. Anat Embryol (Berl) 158(2):179-191.

Gadsby, J. E., R. B. Heap, and R. D. Burton. 1980. Oestrogen production by blastocyst and early embryonic tissue of various species. J Reprod Fertil 60(2):409-417.

Gama, L. L., and R. K. Johnson. 1993. Changes in ovulation rate, uterine capacity, uterine dimensions, and parity effects with selection for litter size in swine. J Anim Sci 71(3):608-617.

Geisert, R. D., G. A. Johnson, and R. C. Burghardt. 2015. Implantation and Establishment of Pregnancy in the Pig. Adv Anat Embryol Cell Biol 216:137-163. doi: 10.1007/978-3-319-15856-3_8

Geisert, R. D., T. N. Pratt, F. W. Bazer, J. S. Mayes, and G. H. Watson. 1994. Immunocytochemical localization and changes in endometrial progestin receptor protein during the porcine oestrous cycle and early pregnancy. Reprod Fertil Dev 6(6):749-760.

Geisert, R. D., R. J. Rasby, J. E. Minton, and R. P. Wetteman. 1986. Role of prostaglandins in development of porcine blastocysts. Prostaglandins 31(2):191-204.

Geisert, R. D., R. H. Renegar, W. W. Thatcher, R. M. Roberts, and F. W. Bazer. 1982a. Establishment of pregnancy in the pig: I. Interrelationships between preimplantation development of the pig blastocyst and uterine endometrial secretions. Biol Reprod 27(4):925-939.

Geisert, R. D., and R. A. M. Schmitt. 2001. Early embryonic survival in the pig: Can it be improved?

Geisert, R. D., W. W. Thatcher, R. M. Roberts, and F. W. Bazer. 1982b. Establishment of pregnancy in the pig: III. Endometrial secretory response to estradiol valerate administered on day 11 of the estrous cycle. Biol Reprod 27(4):957-965.

Geisert, R. D., J. J. Whyte, A. E. Meyer, D. J. Mathew, M. R. Juarez, M. C. Lucy, R. S. Prather, and T. E. Spencer. 2017. Rapid conceptus elongation in the pig: An interleukin 1 beta 2 and estrogen-regulated phenomenon. Mol Reprod Dev 84(9):760-774. doi: 10.1002/mrd.22813

Geisert, R. D., M. T. Zavy, R. J. Moffatt, R. M. Blair, and T. Yellin. 1990. Embryonic steroids and the establishment of pregnancy in pigs. J Reprod Fertil Suppl 40:293-305.

Geisert, R. D., M. T. Zavy, R. P. Wettemann, and B. G. Biggers. 1987. Length of pseudopregnancy and pattern of uterine protein release as influenced by time and duration of oestrogen administration in the pig. J Reprod Fertil 79(1):163-172.

Gregoraszczuk, E. L., and N. Michas. 1999. Progesterone and estradiol secretion by porcine luteal cells is influenced by individual and combined treatment

with prostaglandins E2 and F2alpha throughout the estrus cycle. Prostaglandins Other Lipid Mediat 57(4):231-241.

Gross, T. S., M. A. Mirando, K. H. Young, S. Beers, F. W. Bazer, and W. W. Thatcher. 1990. Reorientation of prostaglandin F secretion by calcium ionophore, estradiol, and prolactin in perifused porcine endometrium. Endocrinology 127(2):637-642. doi: 10.1210/endo-127-2-637

Häggström, M., and D. Richfield. 2014. Diagram of the pathways of human steroidogenesis. WikiJournal of Medicine 1(1)doi: 10.15347/wjm/2014.005

Hall, V. J., J. Christensen, Y. Gao, M. H. Schmidt, and P. Hyttel. 2009. Porcine pluripotency cell signaling develops from the inner cell mass to the epiblast during early development. Dev Dyn 238(8):2014-2024. doi: 10.1002/dvdy.22027

Hayden, M. S., and S. Ghosh. 2012. NF-kappaB, the first quarter-century: remarkable progress and outstanding questions. Genes Dev 26(3):203-234. doi: 10.1101/gad.183434.111

Henricks, D. M., H. D. Guthrie, and D. L. Handlin. 1972. Plasma estrogen, progesterone and luteinizing hormone levels during the estrous cycle in pigs. Biol Reprod 6(2):210-218.

Heuser, C. H., and G. L. Streeter. 1929. Early stages in the development of pig embryos, from the period of initial cleavage to the time of appearance of limb-buds. Contributions to Embryology by Carnegie Institution of Washington 20:3-29.

Huffman, D. W., D. W. MacCorquodale, S. A. Thayer, E. A. Doisy, G. V. Smith, and O. W. Smith. 1940. The isolation of a-dihydrotheelin from human placenta. Journal of Biological Chemistry 133:567-571.

Jaeger, L. A., G. A. Johnson, H. Ka, J. G. Garlow, R. C. Burghardt, T. E. Spencer, and F. W. Bazer. 2001. Functional analysis of autocrine and paracrine signalling at the uterine-conceptus interface in pigs. Reprod Suppl 58:191-207.

Jeong, W., H. Seo, Y. Sung, H. Ka, G. Song, and J. Kim. 2016. Lysophosphatidic Acid (LPA) Receptor 3-Mediated LPA Signal Transduction Pathways: A Possible Relationship with Early Development of Peri-Implantation Porcine Conceptus. Biol Reprod 94(5):104. doi: 10.1095/biolreprod.115.137174

Jinek, M., K. Chylinski, I. Fonfara, M. Hauer, J. A. Doudna, and E. Charpentier. 2012. A programmable dual-RNA-guided DNA endonuclease in adaptive bacterial immunity. Science 337(6096):816-821. doi: 10.1126/science.1225829

Joyce, M. M., R. C. Burghardt, R. D. Geisert, J. R. Burghardt, R. N. Hooper, J. W. Ross, M. D. Ashworth, and G. A. Johnson. 2007. Pig conceptuses secrete estrogen and interferons to differentially regulate uterine STAT1 in a temporal and cell type-specific manner. Endocrinology 148(9):4420-4431. doi: 10.1210/en.2007-0505

Kennedy, T. G., C. Gillio-Meina, and S. H. Phang. 2007. Prostaglandins and the initiation of blastocyst implantation and decidualization. Reproduction 134(5):635-643. doi: 10.1530/REP-07-0328

Kim, D., B. Langmead, and S. L. Salzberg. 2015. HISAT: a fast spliced aligner with low memory requirements. Nature methods 12(4):357-360. doi: 10.1038/nmeth.3317

King, A. E., F. Collins, T. Klonisch, J. M. Sallenave, H. O. Critchley, and P. T. Saunders. 2010. An additive interaction between the NFkappaB and estrogen receptor signalling pathways in human endometrial epithelial cells. Hum Reprod 25(2):510-518. doi: 10.1093/humrep/dep421

Kirby, C. J., M. F. Smith, D. H. Keisler, and M. C. Lucy. 1997. Follicular function in lactating dairy cows treated with sustained-release bovine somatotropin. J Dairy Sci 80(2):273-285. doi: 10.3168/jds.S0022-0302(97)75935-6

Knapczyk-Stwora, K., M. Durlej, M. Duda, K. Czernichowska-Ferreira, A. Tabecka-Lonczynska, and M. Slomczynska. 2011. Expression of oestrogen receptor alpha and oestrogen receptor beta in the uterus of the pregnant swine. Reprod Domest Anim 46(1):1-7. doi: 10.1111/j.1439-0531.2009.01505.x

Knight, J. W., F. W. Bazer, W. W. Thatcher, D. E. Franke, and H. D. Wallace. 1977. Conceptus development in intact and unilaterally hysterectomized-ovariectomized gilts: interrelations among hormonal status, placental development, fetal fluids and fetal growth. J Anim Sci 44(4):620-637.

Kol, S., I. Kehat, and E. Y. Adashi. 2002. Ovarian interleukin-1-induced gene expression: privileged genes threshold theory. Med Hypotheses 58(1):6-8. doi: 10.1054/mehy.2001.1389

Kraeling, R. R., G. B. Rampacek, and N. A. Fiorello. 1985. Inhibition of pregnancy with indomethacin in mature gilts and prepuberal gilts induced to ovulate. Biol Reprod 32(1):105-110.

Laskarin, G., N. Strbo, T. Bogovic Crncic, K. Juretic, N. Ledee Bataille, G. Chaouat, and D. Rukavina. 2005. Physiological role of IL-15 and IL-18 at the maternal-fetal interface. Chemical immunology and allergy 89:10-25. doi: 10.1159/000087906

Lee, K., B. K. Redel, L. Spate, J. Teson, A. N. Brown, K. W. Park, E. Walters, M. Samuel, C. N. Murphy, and R. S. Prather. 2013. Piglets produced from cloned blastocysts cultured in vitro with GM-CSF. Mol Reprod Dev 80(2):145-154. doi: 10.1002/mrd.22143

Liao, Y., G. K. Smyth, and W. Shi. 2014. featureCounts: an efficient general purpose program for assigning sequence reads to genomic features. Bioinformatics 30(7):923-930. doi: 10.1093/bioinformatics/btt656

Lindhard, A., U. Bentin-Ley, V. Ravn, H. Islin, T. Hviid, S. Rex, S. Bangsboll, and S. Sorensen. 2002. Biochemical evaluation of endometrial function at the time of implantation. Fertil Steril 78(2):221-233.

Machaty, Z., W. H. Wang, B. N. Day, and R. S. Prather. 1997. Complete activation of porcine oocytes induced by the sulfhydryl reagent, thimerosal. Biol Reprod 57(5):1123-1127.

Mak, P., J. Li, S. Samanta, and A. M. Mercurio. 2015. ERbeta regulation of NF-kB activation in prostate cancer is mediated by HIF-1. Oncotarget 6(37):40247-40254. doi: 10.18632/oncotarget.5377

Mantovani, A., M. Muzio, P. Ghezzi, C. Colotta, and M. Introna. 1998. Regulation of inhibitory pathways of the interleukin-1 system. Ann N Y Acad Sci 840:338-351.

Mathew, D. J., E. M. Newsom, J. M. Guyton, C. K. Tuggle, R. D. Geisert, and M. C. Lucy. 2015. Activation of the transcription factor nuclear factor-kappa B in uterine luminal epithelial cells by interleukin 1 Beta 2: a novel interleukin 1 expressed by the elongating pig conceptus. Biol Reprod 92(4):107. doi: 10.1095/biolreprod.114.126128

Mathew, D. J., E. M. Sellner, J. C. Green, C. S. Okamura, L. L. Anderson, M. C. Lucy, and R. D. Geisert. 2011. Uterine progesterone receptor expression, conceptus development, and ovarian function in pigs treated with RU 486 during early pregnancy. Biol Reprod 84(1):130-139. doi: 10.1095/biolreprod.110.086843

Moeljono, M. P., W. W. Thatcher, F. W. Bazer, M. Frank, L. J. Owens, and C. J. Wilcox. 1977. A study of prostaglandin F2alpha as the luteolysin in swine: II Characterization and comparison of prostaglandin F, estrogens and progestin concentrations in utero-ovarian vein plasma of nonpregnant and pregnant gilts. Prostaglandins 14(3):543-555.

Nestler, J. E. 1993. Interleukin-1 stimulates the aromatase activity of human placental cytotrophoblasts. Endocrinology 132(2):566-570. doi: 10.1210/endo.132.2.8425476

O'Neill, L. A., R. D. Geisert, M. T. Zavy, G. L. Morgan, and R. P. Wettemann. 1991. Effect of estrogen inhibitors on conceptus estrogen synthesis and development in the gilt. Domest Anim Endocrinol 8(1):139-153.

Patten, B. M., and B. M. Carlson. 1974. Foundations of Embryology. McGraw-Hill Book Company, New York.

Payne, A. H., and D. B. Hales. 2004. Overview of steroidogenic enzymes in the pathway from cholesterol to active steroid hormones. Endocr Rev 25(6):947-970. doi: 10.1210/er.2003-0030

Perry, J. S. 1981. The mammalian fetal membranes. J Reprod Fertil 62(2):321-335.

Perry, J. S., R. B. Heap, and E. C. Amoroso. 1973. Steroid hormone production by pig blastocysts. Nature 245(5419):45-47.

Perry, J. S., and I. W. Rowlands. 1962. Early pregnancy in the pig. Journal of Reproduction and Fertility 4:175-188.

Pohler, K. G., M. H. C. Pereira, F. R. Lopes, J. C. Lawrence, D. H. Keisler, M. F. Smith, J. L. M. Vasconcelos, and J. A. Green. 2016. Circulating concentrations of bovine pregnancy-associated glycoproteins and late embryonic mortality in lactating dairy herds. J Dairy Sci 99(2):1584-1594. doi: 10.3168/jds.2015-10192

Pope, W. F. 1994. Embryonic mortality in swine. In: R. D. Geisert and M. T. Zany, editors, Embryonic Mortality in Domestic Species. CRC Press, Boca Raton, Florida. p. 53-78.

Pope, W. F., R. R. Maurer, and F. Stormshak. 1982. Intrauterine migration of the porcine embryo: influence of estradiol-17 beta and histamine. Biol Reprod 27(3):575-579.

Quaedackers, M. E., C. E. van den Brink, P. T. van der Saag, and L. G. Tertoolen. 2007. Direct interaction between estrogen receptor alpha and NF-kappaB in the nucleus of living cells. Mol Cell Endocrinol 273(1-2):42-50. doi: 10.1016/j.mce.2007.05.002

Reis, A., B. Hornblower, B. Robb, and G. Tzertzinis. 2014. CRISPR/Cas9 and Targeted Genome Editing: A New Era in Molecular Biology. New England Biolabs Expressions (1):1-5.

Robertson, H. A., and G. J. King. 1974. Plasma concentrations of progesterone, oestrone, oestradiol-17beta and of oestrone sulphate in the pig at implantation, during pregnancy and at parturition. J Reprod Fertil 40(1):133-141.

Ross, J. W., M. D. Ashworth, D. R. Stein, O. P. Couture, C. K. Tuggle, and R. D. Geisert. 2009. Identification of differential gene expression during porcine conceptus rapid trophoblastic elongation and attachment to uterine luminal epithelium. Physiol Genomics 36(3):140-148. doi: 10.1152/physiolgenomics.00022.2008

Ross, J. W., J. R. Malayer, J. W. Ritchey, and R. D. Geisert. 2003. Characterization of the interleukin-1beta system during porcine trophoblastic elongation and early placental attachment. Biol Reprod 69(4):1251-1259. doi: 10.1095/biolreprod.103.015842

Rothschild, M. F. 1996. Genetics and reproduction in the pig. Animal Reproduction Science 42(1):143-151. doi: https://doi.org/10.1016/0378-4320(96)01486-8

Schneck, P. 1997. [Selmar Aschheim (1878-1965) and Bernhard Zondek (1891-1966). On the fate of 2 Jewish physicians and researchers at the Berlin Charite Hospital]. Z Arztl Fortbild Qualitatssich 91(2):187-194.

Senger, P. 2003. Pathways to Pregnancy and Parturition 2nd Edition. Current Conceptions, Pullman, WA.

Seo, H., M. Kim, Y. Choi, and H. Ka. 2011. Salivary lipocalin is uniquely expressed in the uterine endometrial glands at the time of conceptus implantation and induced by interleukin 1beta in pigs. Biol Reprod 84(2):279-287. doi: 10.1095/biolreprod.110.086934

Seo, H., M. Kim, Y. Choi, C. K. Lee, and H. Ka. 2008. Analysis of lysophosphatidic acid (LPA) receptor and LPA-induced endometrial prostaglandin-endoperoxide synthase 2 expression in the porcine uterus. Endocrinology 149(12):6166-6175. doi: 10.1210/en.2008-0354

Short, R. V. 1969. Implantation and the maternal recognition of pregnancy Feotal Autonomy, Churchill, London.

Simpson, E., and R. J. Santen. 2015. Celebrating 75 years of oestradiol. J Mol Endocrinol 55(3):T1-20. doi: 10.1530/JME-15-0128

Sorek, R., C. M. Lawrence, and B. Wiedenheft. 2013. CRISPR-mediated adaptive immune systems in bacteria and archaea. Annu Rev Biochem 82:237-266. doi: 10.1146/annurev-biochem-072911-172315

Spencer, T. E., and F. W. Bazer. 2002. Biology of progesterone action during pregnancy recognition and maintenance of pregnancy. Frontiers in bioscience : a journal and virtual library 7:d1879-1898.

Steinach, E., and H. Kun. 1937. Transformation of male sex hormones into a substance with the action of a female hormone. The Lancet 133

Stocco, D. M. 2000. The role of the StAR protein in steroidogenesis: challenges for the future. J Endocrinol 164(3):247-253.

Stone, B. A., and R. F. Seamark. 1985. Steroid hormones in uterine washings and in plasma of gilts between days 9 and 15 after oestrus and between days 9 and 15 after coitus. J Reprod Fertil 75(1):209-221.

Stoner, C. S., F. W. Bazer, W. W. Thatcher, C. J. Wilcox, G. E. Combs, J. W. Knight, R. P. Wettemann, and C. E. White. 1986. Relationship between estrone sulfate in plasma and litter size at farrowing for sows and gilts. Theriogenology 25(5):709-720.

Tomes, G. J., and H. E. Nielsen. 1982. Factors affecting reproductive efficiency of the breeding herd. In: D. J. A. Cole and G. R. Foxcroft, editors, Control of Pig Reproduction. Butterworth Scientific, London.

Trenti, A., S. Tedesco, C. Boscaro, L. Trevisi, C. Bolego, and A. Cignarella. 2018. Estrogen, Angiogenesis, Immunity and Cell Metabolism: Solving the Puzzle. Int J Mol Sci 19(3)doi: 10.3390/ijms19030859

Tuo, W., and F. W. Bazer. 1996. Expression of oncofetal fibronectin in porcine conceptuses and uterus throughout gestation. Reprod Fertil Dev 8(8):1207-1213.

Valdez Magana, G., A. Rodriguez, H. Zhang, R. Webb, and R. Alberio. 2014. Paracrine effects of embryo-derived FGF4 and BMP4 during pig trophoblast elongation. Dev Biol 387(1):15-27. doi: 10.1016/j.ydbio.2014.01.008

Vallet, J. L., J. R. Miles, and B. A. Freking. 2009. Development of the pig placenta. Soc Reprod Fertil Suppl 66:265-279.

Waclawik, A., A. Blitek, M. M. Kaczmarek, J. Kiewisz, and A. J. Ziecik. 2009a. Antiluteolytic mechanisms and the establishment of pregnancy in the pig. Soc Reprod Fertil Suppl 66:307-320.

Waclawik, A., H. N. Jabbour, A. Blitek, and A. J. Ziecik. 2009b. Estradiol-17beta, prostaglandin E2 (PGE2), and the PGE2 receptor are involved in PGE2 positive feedback loop in the porcine endometrium. Endocrinology 150(8):3823-3832. doi: 10.1210/en.2008-1499

Waclawik, A., M. M. Kaczmarek, A. Blitek, P. Kaczynski, and A. J. Ziecik. 2017. Embryo-maternal dialogue during pregnancy establishment and implantation in the pig. Mol Reprod Dev 84(9):842-855. doi: 10.1002/mrd.22835

Watkins, E. D. 2007. In the estrogen elixir: a history of hormone replacement in America. The Johns Hopkins Press, Baltimore.

White, F. J., J. W. Ross, M. M. Joyce, R. D. Geisert, R. C. Burghardt, and G. A. Johnson. 2005. Steroid regulation of cell specific secreted phosphoprotein 1 (osteopontin) expression in the pregnant porcine uterus. Biol Reprod 73(6):1294-1301. doi: 10.1095/biolreprod.105.045153

Whitworth, K. M., K. Lee, J. A. Benne, B. P. Beaton, L. D. Spate, S. L. Murphy, M. S. Samuel, J. Mao, C. O'Gorman, E. M. Walters, C. N. Murphy, J. Driver, A. Mileham, D. McLaren, K. D. Wells, and R. S. Prather. 2014. Use of the CRISPR/Cas9 system to produce genetically engineered pigs from in vitro-derived oocytes and embryos. Biol Reprod 91(3):78. doi: 10.1095/biolreprod.114.121723

Whitworth, K. M., J. Mao, K. Lee, W. G. Spollen, M. S. Samuel, E. M. Walters, L. D. Spate, and R. S. Prather. 2015. Transcriptome Analysis of Pig In Vivo, In Vitro-Fertilized, and Nuclear Transfer Blastocyst-Stage Embryos Treated with Histone Deacetylase Inhibitors Postfusion and Activation Reveals Changes in the Lysosomal Pathway. Cellular reprogramming 17(4):243-258. doi: 10.1089/cell.2015.0022

Whitworth, K. M., and R. S. Prather. 2010. Somatic cell nuclear transfer efficiency: how can it be improved through nuclear remodeling and reprogramming? Mol Reprod Dev 77(12):1001-1015. doi: 10.1002/mrd.21242

Whitworth, K. M., and R. S. Prather. 2017. Gene editing as applied to prevention of reproductive porcine reproductive and respiratory syndrome. Mol Reprod Dev 84(9):926-933. doi: 10.1002/mrd.22811

Whyte, J. J., A. E. Meyer, L. D. Spate, J. A. Benne, R. Cecil, M. S. Samuel, C. N. Murphy, R. S. Prather, and R. D. Geisert. 2018. Inactivation of porcine interleukin-1beta results in failure of rapid conceptus elongation. Proc Natl Acad Sci U S A 115(2):307-312. doi: 10.1073/pnas.1718004115

Wilson, M. E., and S. P. Ford. 2000. Effect of estradiol-17beta administration during the time of conceptus elongation on placental size at term in Meishan pigs. J Anim Sci 78(4):1047-1052.

Yang, H.-J., M. Shozu, K. Murakami, H. Sumitani, T. Segawa, T. Kasai, and M. Inoue. 2002. Spatially Heterogenous Expression of Aromatase P450 through Promoter II Is Closely Correlated with the Level of Steroidogenic Factor-1 Transcript in Endometrioma Tissues. The Journal of Clinical Endocrinology & Metabolism 87(8):3745-3753. doi: 10.1210/jcem.87.8.8733

Zang, Y. C., J. B. Halder, J. Hong, V. M. Rivera, and J. Z. Zhang. 2002. Regulatory effects of estriol on T cell migration and cytokine profile: inhibition of transcription factor NF-kappa B. J Neuroimmunol 124(1-2):106-114.

Zavy, M. T., F. W. Bazer, W. W. Thatcher, and C. J. Wilcox. 1980. A study of prostaglandin F2 alpha as the luteolysin in swine: V. Comparison of prostaglandin F, progestins, estrone and estradiol in uterine flushings from pregnant and nonpregnant gilts. Prostaglandins 20(5):837-851.

Zhao, H., L. Zhou, A. J. Shangguan, and S. E. Bulun. 2016. Aromatase expression and regulation in breast and endometrial cancer. J Mol Endocrinol 57(1):R19-33. doi: 10.1530/JME-15-0310

Zhengxing, L., Z. Yaofeng, L. I. U. Guoshi, L. I. Ning, W. Feng, L. I. Kongpan, D. Shoulong, H. U. Rui, T. Xiuzhi, L. Ling, W. Tao, M. A. Yonghe, and H. A. N. Hongbing. 2014. One-step generation of myostatin gene knockout

sheep via the CRISPR/Cas9 system. Frontiers of Agricultural Science and Engineering 1(1)doi: 10.15302/j-fase-2014007

Zhou, X., H. Lindsay, and M. D. Robinson. 2014. Robustly detecting differential expression in RNA sequencing data using observation weights. Nucleic acids research 42(11):e91. doi: 10.1093/nar/gku310

Zondek, B. 1934. Oestrogenic hormone in the urine of the stallion. Nature 133

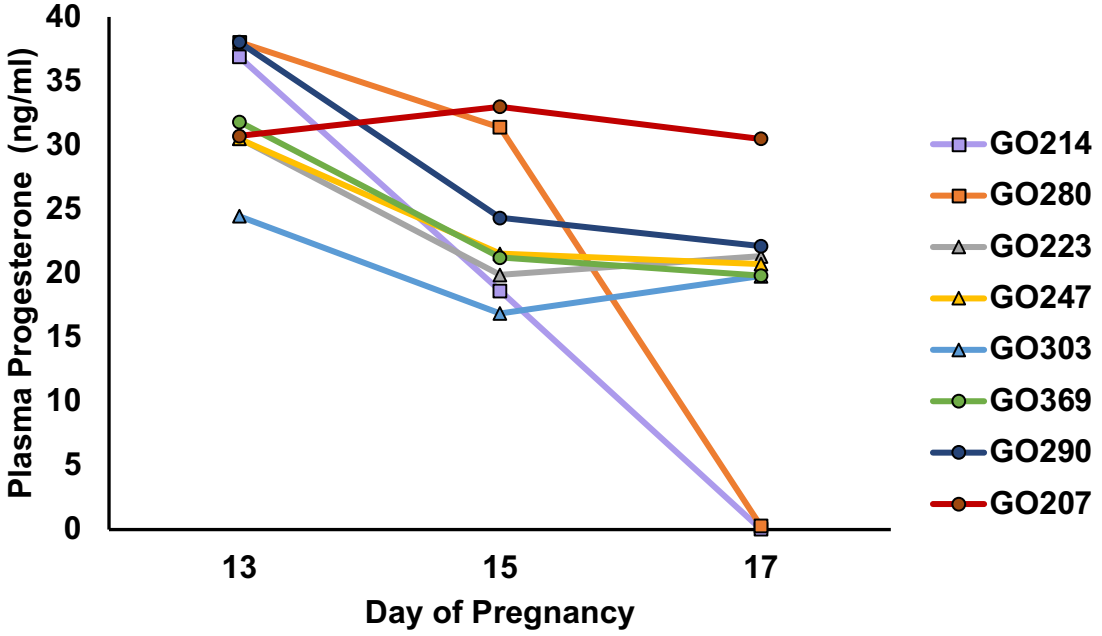

Figure S1: Plasma Progesterone of Day 17 Collections. Blood was drawn on days 13, 15, 17 of cyclic gilts (n=3) and the recipient gilts carrying *CYP19A1*$^{+/+}$ (n=3) or *CYP19A1*$^{-/-}$ (n=3). Cyclic gilts have lines with square points, *CYP19A1*$^{+/+}$ have lines circle points, and *CYP19A1*$^{-/-}$ have lines with triangle points. This demonstrates the functionality of the CL of pregnancy gilts to day 17, despite carrying *CYP19A1*$^{+/+}$ or *CYP19A1*$^{-/-}$.

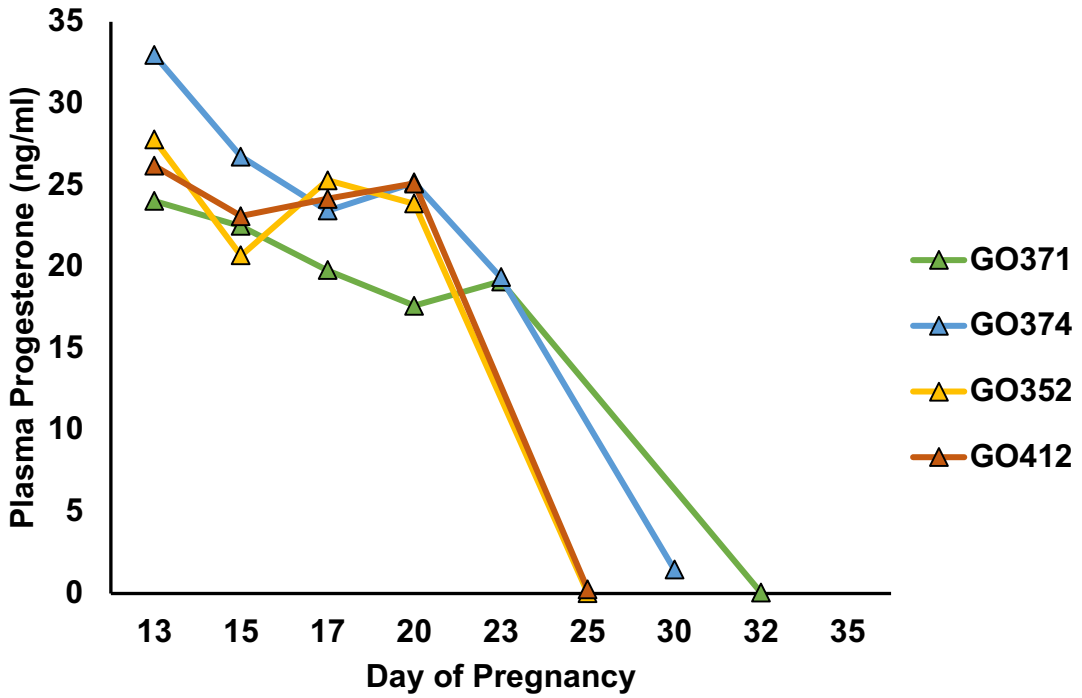

Figure S2: Plasma Progesterone of *CYP19A1*$^{-/-}$ Pregnancies. Blood was drawn on recipient gilts carrying *CYP19A1*$^{-/-}$ (n=4). Gilts, O412 and O352, had plasma concentrations of progesterone decreased to <1 ng/ml by day 25 and displayed estrus on day 27. Gilt O374 and gilt O371 had plasma concentrations of progesterone decreased to <1 ng/ml by day 30.

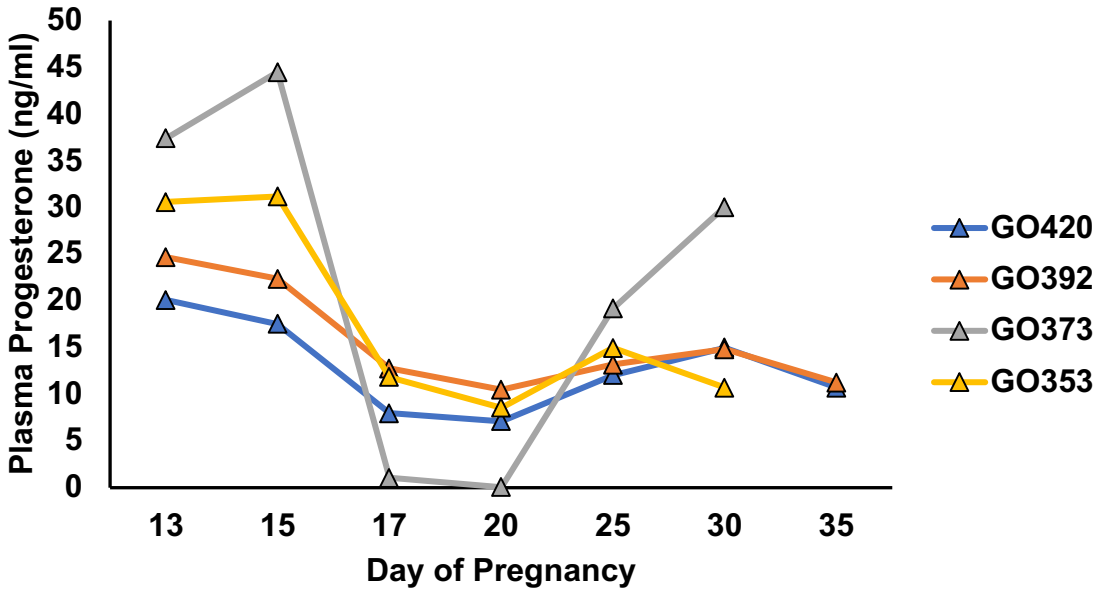

Figure S3: Plasma Progesterone of Estradiol-Benzoate Injected Recipient Gilts with *CYP19A1*$^{-/-}$ Conceptuses. Two recipient gilts, O420 and O392, received estradiol-benzoate injections on days 14, 17, 18 and 19 of pregnancy. The injections of estradiol-benzoate maintained CL production of progesterone but there were no embryos present on day 26 via ultrasound in both gilts. Recipient gilts, O373 and O353, received injections on days 15, 18, 19, and 20. O353 had function CL up until day 30 but embryos were not present on ultrasound by day 27. O373 did not respond to the estradiol-benzoate injections and was not pregnant with *CYP19A1*$^{-/-}$ conceptuses, therefore lost progesterone production by day 17 and showed standing heat on day 20.

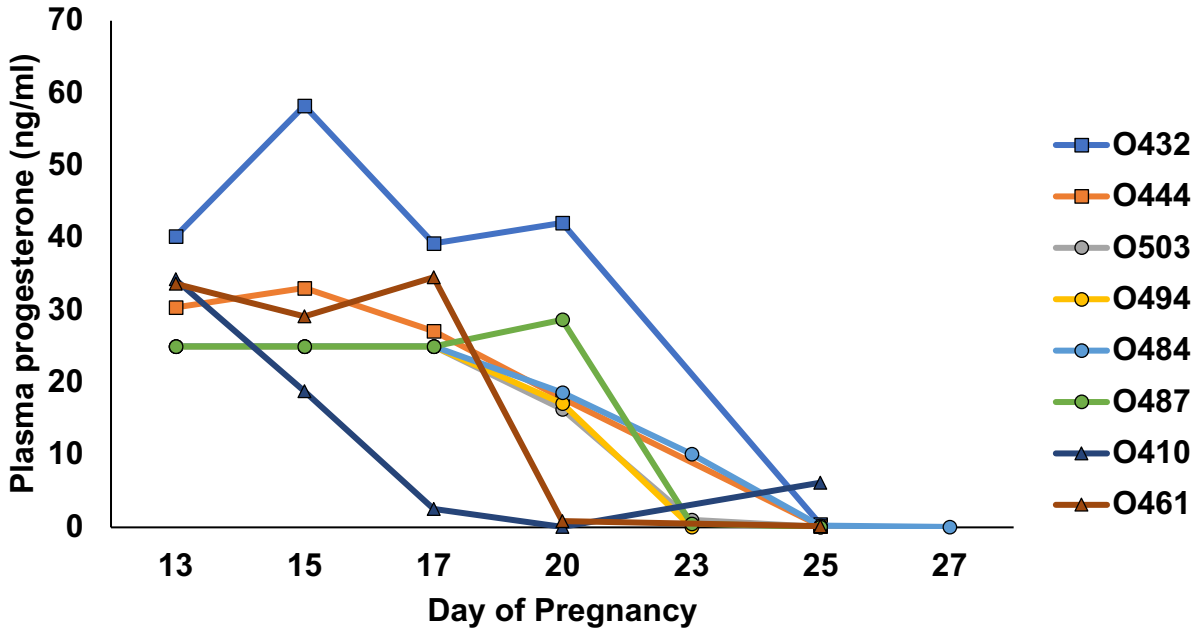

Figure S4: Plasma Progesterone Concentrations from Co-Embryo Transferred Recipient Gilts of *CYP19A1*$^{-/-}$ and *CYP19A1*$^{+/+}$ Blastocyst. Recipient gilts were embryo transferred *CYP19A1*$^{-/-}$ blastocysts and *CYP19A1*$^{+/+}$ blastocysts derived from one of three *CYP19A1*$^{+/+}$ cell lines: cell line B (n=2) (square points), cell line C (n=4) (circle points), or cell line C (n=2) (triangle points). Recipient gilt O410 was not pregnant and showed heat on day 21. All the other recipient gilts showed estrus and was confirmed open between days 24 to 27 of pregnancy.

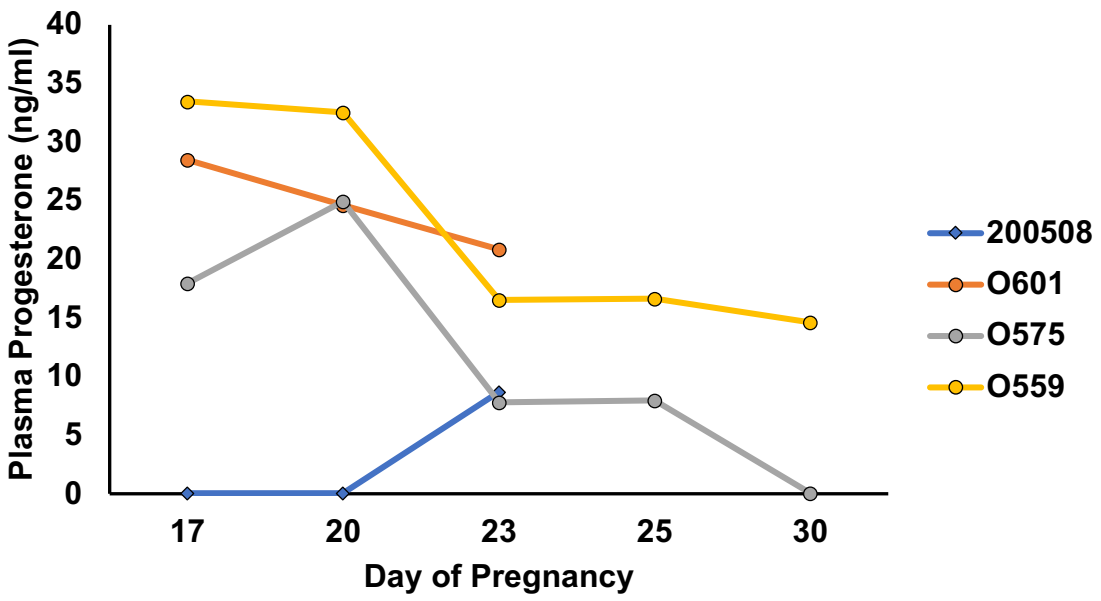

Figure S5: Plasma Progesterone Concentrations from Co-Embryo Transferred Recipient Gilts of *CYP19A1*$^{-/-}$ Clones and IVF *CYP19A1*$^{+/+}$ Blastocysts. Recipient gilt 200508, control IVF embryo transfer (diamond points), was not pregnant and displayed standing heat on day 20. Recipient gilts O575, O559, and O601 were co-transferred with *CYP19A1*$^{+/+}$ IVF blastocyst and *CYP19A1*$^{-/-}$ clones Gilt O575 lost her pregnancy and expressed standing heat on day 28. Gilt O559 and O601 both maintained pregnancy until euthanized on day 34. Blood draws on gilt O601 was stopped after day 23 due to injury.

Table S1: Top Endometrial Up-regulated Genes in Day 14 *CYP19A1*$^{-/-}$ Verses *CYP19A1*$^{+/+}$.

Gene Name	FC	FDR	Day 14 *CYP19A1+/+* CPM average	Day 14 *CYP19A1-/-* CPM average
matrix metallopeptidase 8	69.81	1.60E-03	0.91	30.21
Unknown, ENSSSCG00000039569	39.24	1.89E-03	1.61	33.26
Sus scrofa S100 calcium binding protein A8 (S100A8), mRNA.	23.20	1.41E-02	20.54	657.40
Protein S100-A12	20.14	5.32E-05	2.56	51.39
aconitate decarboxylase 1	13.18	1.46E-02	10.53	16.93
aldo-keto reductase family 1 member B	12.45	1.25E-03	8.67	86.35
1,25-dihydroxyvitamin D(3) 24-hydroxylase, mitochondrial	10.83	2.47E-02	1.40	15.24
tumor necrosis factor-inducible gene 6 protein precursor	9.51	1.25E-02	0.36	4.17
Unknown, ENSSSCG00000020872	9.36	2.36E-10	3.14	27.32
Unknown, ENSSSCG00000036177	6.48	1.01E-03	0.75	4.80
Unknown, ENSSSCG00000036778	5.98	8.69E-04	1.22	6.72
vanin 2	5.79	3.62E-07	29.69	111.72
branched chain amino acid transaminase 1	5.31	2.03E-13	20.64	97.57
S100 calcium binding protein A2	5.24	1.94E-07	84.43	396.95
transmembrane protein 139	5.08	1.01E-03	1.20	5.92
Unknown, ENSSSCG00000004180	4.95	3.15E-02	4.26	12.48
fibrinogen gamma chain	4.93	1.46E-02	4.82	22.43
cholinergic receptor muscarinic 3	4.86	2.97E-02	0.50	2.44
DCC netrin 1 receptor	4.73	7.74E-05	0.60	2.63
synaptosome associated protein 25	4.63	4.03E-02	0.22	0.88
Unknown, ENSSSCG00000036728	4.61	5.13E-03	0.89	3.95
olfactory receptor family 10 subfamily G member 3	4.56	7.79E-03	0.97	5.43
Unknown, ENSSSCG00000040146	4.53	1.13E-02	0.22	1.02
Unknown, ENSSSCG00000012200	4.41	4.51E-02	1.50	8.90
phosphoenolpyruvate carboxykinase 2, mitochondrial	4.35	6.05E-04	3.07	12.37
Dehydrogenase/reductase SDR family member 4	4.12	6.99E-03	8.73	35.15
aminoadipate aminotransferase	4.11	5.13E-03	0.34	1.35
proenkephalin	4.02	1.45E-03	0.73	2.60
cytochrome P450 family 26 subfamily A member 1	3.93	3.82E-04	3.23	10.49
serum amyloid A-3 protein precursor	3.92	3.75E-02	8.56	98.13
opsin 4	3.75	1.89E-03	3.17	10.61
Unknown, ENSSSCG00000013714	3.61	4.40E-02	2.07	7.14
early activation antigen CD69	3.51	3.74E-06	7.95	26.27
gamma-glutamyltranspeptidase 1	3.48	3.91E-02	0.89	3.05
leucine rich repeat transmembrane neuronal 4	3.48	2.47E-02	3.24	12.06

solute carrier family 5 member 1	3.42	4.52E-02	9.22	30.59
ectodysplasin A receptor	3.37	3.50E-02	0.27	0.74
Sus scrofa vanin 1 (VNN1), mRNA.	3.35	1.45E-02	22.46	63.38
Unknown, ENSSSCG00000037206	3.31	5.15E-03	1.21	3.93
hepatocyte nuclear factor 4 alpha	3.20	1.87E-02	0.50	1.51
Sus scrofa coagulation factor V (F5), mRNA.	3.20	2.51E-03	4.04	12.76
lecithin retinol acyltransferase	3.14	2.77E-04	4.23	7.02
Unknown, ENSSSCG00000038037	3.10	2.99E-02	11.86	33.68
peroxisomal trans-2-enoyl-CoA reductase	3.07	1.59E-06	9.91	31.69
Unknown, ENSSSCG00000011676	3.01	4.44E-02	18.08	55.49
calpain 8	2.93	1.60E-03	3.00	8.59
RAB17, member RAS oncogene family	2.91	2.97E-02	0.49	1.27
relaxin/insulin like family peptide receptor 1	2.82	1.25E-03	11.69	31.10
Sus scrofa Epididymal secretory protein E4 (E4), mRNA.	2.70	2.34E-02	63.09	156.56
CD109 molecule	2.69	4.75E-02	6.51	17.01
mitotic spindle positioning	2.64	1.66E-02	2.08	5.71
Unknown, ENSSSCG00000005278	2.63	2.06E-03	1.38	3.27
estradiol 17-beta-dehydrogenase 2	2.59	5.03E-04	7.58	14.21
solute carrier family 6 member 2	2.59	9.34E-03	1.53	3.85
neuromedin U	2.57	1.72E-02	86.91	181.26
sodium voltage-gated channel alpha subunit 4	2.54	1.11E-02	0.43	1.10
interleukin 17 receptor D	2.44	2.81E-02	8.52	23.35
regulator of G protein signaling 4	2.36	2.47E-02	3.07	7.08
Rieske Fe-S domain containing	2.34	2.65E-02	7.27	26.85
solute carrier family 2 member 8	2.31	2.65E-02	5.34	10.80
sphingomyelin phosphodiesterase acid like 3B	2.29	2.05E-03	1.71	3.55
phospholipase A2 group IVA	2.28	1.19E-03	27.31	62.64
transmembrane channel like 7	2.27	1.19E-03	2.01	4.69
glycerol kinase	2.26	4.40E-02	5.00	10.94
NACHT and WD repeat domain containing 2	2.25	4.90E-02	1.05	2.31
glutathione S-transferase Mu 3-like	2.24	3.41E-04	64.89	134.14
contactin 3	2.23	5.67E-04	16.97	35.07
solute carrier family 6 member 15	2.20	2.34E-02	1.65	3.92
type II iodothyronine deiodinase	2.19	2.34E-02	12.56	23.57
myomesin 1	2.18	4.46E-03	3.86	10.36
Unknown, ENSSSCG00000027232	2.15	3.65E-02	4.21	9.45
transient receptor potential cation channel subfamily M member 6	2.06	2.06E-03	20.32	38.23
syndecan 1	2.05	4.40E-02	2.67	5.62
lactate dehydrogenase D	2.02	7.79E-03	5.97	10.99
glutathione S-transferase kappa 1	2.02	1.83E-03	5.62	10.73

chimerin 1	2.01	3.15E-02	7.97	14.94
transmembrane protein 243	2.00	4.51E-02	35.09	60.52

Table S2: Top Endometrial Down-regulated Genes in Day 14 *CYP19A1*$^{-/-}$ Verses *CYP19A1*$^{+/+}$.

Gene Name	FC	FDR	Day 14 *CYP19A1*+/+ CPM average	Day 14 *CYP19A1*-/- CPM average
transforming growth factor beta 2	-2.01	3.65E-02	22.47	11.70
basic helix-loop-helix family member e40	-2.06	5.63E-04	9.20	4.50
aminoacyl tRNA synthase complex-interacting multifunctional protein 2 isoform 1	-2.10	9.34E-03	3.05	1.44
Matrix Gla protein	-2.11	1.46E-05	22.98	10.59
Unknown, ENSSSCG00000024911	-2.18	4.44E-02	223.23	102.87
dual specificity phosphatase 1	-2.34	3.13E-04	90.27	42.39
solute carrier family 52 member 3	-2.36	1.37E-02	2.63	1.05
ELAV like RNA binding protein 2	-2.38	1.61E-02	5.04	2.39
activating transcription factor 3	-2.41	1.89E-03	20.58	8.19
Unknown, ENSSSCG00000036125	-2.45	2.12E-02	3.31	1.11
Metallothionein-1A	-2.48	1.72E-02	30.00	11.27
mitogen-activated protein kinase kinase 6	-2.56	2.68E-03	11.89	4.45
DNA-binding protein inhibitor ID-2	-2.80	9.15E-04	31.52	10.93
endonuclease domain containing 1	-3.05	2.06E-03	37.50	13.43
Metalloreductase STEAP1	-3.46	4.13E-02	19.65	9.49
Xg blood group	-4.34	8.18E-07	3.87	0.86
testis expressed 12	-4.53	3.96E-02	2.42	0.93
cation channel sperm associated auxiliary subunit beta	-4.73	2.06E-03	26.44	5.44
Unknown, ENSSSCG00000031957	-4.74	3.62E-07	3.12	0.67
glycine-N-acyltransferase like 2	-5.18	1.00E-10	29.95	8.58
glutamate carboxypeptidase 2	-6.15	1.26E-11	28.80	7.93
testis expressed 15, meiosis and synapsis associated	-7.12	8.18E-06	1.67	0.42
dimethylglycine dehydrogenase	-8.06	5.32E-05	0.58	0.14
lithostathine-like precursor	-8.22	3.50E-02	0.55	0.09
S-methylmethionine--homocysteine S-methyltransferase BHMT2	-10.58	3.26E-06	0.78	0.13

Table S3: Top Endometrial Up-regulated Genes from Day 14 *CYP19A1*$^{+/+}$ to Day 17 *CYP19A1*$^{+/+}$.

Gene Name	FC	FDR	Day 14 *CYP19A1*+/+ CPM average	Day 17 *CYP19A1*+/+ CPM average

Sus scrofa corneodesmosin (CDSN), mRNA.	35.28	1.16E-04	2.04	22.86
secreted phosphoprotein 1	22.05	4.51E-07	16.63	362.22
Sus scrofa C-X-C motif chemokine ligand 14 (CXCL14), mRNA.	18.18	2.18E-18	1.99	33.59
histidine decarboxylase	14.99	5.76E-18	2.37	27.19
vanin 2	10.77	4.71E-05	29.69	263.10
N-acylethanolamine acid amidase	10.03	1.03E-11	14.82	134.46
C-X-C motif chemokine 10 precursor	9.84	7.40E-06	33.20	45.62
trace amine associated receptor 1	9.42	2.62E-09	1.67	16.69
DCC netrin 1 receptor	7.76	3.61E-04	0.60	5.00
1,25-dihydroxyvitamin D(3) 24-hydroxylase, mitochondrial	7.47	1.16E-04	1.40	6.61
neuromedin U	6.97	2.17E-12	86.91	519.53
Sus scrofa alpha-1-antichymotrypsin 2 (SERPINA3-2), mRNA.	6.54	1.73E-02	0.28	2.50
Unknown, ENSSSCG00000031703	6.44	1.96E-03	0.18	1.12
neurotrimin	6.32	5.73E-03	1.00	6.34
aquaporin 8	6.23	1.55E-04	0.54	2.57
SPHK1 interactor, AKAP domain containing	6.06	1.16E-04	1.37	6.07
calcium dependent secretion activator	5.83	3.68E-04	0.21	1.20
colony stimulating factor 3 receptor	5.82	3.78E-05	1.70	10.31
ATP binding cassette subfamily A member 12	5.81	3.27E-15	1.65	10.35
lecithin retinol acyltransferase	5.74	2.18E-12	4.23	13.65
estradiol 17-beta-dehydrogenase 2	5.73	1.02E-11	7.58	37.25
Unknown, ENSSSCG00000034371	5.60	4.52E-02	34.59	173.22
PKHD1, fibrocystin/polyductin	5.57	1.57E-30	1.49	8.67
gamma-glutamyltranspeptidase 1	5.46	7.86E-13	0.89	5.16
Unknown, ENSSSCG00000035073	5.38	2.10E-04	1.02	6.34
Unknown, ENSSSCG00000031023	5.23	2.77E-04	100.31	265.65
solute carrier organic anion transporter family member 1A2	5.11	1.57E-30	7.86	41.50
polypeptide N-acetylgalactosaminyltransferase 9	5.07	2.11E-06	3.10	16.45
Unknown, ENSSSCG00000001040	5.06	4.82E-13	7.13	32.73
FosB proto-oncogene, AP-1 transcription factor subunit	4.91	4.45E-02	1.46	4.01
LDL receptor related protein 2	4.90	1.28E-24	10.28	52.44
Unknown, ENSSSCG00000037345	4.84	2.96E-02	1.51	7.45
fibroblast growth factor receptor 4	4.58	1.05E-03	0.94	3.32
serpin family B member 2	4.53	8.71E-03	0.31	0.65
chromosome 11 open reading frame 87	4.52	1.75E-02	0.09	0.40
Unknown, ENSSSCG00000037798	4.44	6.08E-03	2.15	6.04
calcium homeostasis modulator family member 6	4.35	1.54E-04	1.19	3.79
aldehyde dehydrogenase 3 family member B2	4.32	3.27E-05	1.22	5.78
purinergic receptor P2Y2	4.32	5.71E-03	2.01	6.79

sodium channel epithelial 1 gamma subunit	4.23	1.58E-02	0.45	1.85
Unknown, ENSSSCG00000004839	4.01	2.86E-03	0.21	1.05
Dipeptidyl peptidase 4 Dipeptidyl peptidase 4 membrane form Dipeptidyl peptidase 4 soluble form	4.01	2.18E-12	17.13	76.71
carbonic anhydrase 2	3.96	4.24E-20	41.08	157.97
interleukin 1 alpha	3.95	3.78E-05	8.92	31.06
Wnt family member 7A	3.94	1.16E-04	0.48	1.98
neurotrophic receptor tyrosine kinase 2	3.93	6.64E-07	7.42	24.62
potassium voltage-gated channel subfamily J member 15	3.85	1.45E-04	2.21	8.56
matrilysin	3.84	3.57E-03	1.24	5.12
RAB17, member RAS oncogene family	3.78	1.31E-02	0.49	2.07
Unknown, ENSSSCG00000029020	3.73	1.97E-03	2.90	10.50
hyaluronan binding protein 2	3.73	3.20E-03	0.29	1.16
homeobox protein NANOG	3.71	2.73E-02	0.76	2.36
RBBP8 N-terminal like	3.62	3.62E-04	0.35	1.31
solute carrier family 26 member 4	3.60	1.03E-11	4.96	17.16
anterior gradient 2, protein disulphide isomerase family member	3.59	7.87E-04	34.06	114.76
cholinergic receptor muscarinic 3	3.51	1.81E-02	0.50	2.11
Unknown, ENSSSCG00000032980	3.46	3.49E-03	0.19	0.69
retinoic acid induced 2	3.35	1.57E-02	0.83	2.68
Unknown, ENSSSCG00000039858	3.34	1.66E-02	0.27	1.02
retinal pigment epithelium-derived rhodopsin homolog	3.30	1.70E-02	0.70	2.41
FXYD domain containing ion transport regulator 2	3.28	2.24E-03	36.89	96.37
protocadherin alpha 13	3.23	5.79E-03	0.34	1.16
Sus scrofa cytochrome P450, family 2, subfamily J, polypeptide 34 (CYP2J34), mRNA.	3.16	1.50E-05	1.80	5.24
LY6/PLAUR domain containing 6B	3.14	2.31E-06	5.05	16.53
early activation antigen CD69	3.13	2.78E-03	7.95	26.62
arylformamidase	3.13	6.09E-06	3.56	11.95
Sus scrofa Epididymal secretory protein E4 (E4), mRNA.	3.12	4.04E-02	63.09	239.36
Unknown, ENSSSCG00000000194	3.11	1.61E-02	6.91	16.37
Unknown, ENSSSCG00000026653	3.05	2.97E-02	0.40	1.28
Unknown, ENSSSCG00000008001	3.05	4.47E-03	2.82	8.00
Unknown, ENSSSCG00000023956	3.02	7.91E-11	5.31	18.42
solute carrier family 6 member 15	3.02	6.21E-04	1.65	6.45
delta 4-desaturase, sphingolipid 2	3.01	9.42E-03	0.42	1.31
ADM Adrenomedullin Proadrenomedullin N-20 terminal peptide	3.01	1.58E-07	18.65	58.15
additional sex combs like 3, transcriptional regulator	3.00	2.09E-04	1.37	4.56
immunoglobulin superfamily member 1	2.98	7.87E-03	0.43	1.32
Unknown, ENSSSCG00000025992	2.97	1.77E-04	22.85	60.94

adaptor related protein complex 1 sigma 3 subunit	2.97	1.09E-12	8.87	28.02
carbohydrate sulfotransferase 9	2.92	2.96E-15	5.50	16.66
islet amyloid polypeptide	2.85	3.39E-04	2.38	6.67
Sus scrofa solute carrier family 1 (neuronal/epithelial high affinity glutamate transporter, system Xag), member 1 (SLC1A1), mRNA.	2.80	1.22E-11	7.08	20.36
uridine phosphorylase 1	2.78	4.40E-02	2.09	5.76
EvC ciliary complex subunit 1	2.77	1.07E-05	5.88	15.54
potassium voltage-gated channel subfamily J member 16	2.75	1.44E-02	8.61	20.67
semaphorin 3D	2.75	1.34E-06	16.55	43.05
threonyl-tRNA synthetase like 2	2.73	1.49E-03	3.86	9.98
Unknown, ENSSSCG00000037927	2.71	6.78E-03	6.08	17.28
Unknown, ENSSSCG00000024518	2.69	3.04E-02	0.48	1.49
structural maintenance of chromosomes 1B	2.68	4.08E-03	0.72	2.01
erb-b2 receptor tyrosine kinase 4	2.66	5.02E-05	3.90	10.01
calcium homeostasis modulator family member 5	2.63	4.65E-06	6.45	18.96
zinc finger protein 608	2.62	4.76E-07	7.21	16.46
crystallin alpha B	2.59	9.50E-03	2.27	5.86
Unknown, ENSSSCG00000004197	2.59	3.21E-02	4.23	11.48
cholinergic receptor nicotinic alpha 3 subunit	2.58	1.91E-02	0.42	1.07
pleckstrin homology domain containing S1	2.58	2.41E-11	10.16	27.04
epsin 3	2.57	5.95E-05	0.88	2.35
inhibin beta B chain precursor	2.57	1.46E-02	8.37	22.78
serpin family B member 5	2.54	5.31E-05	13.24	38.49
Unknown, ENSSSCG00000031367	2.51	1.55E-02	3.35	9.90
15-hydroxyprostaglandin dehydrogenase	2.49	2.77E-04	13.19	36.18
branched chain amino acid transaminase 1	2.48	4.84E-03	20.64	45.41
UDP-GlcNAc:betaGal beta-1,3-N-acetylglucosaminyltransferase 3	2.47	2.31E-04	4.64	10.09
alkaline phosphatase, liver/bone/kidney	2.46	6.17E-08	14.04	34.54
adhesion G protein-coupled receptor F1	2.45	5.00E-04	13.02	32.99
CUB and Sushi multiple domains 1	2.44	1.21E-04	0.51	1.28
prominin 2	2.44	2.36E-04	1.69	4.18
alpha 2-HS glycoprotein	2.43	1.69E-02	1.80	4.34
carbonic anhydrase 8	2.42	1.30E-03	5.08	13.35
Unknown, ENSSSCG00000023305	2.41	3.04E-03	51.91	134.60
estrogen sulfotransferase	2.41	9.83E-03	10.29	18.23
leucine rich repeat and fibronectin type III domain containing 4	2.40	1.16E-04	1.43	3.56
sphingosine-1-phosphate phosphatase 2	2.39	1.40E-02	1.21	2.73
interleukin 18 receptor 1	2.38	2.47E-04	2.67	6.08
Sus scrofa radical S-adenosyl methionine domain containing 2 (RSAD2), mRNA.	2.38	6.43E-03	6.31	13.19

Unknown, ENSSSCG00000034049	2.34	3.99E-03	20.12	40.32
aminoadipate-semialdehyde synthase	2.34	5.81E-09	9.66	23.47
dual specificity phosphatase 9	2.32	5.80E-04	3.11	7.53
farnesyl diphosphate synthase	2.31	1.01E-03	1.89	4.42
solute carrier family 37 member 2	2.30	5.15E-05	31.53	75.15
solute carrier family 19 member 3	2.30	2.24E-06	9.38	22.30
ubiquitin-like protein ISG15	2.29	4.83E-04	6.59	14.85
Unknown, ENSSSCG00000040056	2.28	2.91E-06	37.12	96.36
Unknown, ENSSSCG00000029281	2.27	4.93E-05	5.54	13.75
family with sequence similarity 196 member B	2.27	7.62E-04	2.39	6.56
sodium channel epithelial 1 beta subunit	2.24	1.93E-02	1.23	2.85
interferon alpha inducible protein 6	2.23	2.90E-03	155.05	348.12
protein tyrosine phosphatase, receptor type Z1	2.22	4.71E-03	1.65	3.11
myosin IIIA	2.22	7.53E-04	4.85	10.66
semaphorin 3A	2.22	1.93E-02	3.79	7.75
small integral membrane protein 3	2.21	4.24E-03	6.08	13.40
prostaglandin G/H synthase 2 precursor	2.21	6.37E-03	35.06	83.85
ADCYAP receptor type I	2.20	1.98E-02	1.79	3.89
interferon-induced GTP-binding protein Mx1	2.20	9.12E-04	33.45	64.76
phytanoyl-CoA 2-hydroxylase interacting protein like	2.20	6.54E-08	6.23	14.20
aarF domain containing kinase 5	2.18	2.25E-04	27.46	61.69
ATPase H+ transporting V0 subunit a1	2.16	7.58E-04	11.30	26.01
SLIT-ROBO Rho GTPase activating protein 3	2.15	1.80E-04	20.32	43.56
synaptotagmin like 1	2.14	3.98E-02	1.21	2.60
low density lipoprotein receptor	2.14	4.55E-02	11.46	25.91
ovo like transcriptional repressor 1	2.14	2.29E-02	1.69	3.74
solute carrier family 29 member 1 (Augustine blood group)	2.14	3.53E-03	1.31	2.61
Unknown, ENSSSCG00000036208	2.14	2.54E-02	1.42	2.67
solute carrier family 4 member 11	2.12	8.79E-04	3.69	8.00
dihydrouridine synthase 4 like	2.12	3.81E-04	2.06	4.52
chromosome 9 open reading frame 72	2.11	8.02E-04	19.84	42.34
thyroid hormone receptor beta	2.11	2.66E-03	2.03	4.53
MX dynamin like GTPase 2	2.09	5.76E-03	8.23	15.14
interleukin 17 receptor D	2.09	3.53E-03	8.52	19.42
DNA-binding protein inhibitor ID-2	2.08	1.87E-02	31.52	61.56
stearoyl-CoA desaturase	2.07	5.92E-03	7.79	18.57
ATPase 13A4	2.07	4.65E-04	47.36	100.08
serum/glucocorticoid regulated kinase 1	2.07	1.41E-04	47.49	104.85
Unknown, ENSSSCG00000034592	2.06	1.63E-03	7.03	15.08
interleukin 1 receptor accessory protein	2.06	1.06E-04	16.59	32.70

G protein subunit alpha z	2.05	4.10E-03	1.85	3.95
aldo-keto reductase family 1, member C-like 1	2.04	2.03E-02	2.78	5.40
formin homology 2 domain containing 3	2.04	3.06E-03	3.21	6.26
DExH-box helicase 58	2.02	1.98E-02	2.28	4.45
Unknown, ENSSSCG00000006851	2.01	8.00E-03	15.42	32.15

Table S4: Top Endometrial Down-regulated Genes from Day 14 *CYP19A1*$^{+/+}$ to Day 17 *CYP19A1*$^{+/+}$.

Gene Name	FC	FDR	Day 14 *CYP19A1*+/+ CPM AVG	Day 17 *CYP19A1*+/+ CPM AVG
NSF attachment protein beta	-2.00	5.02E-04	8.91	4.60
collagen type I alpha 1 chain	-2.00	3.78E-05	201.22	101.68
S100 calcium binding protein A6	-2.01	1.67E-03	57.94	28.95
Unknown, ENSSSCG00000012627	-2.02	3.97E-02	5.59	2.73
matrix metallopeptidase 15	-2.02	9.58E-03	5.36	2.76
diacylglycerol kinase eta	-2.02	8.39E-04	38.63	20.24
tetraspanin 15	-2.02	2.28E-04	17.35	8.84
collagen type XVI alpha 1 chain	-2.03	2.12E-03	19.23	10.75
sodium/hydrogen exchanger 1	-2.03	9.70E-05	6.02	3.06
Metalloreductase STEAP1	-2.04	3.09E-02	19.65	11.01
sortilin related receptor 1	-2.04	2.07E-05	98.92	50.03
lysosomal protein transmembrane 4 beta	-2.05	4.25E-04	100.44	49.83
syncoilin, intermediate filament protein	-2.05	3.50E-04	6.77	3.43
dual specificity phosphatase 4	-2.05	1.05E-03	15.19	7.66
sosondowah ankyrin repeat domain family member A	-2.05	5.38E-03	7.94	4.13
Unknown, ENSSSCG00000036483	-2.06	7.12E-04	29.37	14.82
Rho guanine nucleotide exchange factor 37	-2.06	2.86E-02	15.28	7.76
Sus scrofa synuclein alpha interacting protein (SNCAIP), transcript variant 1, mRNA.	-2.06	4.47E-02	3.25	1.63
3-hydroxybutyrate dehydrogenase 1	-2.08	2.04E-03	26.13	13.10
intraflagellar transport 122	-2.09	1.45E-04	18.42	9.48
Unknown, ENSSSCG00000017129	-2.09	1.77E-02	7.20	3.58
ephrin-B2	-2.10	1.55E-04	20.27	9.84
transglutaminase 2	-2.10	2.97E-04	96.61	48.80
Unknown, ENSSSCG00000004709	-2.10	1.95E-03	32.00	16.41
WW domain containing E3 ubiquitin protein ligase 2	-2.10	2.03E-02	22.01	9.06
Carbonic anhydrase 3	-2.10	3.25E-02	3.31	1.54
solute carrier organic anion transporter family member 4C1	-2.10	3.05E-02	33.13	14.00
dynamin 3	-2.10	6.35E-04	18.53	9.23
coiled-coil domain containing 190	-2.10	2.12E-03	15.08	7.16

calmodulin-like 4	-2.11	6.09E-05	8.27	4.06
TSC22 domain family member 1	-2.12	4.25E-05	58.34	29.40
connector enhancer of kinase suppressor of Ras 2	-2.12	8.40E-03	4.12	1.67
phospholipid phosphatase related 1	-2.12	3.38E-02	6.11	3.29
thrombospondin 3	-2.12	6.21E-03	2.15	1.04
Sus scrofa phosphoglycerate dehydrogenase (PHGDH), mRNA.	-2.13	3.14E-02	70.05	39.79
phosphoglucomutase 3	-2.14	9.21E-04	33.61	17.61
neuralized E3 ubiquitin protein ligase 1	-2.15	1.80E-04	10.02	4.68
chromosome 10 open reading frame 10	-2.15	5.83E-03	11.90	5.71
adenylate cyclase 6	-2.17	4.53E-04	24.13	12.28
Unknown, ENSSSCG00000037530	-2.18	1.16E-04	3.49	1.67
Sus scrofa cytochrome P450, family 4, subfamily F, polypeptide 55 (CYP4F55), mRNA.	-2.18	1.22E-02	9.92	4.97
beta-1,3-galactosyltransferase 5	-2.18	2.49E-02	1.75	0.86
Unknown, ENSSSCG00000005398	-2.19	3.21E-02	65.29	33.22
kynurenine 3-monooxygenase	-2.19	4.16E-04	46.39	24.78
solute carrier family 16 member 1	-2.20	1.62E-04	30.46	13.03
lactate dehydrogenase B	-2.20	1.91E-05	271.05	130.06
matrix metallopeptidase 23B	-2.20	2.89E-02	4.75	2.22
Sus scrofa collagen type III alpha 1 chain (COL3A1), mRNA.	-2.20	4.55E-06	1446.25	701.92
cadherin 20	-2.21	1.65E-03	10.08	4.81
Sus scrofa complement C7 (C7), mRNA.	-2.21	8.69E-06	24.90	11.30
family with sequence similarity 129 member B	-2.21	1.05E-06	75.57	35.85
Unknown, ENSSSCG00000000951	-2.22	1.69E-06	116.59	55.45
Unknown, ENSSSCG00000027790	-2.22	7.36E-05	48.78	21.82
adenosylhomocysteinase like 1	-2.23	8.05E-06	49.28	24.04
reelin	-2.24	1.95E-03	1.62	0.75
nebulette	-2.24	1.82E-08	9.62	4.46
Protein S100-G Protein S100-G, minor isoform	-2.24	4.12E-02	3.50	1.68
beta-1,4-N-acetyl-galactosaminyltransferase 3	-2.24	4.83E-03	18.46	8.60
transmembrane protein 72	-2.25	2.55E-03	27.52	12.40
biglycan	-2.25	2.56E-02	2.46	1.02
abhydrolase domain containing 12B	-2.25	2.52E-02	4.58	2.16
phosphotriesterase related	-2.27	1.06E-03	4.51	2.04
fibrillin 2	-2.27	3.14E-03	1.47	0.68
V-set domain containing T-cell activation inhibitor 1	-2.28	6.52E-03	18.76	8.06
solute carrier family 24 member 4	-2.29	1.72E-02	45.91	21.85
NDP, norrin cystine knot growth factor	-2.29	1.70E-03	5.66	2.56
cAMP responsive element modulator	-2.29	2.06E-04	84.66	44.45
Sus scrofa fibrinogen like 2 (FGL2), mRNA.	-2.29	5.95E-03	74.08	44.22

cysteine dioxygenase type 1	-2.31	3.37E-07	98.10	45.21
Unknown, ENSSSCG00000016426	-2.35	1.94E-04	16.65	7.64
SH3 and PX domains 2A	-2.36	1.15E-06	15.51	7.01
transforming growth factor beta 2	-2.36	3.68E-04	22.47	10.07
talin 2	-2.37	1.46E-04	34.56	16.12
cell adhesion molecule L1 like	-2.38	2.59E-03	3.27	1.30
oxoglutarate dehydrogenase	-2.38	4.86E-03	62.54	26.15
PHD finger protein 19	-2.38	8.63E-05	4.88	2.13
syntaxin binding protein 6	-2.38	4.33E-03	35.02	15.14
Unknown, ENSSSCG00000010499	-2.41	4.16E-03	34.34	14.96
DLG associated protein 1	-2.42	2.03E-02	4.39	1.94
Matrix Gla protein	-2.42	3.44E-06	22.98	9.62
family with sequence similarity 189 member A2	-2.43	6.04E-05	21.05	9.02
acyl-CoA synthetase long chain family member 3	-2.45	2.19E-05	75.95	32.89
dihydropyrimidinase	-2.46	1.80E-04	4.56	1.84
5'-aminolevulinate synthase 2	-2.46	4.07E-02	20.09	7.32
cAMP responsive element binding protein 3 like 4	-2.47	4.69E-02	4.50	1.84
protein phosphatase 1 regulatory subunit 3B	-2.49	4.64E-05	34.35	14.15
Sus scrofa mitochondrial carrier 1 (MTCH1), transcript variant 1, mRNA.	-2.50	4.55E-06	101.15	43.59
C-C motif chemokine 21 precursor	-2.51	1.35E-02	2.43	0.99
adenylate cyclase 9	-2.51	1.06E-04	21.80	9.60
ATP binding cassette subfamily G member 1	-2.52	1.28E-03	9.99	4.34
hemoglobin subunit beta	-2.53	4.66E-02	1277.31	486.27
docking protein 5	-2.54	2.51E-02	5.03	1.75
spalt like transcription factor 2	-2.55	2.37E-03	24.28	11.33
Unknown, ENSSSCG00000032569	-2.56	1.93E-02	30.96	12.15
growth regulation by estrogen in breast cancer 1 like	-2.57	1.74E-06	10.72	4.49
solute carrier family 12 member 8	-2.57	8.38E-05	4.22	1.69
Unknown, ENSSSCG00000035617	-2.57	4.38E-02	7.10	3.12
Rho GTPase activating protein 22	-2.58	1.18E-03	20.00	8.24
keratin 14	-2.59	4.50E-04	9.87	3.87
copine 5	-2.60	2.03E-02	1.23	0.48
peptidyl arginine deiminase 2	-2.60	1.16E-04	4.22	1.68
Unknown, ENSSSCG00000040088	-2.60	2.80E-10	4.69	1.86
glutamate ionotropic receptor delta type subunit 2	-2.61	1.24E-03	10.22	3.99
ATP binding cassette subfamily A member 8	-2.63	1.41E-07	14.85	5.99
polypeptide N-acetylgalactosaminyltransferase like 5	-2.64	1.18E-04	21.19	8.64
syntrophin beta 1	-2.65	1.54E-02	73.22	25.94
sodium voltage-gated channel alpha subunit 3	-2.67	1.66E-02	1.09	0.49

ubiquitin specific peptidase 43	-2.70	1.16E-04	6.15	2.53
discs large MAGUK scaffold protein 2	-2.71	4.79E-04	9.41	3.21
Unknown, ENSSSCG00000031957	-2.71	6.21E-04	3.12	1.14
Unknown, ENSSSCG00000038043	-2.72	4.09E-02	0.52	0.19
G protein-coupled receptor 68	-2.76	2.03E-02	2.90	1.06
Sus scrofa S100 calcium binding protein A14 (S100A14), mRNA.	-2.76	4.10E-05	35.99	14.21
Unknown, ENSSSCG00000036946	-2.79	4.79E-04	65.97	22.38
glycogen phosphorylase, liver form	-2.79	2.01E-06	21.63	7.80
zinc finger DHHC-type containing 2	-2.80	4.68E-05	18.29	6.85
eva-1 homolog A, regulator of programmed cell death	-2.81	8.22E-03	4.68	2.13
zinc finger protein ZFPM2	-2.81	2.58E-04	3.23	1.12
synaptotagmin 1	-2.81	1.18E-03	2.40	0.89
Unknown, ENSSSCG00000036785	-2.85	2.58E-04	14.00	5.03
ectonucleoside triphosphate diphosphohydrolase 3	-2.87	5.11E-08	10.76	3.78
flavin containing monooxygenase 5	-2.87	1.81E-05	56.73	27.29
leucine rich repeat neuronal 1	-2.88	1.25E-04	3.29	1.13
Unknown, ENSSSCG00000010086	-2.89	1.02E-02	2.98	1.06
protein phosphatase 1 regulatory subunit 3D	-2.90	3.60E-05	14.09	5.09
Unknown, ENSSSCG00000017608	-2.90	4.91E-05	34.40	12.60
ATPase phospholipid transporting 8B3	-2.93	7.78E-03	0.67	0.23
CD209 antigen	-2.93	1.30E-03	5.61	1.95
stomatin	-2.93	1.95E-11	100.65	32.78
potassium voltage-gated channel interacting protein 1	-2.94	1.11E-04	3.96	1.44
SUN domain containing ossification factor	-2.94	1.03E-10	244.02	89.09
Unknown, ENSSSCG00000036224	-2.95	1.02E-02	3.56	2.98
5-hydroxytryptamine receptor 1D	-2.98	1.67E-06	4.55	1.59
glutathione S-transferase Mu 3-like	-3.01	3.05E-04	64.89	22.46
exostosin like glycosyltransferase 1	-3.02	3.05E-02	5.36	2.53
fibroblast growth factor 13	-3.02	1.37E-05	16.14	5.19
Sus scrofa annexin A8 (ANXA8), mRNA.	-3.05	2.38E-02	6.70	1.74
phosphatidylinositol transfer protein, cytoplasmic 1	-3.06	1.67E-06	152.61	62.04
Sus scrofa cell division cycle 25C (CDC25C), mRNA.	-3.06	4.63E-02	6.24	1.84
arylsulfatase E (chondrodysplasia punctata 1)	-3.07	4.14E-08	20.63	5.96
lymphatic vessel endothelial hyaluronan receptor 1	-3.08	7.50E-04	3.83	1.26
zinc finger homeobox 4	-3.10	5.39E-04	2.15	0.70
cytidine deaminase	-3.11	1.11E-05	37.33	12.03
Unknown, ENSSSCG00000034750	-3.12	3.97E-02	1.12	0.38
embigin	-3.12	6.53E-04	161.59	42.13
rho-related GTP-binding protein RhoV	-3.15	1.14E-02	2.33	0.68

GRB2 binding adaptor protein, transmembrane	-3.17	3.56E-03	2.67	0.87
Unknown, ENSSSCG00000031906	-3.21	1.05E-06	61.55	20.31
solute carrier family 38 member 1	-3.21	6.81E-09	282.07	96.88
chromosome 12 open reading frame 56	-3.23	9.14E-03	1.76	0.56
selectin L	-3.24	1.93E-03	74.66	19.21
integrin subunit beta like 1	-3.26	6.08E-03	2.86	0.82
ADAM metallopeptidase with thrombospondin type 1 motif 18	-3.31	2.69E-04	31.46	10.23
fibronectin type III domain containing 1	-3.31	1.61E-09	18.82	6.23
ST6 N-acetylgalactosaminide alpha-2,6-sialyltransferase 1	-3.32	2.76E-04	1.44	0.46
mitogen-activated protein kinase 13	-3.32	2.22E-05	16.85	5.61
Unknown, ENSSSCG00000039147	-3.36	1.67E-06	115.13	32.54
putative monooxygenase p33MONOX	-3.38	6.76E-07	46.16	13.13
Unknown, ENSSSCG00000010703	-3.39	3.94E-07	104.41	32.41
joining chain of multimeric IgA and IgM	-3.39	2.16E-06	63.28	17.56
creatine kinase, mitochondrial 2	-3.42	2.13E-03	2.14	0.70
radial spoke head 14 homolog	-3.44	4.62E-03	4.19	1.23
EPH receptor A7	-3.45	9.21E-04	5.28	1.30
Xg blood group	-3.48	7.20E-05	3.87	1.13
Unknown, ENSSSCG00000017577	-3.48	1.40E-02	1.15	0.36
S-methylmethionine--homocysteine S-methyltransferase BHMT2	-3.50	8.40E-03	0.78	0.23
xanthine dehydrogenase	-3.54	1.26E-02	0.72	0.20
collagen beta(1-O)galactosyltransferase 2	-3.55	3.41E-10	11.60	3.48
embryonal Fyn-associated substrate	-3.56	1.32E-05	14.34	4.38
Unknown, ENSSSCG00000037206	-3.57	2.93E-02	1.21	0.36
nanos C2HC-type zinc finger 1	-3.59	2.61E-03	4.56	1.20
cell wall biogenesis 43 C-terminal homolog	-3.59	1.87E-04	46.97	11.93
ring finger protein 152	-3.69	8.87E-15	44.67	12.10
POF1B, actin binding protein	-3.70	3.32E-04	6.76	1.81
multimerin 1	-3.71	3.83E-04	2.76	0.87
Unknown, ENSSSCG00000031550	-3.82	1.50E-02	33.60	8.57
type II iodothyronine deiodinase	-3.89	3.77E-03	12.56	4.98
diacylglycerol kinase gamma	-3.89	1.36E-07	23.86	6.61
fibroblast growth factor 12	-3.94	2.86E-02	1.41	0.26
USH1 protein network component harmonin	-3.97	3.06E-04	4.93	1.29
melanophilin	-3.98	2.31E-06	14.11	4.14
spexin hormone	-4.05	1.56E-03	7.48	1.86
Unknown, ENSSSCG00000024669	-4.09	3.57E-09	57.53	15.20
RAN binding protein 17	-4.11	1.19E-08	110.70	30.11
growth arrest and DNA damage-inducible protein GADD45 gamma	-4.12	3.98E-04	6.28	1.61
fin bud initiation factor homolog (zebrafish)	-4.15	5.38E-03	9.96	2.42

chordin like 1	-4.19	3.69E-05	85.23	18.95
Unknown, ENSSSCG00000015401	-4.28	1.16E-08	1.92	0.49
blood vessel epicardial substance	-4.36	1.97E-03	4.00	0.68
Unknown, ENSSSCG00000017032	-4.42	6.23E-03	2.85	0.61
leucine rich repeat LGI family member 2	-4.48	1.54E-03	10.34	1.51
Unknown, ENSSSCG00000036279	-4.59	1.11E-02	3.53	0.74
notum, palmitoleoyl-protein carboxylesterase	-4.63	1.16E-03	3.09	0.59
cytochrome b5 reductase 1	-4.68	8.66E-06	5.86	1.28
Unknown, ENSSSCG00000036125	-4.68	3.27E-06	3.31	0.62
CDC42 small effector 2	-4.69	1.95E-11	143.52	28.84
opsin 4	-4.74	9.52E-05	3.17	0.69
armadillo repeat containing 12	-4.84	1.77E-03	3.51	0.75
Unknown, ENSSSCG00000038037	-4.84	1.21E-02	11.86	2.45
solute carrier family 7 member 2	-4.89	6.00E-05	18.05	3.68
fibrinogen gamma chain	-4.97	1.44E-04	4.82	0.91
Unknown, ENSSSCG00000000983	-4.98	4.44E-03	4.19	0.72
alanine and arginine rich domain containing protein	-5.05	1.80E-04	3.28	0.62
solute carrier family 46 member 2	-5.07	5.16E-11	11.96	2.74
Protein S100-A12	-5.07	1.11E-03	2.56	0.58
fibromodulin	-5.13	2.22E-05	12.91	2.81
4-hydroxyphenylpyruvate dioxygenase	-5.26	1.82E-03	2.36	0.45
proline rich basic protein 1	-5.26	6.35E-04	3.00	0.57
sarcosine dehydrogenase	-5.30	2.86E-03	0.39	0.08
T-box 20	-5.42	1.31E-03	2.70	0.37
Unknown, ENSSSCG00000032922	-5.47	9.82E-06	21.58	4.95
huntingtin associated protein 1	-5.56	4.92E-04	1.16	0.19
Unknown, ENSSSCG00000027874	-5.64	3.62E-02	1.43	0.26
Unknown, ENSSSCG00000038475	-5.66	2.36E-09	13.21	2.64
synaptonemal complex protein 2	-5.80	1.87E-16	56.26	8.82
junctophilin 4	-5.98	2.73E-05	1.99	0.36
annexin A10	-6.04	4.58E-02	2.10	1.03
betaine--homocysteine S-methyltransferase 1	-6.05	4.46E-02	1.38	0.50
cytochrome P450 family 4 subfamily B member 1	-6.12	2.94E-03	1.46	0.22
integrin subunit beta 6	-6.14	2.18E-12	9.47	1.94
solute carrier family 23 member 1	-6.15	1.39E-04	25.18	4.32
dpy-19 like 2	-6.28	3.03E-07	9.50	1.02
mucin 6, oligomeric mucus/gel-forming	-6.41	4.49E-02	0.55	0.07
Unknown, ENSSSCG00000028567	-6.61	3.25E-03	7.35	0.83
ankyrin repeat domain 34B	-6.86	1.58E-10	17.83	2.60
molybdenum cofactor sulfurase	-6.98	3.80E-08	40.40	5.42

keratocan	-7.46	8.80E-04	36.72	17.44
C-C motif chemokine ligand 28	-8.10	6.12E-06	110.73	10.85
phospholipid phosphatase 4	-8.44	4.95E-13	26.00	3.21
dispatched RND transporter family member 3	-8.49	1.41E-02	4.77	0.26
marginal zone B and B1 cell specific protein	-8.78	5.99E-05	2.65	0.55
carboxylesterase 3 precursor	-8.99	3.96E-11	115.47	14.27
neuromedin B	-9.12	6.29E-18	250.98	26.85
glycine-N-acyltransferase like 2	-9.22	1.87E-16	29.95	3.49
gamma-aminobutyric acid type A receptor pi subunit	-9.61	6.93E-12	17.60	2.29
Unknown, ENSSSCG00000032503	-13.57	3.69E-05	1205.89	162.36
cation channel sperm associated auxiliary subunit beta	-14.52	3.38E-08	26.44	10.19
Sus scrofa claudin 22 (CLDN22), mRNA.	-14.69	2.97E-04	3.64	0.20
alkylglycerol monooxygenase	-18.36	7.03E-08	3.06	0.17
Sus scrofa opticin (OPTC), mRNA.	-18.52	1.44E-03	16.21	0.21
actin, beta like 2	-19.68	4.76E-08	5.78	0.35
Unknown, ENSSSCG00000030554	-22.60	1.81E-05	4.75	0.17
Unknown, ENSSSCG00000004213	-24.58	2.30E-14	4.45	0.18
Sus scrofa salivary lipocalin (SAL1), mRNA.	-26.16	3.08E-15	330.27	8.99
thioesterase superfamily member 5	-26.66	4.89E-06	8.61	0.26
Unknown, ENSSSCG00000031475	-61.69	6.08E-08	27.99	0.58
Unknown, ENSSSCG00000037293	-67.85	2.31E-07	9.95	0.10
Sus scrofa S100 calcium binding protein A8 (S100A8), mRNA.	-114.85	4.34E-06	20.54	0.22
S100 calcium binding protein A9	-181.93	1.47E-13	113.43	0.69

Table S5: Top Endometrial Up-regulated Genes from Day 14 *CYP19A1*$^{-/-}$ to Day 17 *CYP19A1*$^{-/-}$.

Gene Name	FC	FDR	Day 14 *CYP19A1*-/- CPM average	Day 17 *CYP19A1*-/- CPM average
Sus scrofa pregnancy-associated glycoprotein 6 (PAG6), mRNA.	230.17	7.56E-04	0.02	10.25
synaptotagmin 4	33.41	1.06E-13	0.08	2.62
Unknown, ENSSSCG00000015159	20.18	4.08E-04	0.58	3.16
Sus scrofa corneodesmosin (CDSN), mRNA.	16.06	2.40E-12	0.24	3.22
trace amine associated receptor 1	15.83	6.09E-04	1.14	20.08
Unknown, ENSSSCG00000031023	15.29	3.35E-05	17.68	276.61
histidine decarboxylase	12.29	1.06E-07	1.78	26.73
solute carrier family 36 member 2	9.95	7.95E-04	0.80	3.74
ATP binding cassette subfamily A member 12	8.93	6.01E-04	0.62	5.55
secreted phosphoprotein 1	8.84	8.99E-08	14.06	185.36
lithostathine-like precursor	8.33	1.76E-04	0.09	0.49

carbonic anhydrase 8	8.32	6.59E-06	2.71	16.16
pyrimidinergic receptor P2Y6	8.12	1.31E-06	0.36	2.80
adenosine A1 receptor	8.11	2.66E-03	0.48	1.57
aquaporin 8	7.93	1.41E-02	0.18	2.16
Wnt family member 7A	7.62	2.78E-08	0.33	2.16
Sus scrofa C-X-C motif chemokine ligand 14 (CXCL14), mRNA.	6.96	4.54E-06	1.35	20.05
Unknown, ENSSSCG00000009239	6.74	1.12E-03	2.65	15.29
adenylate cyclase 8	6.56	8.80E-06	0.09	0.61
activating transcription factor 3	6.43	2.53E-08	8.19	92.04
suppressor of cytokine signaling 1	6.28	7.22E-04	0.68	6.79
Unknown, ENSSSCG00000037927	6.21	7.43E-03	2.97	15.91
hepatitis A virus cellular receptor 1 precursor	6.17	4.28E-02	0.06	1.49
PKHD1, fibrocystin/polyductin	6.06	7.36E-06	1.35	10.61
Interferon gamma	6.00	1.32E-02	0.12	4.64
N-acylethanolamine acid amidase	6.00	9.66E-08	20.09	111.12
Unknown, ENSSSCG00000033570	5.96	8.70E-05	4.92	25.95
basic helix-loop-helix family member e40	5.87	4.13E-14	4.50	25.36
SLIT-ROBO Rho GTPase activating protein 3	5.75	4.84E-07	9.30	47.50
Unknown, ENSSSCG00000035073	5.70	8.55E-04	0.98	8.39
serine peptidase inhibitor, Kazal type 9	5.53	2.90E-03	10.02	40.98
amphiregulin precursor	5.50	2.87E-05	0.10	0.55
Unknown, ENSSSCG00000007978	5.48	1.49E-02	9.37	49.97
alpha hemoglobin stabilizing protein	5.43	3.12E-02	0.89	2.59
Metalloreductase STEAP1	5.30	1.41E-05	9.49	31.16
Unknown, ENSSSCG00000038652	5.28	5.23E-04	0.62	3.46
Unknown, ENSSSCG00000033677	5.23	7.94E-04	7.82	35.87
carbonic anhydrase 2	5.19	3.04E-03	27.26	145.42
Unknown, ENSSSCG00000038257	5.16	5.30E-03	0.17	0.91
interferon stimulated exonuclease gene 20	5.07	1.49E-02	1.30	2.73
cytochrome P450 family 26 subfamily B member 1	4.92	1.04E-05	5.15	21.25
Unknown, ENSSSCG00000022839	4.68	2.90E-04	1.23	5.35
teneurin transmembrane protein 2	4.64	1.31E-02	0.07	0.48
protein phosphatase with EF-hand domain 2	4.57	1.12E-05	2.25	10.44
purinergic receptor P2Y2	4.37	3.14E-03	1.25	6.63
cyclic nucleotide gated channel alpha 1	4.36	9.78E-04	0.26	1.21
C-X-C motif chemokine 9 precursor	4.33	9.71E-05	2.02	10.57
LDL receptor related protein 2	4.28	3.71E-06	22.05	72.12
family with sequence similarity 237 member B	4.21	4.15E-03	9.15	34.17
adaptor related protein complex 1 sigma 3 subunit	4.21	1.18E-17	8.04	34.62

Sus scrofa pleckstrin homology like domain family A member 2 (PHLDA2), mRNA.	4.18	1.75E-03	1.89	12.63
DNA-binding protein inhibitor ID-2	4.10	2.78E-08	10.93	46.02
glutamate decarboxylase like 1	4.08	2.12E-03	0.16	0.72
CUGBP Elav-like family member 4	4.06	1.47E-03	0.17	0.77
makorin ring finger protein 3	4.05	3.04E-03	0.49	2.05
Sus scrofa CD163 molecule-like 1 (CD163L1), mRNA.	4.02	1.70E-03	0.13	0.53
solute carrier organic anion transporter family member 1A2	3.97	3.45E-06	8.10	37.81
glutamate carboxypeptidase 2	3.94	5.62E-07	7.93	18.43
tubulin alpha like 3	3.91	2.53E-08	0.95	3.83
Unknown, ENSSSCG00000040056	3.91	9.12E-15	29.41	116.55
aldehyde dehydrogenase 3 family member B2	3.87	1.45E-02	0.79	2.72
hemoglobin subunit beta	3.84	3.39E-03	643.03	1998.10
proto-oncogene c-Fos	3.82	1.68E-02	30.77	136.77
Dipeptidyl peptidase 4 Dipeptidyl peptidase 4 membrane form Dipeptidyl peptidase 4 soluble form	3.79	4.56E-04	14.59	70.52
Unknown, ENSSSCG00000014727	3.75	3.24E-03	18.27	55.37
Unknown, ENSSSCG00000024161	3.74	8.91E-04	4.21	14.66
SLIT and NTRK like family member 4	3.62	1.01E-03	0.32	1.21
SPHK1 interactor, AKAP domain containing	3.60	1.05E-02	1.64	6.60
matrilysin	3.57	3.13E-02	0.96	4.82
5'-aminolevulinate synthase 2	3.57	8.03E-03	9.16	29.98
Unknown, ENSSSCG00000002849	3.53	2.98E-04	1.40	3.90
protein MGARP	3.49	2.97E-04	0.67	2.42
Unknown, ENSSSCG00000034592	3.45	5.01E-06	5.74	21.39
solute carrier family 26 member 3	3.42	2.05E-02	0.42	1.26
epsin 3	3.40	1.52E-04	0.86	2.63
solute carrier family 37 member 2	3.40	8.70E-05	26.09	89.25
dual specificity phosphatase 9	3.33	9.71E-05	2.41	7.97
phosphoserine aminotransferase 1	3.33	5.96E-07	55.81	187.55
FXYD domain containing ion transport regulator 2	3.31	7.07E-03	22.32	74.02
BRCA1 associated RING domain 1	3.30	8.27E-07	2.29	6.32
Unknown, ENSSSCG00000031957	3.28	2.93E-02	0.67	2.76
hyaluronan binding protein 2	3.25	1.01E-02	0.21	0.69
methylenetetrahydrofolate dehydrogenase (NADP+ dependent) 2, methenyltetrahydrofolate cyclohydrolase	3.17	6.21E-06	8.60	26.10
15-hydroxyprostaglandin dehydrogenase	3.15	7.17E-10	11.52	36.68
potassium voltage-gated channel subfamily J member 16	3.11	1.60E-02	4.58	12.36
prolyl 3-hydroxylase 1	3.10	1.70E-05	19.85	58.11
gap junction protein beta 1	3.09	2.05E-02	0.49	1.57

phosphatidylethanolamine-binding protein 4 precursor	3.09	3.73E-02	0.51	1.58
colony stimulating factor 3 receptor	3.07	2.68E-02	1.33	6.48
Unknown, ENSSSCG00000008314	3.04	1.04E-04	24.55	70.43
hemoglobin subunit mu	3.00	1.40E-02	1.61	5.00
adhesion G protein-coupled receptor B1	2.98	1.88E-02	0.20	0.62
interleukin 1 alpha	2.98	3.10E-04	10.00	26.88
neuronal vesicle trafficking associated 2	2.96	4.45E-02	0.33	1.00
extended synaptotagmin 3	2.96	2.20E-03	1.00	3.21
Sus scrofa radical S-adenosyl methionine domain containing 2 (RSAD2), mRNA.	2.94	1.57E-02	5.93	13.39
endonuclease domain containing 1	2.92	1.20E-03	13.43	36.13
family with sequence similarity 196 member B	2.89	5.26E-08	2.17	5.92
Unknown, ENSSSCG00000035559	2.88	3.55E-02	5.63	16.78
electrogenic sodium bicarbonate cotransporter 4	2.87	2.68E-03	0.32	0.95
solute carrier family 9 member A4	2.87	4.69E-03	7.51	16.11
mitogen-activated protein kinase kinase 6	2.87	4.59E-05	4.45	11.89
ovo like transcriptional repressor 1	2.87	3.21E-02	1.82	6.49
Unknown, ENSSSCG00000023956	2.84	6.42E-06	5.53	19.91
dual specificity phosphatase 1	2.83	1.49E-03	42.39	179.88
ADM Adrenomedullin Proadrenomedullin N-20 terminal peptide	2.82	2.04E-04	13.26	39.28
SMAD family member 6	2.81	1.77E-02	1.13	3.49
Unknown, ENSSSCG00000026653	2.77	2.07E-02	0.35	1.00
FAM20A, golgi associated secretory pathway pseudokinase	2.77	2.81E-06	8.11	21.41
UDP-GlcNAc:betaGal beta-1,3-N-acetylglucosaminyltransferase 3	2.75	5.05E-05	4.11	12.26
eukaryotic translation initiation factor 4E family member 3	2.75	2.68E-06	31.75	89.79
ankyrin repeat domain 22	2.74	2.05E-04	4.93	12.51
Unknown, ENSSSCG00000040980	2.68	4.22E-02	0.21	0.53
Unknown, ENSSSCG00000034514	2.67	4.07E-02	2.59	7.16
nephronectin	2.66	2.09E-03	8.36	20.58
Unknown, ENSSSCG00000013788	2.65	1.11E-03	0.84	2.23
glucosaminyl (N-acetyl) transferase family member 7	2.64	2.62E-03	2.92	8.33
dihydrouridine synthase 4 like	2.62	1.39E-03	1.36	3.59
GLI pathogenesis related 1	2.60	1.02E-06	2.86	7.63
STAM binding protein like 1	2.59	5.18E-03	1.43	3.60
tubulointerstitial nephritis antigen like 1	2.56	1.53E-02	28.54	70.20
sorting nexin 10	2.56	3.42E-03	2.29	4.86
inhibin beta B chain precursor	2.54	2.47E-05	6.85	17.60
zinc finger DHHC-type containing 13	2.53	1.20E-05	12.29	30.99
Fatty acid-binding protein, heart	2.53	4.27E-05	5.28	14.08

serum/glucocorticoid regulated kinase 1	2.51	9.66E-08	45.39	121.50
homeobox protein DLX-5	2.50	2.15E-08	6.46	16.63
serpin family B member 5	2.50	2.62E-03	17.25	46.56
formin homology 2 domain containing 3	2.50	4.47E-06	2.24	6.10
Unknown, ENSSSCG00000009162	2.50	2.28E-02	2.86	7.32
cilia and flagella associated protein 69	2.49	2.85E-04	30.44	72.58
crystallin alpha B	2.49	1.20E-02	3.02	7.24
arginase 1	2.47	2.05E-02	1.11	2.83
potassium voltage-gated channel subfamily E regulatory subunit 3	2.46	1.65E-03	6.45	15.58
keratin associated protein 24-1	2.43	1.83E-03	9.65	26.04
neurotrophic receptor tyrosine kinase 2	2.41	4.23E-03	4.33	17.46
G protein-coupled receptor 22	2.41	7.31E-05	9.78	23.36
aminoadipate-semialdehyde synthase	2.40	1.12E-04	9.49	21.23
allograft inflammatory factor 1 like	2.39	1.32E-02	4.66	9.52
heparin binding EGF like growth factor	2.38	3.01E-02	1.23	3.01
Unknown, ENSSSCG00000033338	2.36	4.18E-02	20.66	47.85
transient receptor potential cation channel subfamily V member 5	2.35	1.33E-03	61.06	131.86
Unknown, ENSSSCG00000038778	2.35	9.91E-03	14.28	34.54
ecto-NOX disulfide-thiol exchanger 1	2.33	1.10E-02	0.74	1.79
zinc finger DHHC-type containing 18	2.33	2.91E-03	1.47	3.31
Unknown, ENSSSCG00000023305	2.29	4.71E-02	25.96	61.14
Rho GTPase activating protein 18	2.27	1.05E-07	16.85	39.25
SH3 domain containing GRB2 like 2, endophilin A1	2.24	2.05E-02	14.30	35.16
Unknown, ENSSSCG00000040854	2.22	2.40E-03	9.58	21.88
additional sex combs like 3, transcriptional regulator	2.22	7.36E-03	1.29	3.70
UBX domain protein 2B	2.22	2.14E-02	7.42	15.38
zinc finger protein 608	2.22	2.52E-05	7.11	16.14
leucine rich repeat and fibronectin type III domain containing 4	2.21	7.60E-03	1.47	3.33
H2.0 like homeobox	2.21	2.03E-02	1.12	2.40
Unknown, ENSSSCG00000038811	2.20	7.70E-03	6.28	13.74
WNT1 inducible signaling pathway protein 2	2.20	2.20E-02	1.61	3.13
protein tyrosine phosphatase, receptor type Z1	2.18	1.88E-02	1.03	2.27
Sus scrofa solute carrier family 1 (neuronal/epithelial high affinity glutamate transporter, system Xag), member 1 (SLC1A1), mRNA.	2.17	1.04E-02	5.13	15.33
reticulon 4 interacting protein 1	2.17	2.74E-03	1.94	4.15
LDL receptor related protein 8	2.16	3.55E-03	5.85	12.78
myomesin 3	2.15	3.15E-02	0.46	1.03
GRAM domain containing 1B	2.15	3.85E-02	2.76	6.31
platelet derived growth factor subunit A	2.15	9.78E-04	1.39	3.07

estradiol 17-beta-dehydrogenase 2	2.15	3.95E-03	14.21	29.67
erb-b2 receptor tyrosine kinase 4	2.13	2.57E-03	5.12	11.29
kelch like family member 14	2.13	1.40E-03	3.06	6.58
aldehyde dehydrogenase 7 family member A1	2.13	7.13E-03	49.71	96.83
ATPase 13A4	2.12	1.57E-04	48.09	105.44
CUB and Sushi multiple domains 1	2.11	2.05E-02	0.40	0.87
Unknown, ENSSSCG00000039473	2.11	2.93E-07	49.42	106.93
NIPA like domain containing 1	2.11	1.12E-04	6.46	14.25
RELT like 1	2.10	4.69E-03	15.78	32.03
T-cell surface antigen CD2 precursor	2.10	6.04E-04	3.86	8.32
ZFP64 zinc finger protein	2.09	1.76E-04	2.91	6.26
LY6/PLAUR domain containing 6B	2.08	3.66E-02	8.29	17.73
myelin regulatory factor-like	2.08	6.07E-03	1.59	3.35
kinesin family member 12	2.08	4.15E-03	3.33	7.46
phytanoyl-CoA 2-hydroxylase interacting protein like	2.07	2.83E-04	6.48	13.87
zinc finger and BTB domain containing 10	2.07	9.53E-08	95.74	203.25
zinc finger homeobox 4	2.07	4.45E-02	1.09	2.17
gap junction protein beta 3	2.06	2.10E-02	7.29	14.87
FYVE, RhoGEF and PH domain containing 4	2.06	2.74E-06	24.44	51.87
Unknown, ENSSSCG00000025992	2.06	1.90E-02	15.22	34.87
coiled-coil-helix-coiled-coil-helix domain containing 10	2.06	1.91E-02	4.21	8.92
aminoacyl tRNA synthase complex-interacting multifunctional protein 2 isoform 1	2.06	1.60E-02	1.44	3.39
ubiquitin-like protein ISG15	2.05	2.09E-02	10.08	17.82
SLIT and NTRK like family member 6	2.03	3.39E-02	3.76	5.22
solute carrier family 29 member 1 (Augustine blood group)	2.03	4.67E-02	1.17	2.21
PX domain containing serine/threonine kinase like	2.02	5.87E-05	15.76	32.68
Unknown, ENSSSCG00000039222	2.01	2.27E-02	29.79	62.72
mal, T-cell differentiation protein 2 (gene/pseudogene)	2.01	5.10E-03	100.78	214.91

Table S6: Top Endometrial Down-regulated Genes from Day 14 *CYP19A1*$^{-/-}$ to Day 17 *CYP19A1*$^{-/-}$.

Gene Name	FC	FDR	Day 14 *CYP19A1-/-* CPM average	Day 17 *CYP19A1-/-* CPM average
Rho GTPase activating protein 22	-2.00	3.73E-02	16.43	8.24
syntaphilin	-2.01	1.12E-02	8.81	4.51
thrombospondin 3	-2.01	8.43E-03	2.05	1.05
sodium voltage-gated channel alpha subunit 1	-2.01	1.60E-02	2.33	1.19
cilia and flagella associated protein 46	-2.01	2.85E-03	4.89	2.68

glutathione S-transferase kappa 1	-2.02	7.53E-03	10.73	5.56
Unknown, ENSSSCG00000032949	-2.02	1.36E-02	21.00	11.02
pleckstrin and Sec7 domain containing	-2.03	1.41E-02	1.61	0.81
collagen type XVI alpha 1 chain	-2.03	3.58E-05	22.50	11.41
MGAT4 family member D	-2.03	1.16E-02	11.89	5.70
transmembrane protein 72	-2.04	8.42E-04	24.49	12.95
solute carrier family 38 member 1	-2.04	1.31E-03	246.21	120.63
syndecan 1	-2.05	2.29E-02	5.62	2.68
protein phosphatase 1 regulatory subunit 3B	-2.05	1.24E-02	35.82	16.26
ubiquitin specific peptidase 43	-2.06	1.15E-02	5.49	3.31
beta-1,4-N-acetyl-galactosaminyltransferase 3	-2.06	7.21E-03	17.26	11.06
Sus scrofa translocator protein (TSPO), mRNA.	-2.06	7.30E-03	52.07	25.87
Unknown, ENSSSCG00000036785	-2.06	2.95E-03	10.47	5.54
lactamase beta	-2.06	1.63E-04	21.31	10.60
atypical chemokine receptor 4	-2.07	2.61E-02	6.25	3.09
Kruppel like factor 8	-2.07	2.21E-03	5.59	2.77
UEV and lactate/malate dehyrogenase domains	-2.07	6.99E-04	33.02	15.99
non-SMC condensin I complex subunit G	-2.08	3.97E-03	2.86	1.36
solute carrier family 16 member 14	-2.08	3.64E-02	6.03	3.01
intraflagellar transport 122	-2.09	4.66E-06	16.40	8.08
regulator of G protein signaling 4	-2.09	3.43E-02	7.08	3.47
natriuretic peptide receptor 3	-2.09	4.00E-02	16.46	8.53
netrin G1	-2.09	4.12E-03	14.30	7.48
solute carrier family 38 member 4	-2.10	2.38E-03	5.42	2.78
solute carrier family 46 member 2	-2.10	1.12E-02	11.29	4.98
mitogen-activated protein kinase 13	-2.13	1.05E-02	13.27	6.18
transmembrane protein 100	-2.15	1.25E-02	22.46	11.41
diacylglycerol kinase gamma	-2.15	3.80E-04	15.58	7.09
glycogen phosphorylase, liver form	-2.15	7.71E-04	16.57	7.92
discs large MAGUK scaffold protein 2	-2.16	1.87E-02	9.78	4.29
Unknown, ENSSSCG00000031979	-2.16	1.33E-03	23.92	12.13
phosphotriesterase related	-2.16	5.73E-03	4.63	2.16
connective tissue growth factor precursor	-2.17	6.82E-05	201.07	95.45
phosphatidylinositol transfer protein, cytoplasmic 1	-2.17	2.86E-02	179.06	75.26
collagen type I alpha 1 chain	-2.17	1.87E-02	245.82	125.08
PRELI domain containing 2	-2.19	1.99E-03	34.36	17.51
cell wall biogenesis 43 C-terminal homolog	-2.19	2.94E-02	44.52	20.91
oxoglutarate dehydrogenase	-2.19	2.14E-05	53.42	24.78
interferon alpha and beta receptor subunit 1	-2.20	3.26E-02	68.27	28.21

alpha-2-macroglobulin	-2.20	7.88E-04	84.12	38.19
polypeptide N-acetylgalactosaminyltransferase like 5	-2.20	2.11E-02	21.87	9.16
Rho guanine nucleotide exchange factor 37	-2.21	7.41E-04	19.94	8.95
SEC14 like lipid binding 3	-2.21	3.42E-03	3.68	1.78
sperm associated antigen 1	-2.21	5.55E-05	42.16	19.08
von Willebrand factor A domain containing 3A	-2.22	9.33E-04	8.90	4.59
caspase-3	-2.23	9.32E-03	55.18	27.55
tectonic family member 3	-2.24	3.91E-02	133.78	78.25
annexin A4	-2.24	6.68E-07	287.72	128.90
synaptotagmin like 5	-2.25	9.32E-03	2.46	1.13
cilia and flagella associated protein 74	-2.25	3.41E-02	2.02	0.95
Unknown, ENSSSCG00000017608	-2.26	8.04E-05	27.18	12.64
coiled-coil domain containing 190	-2.28	1.70E-02	15.50	7.24
Unknown, ENSSSCG00000033566	-2.29	4.34E-03	137.70	73.68
phosphoglucomutase 3	-2.29	3.09E-06	40.95	18.36
lymphatic vessel endothelial hyaluronan receptor 1	-2.29	1.44E-03	4.13	1.88
stomatin	-2.29	9.36E-06	79.76	35.28
ring finger protein 125	-2.30	9.64E-05	49.50	23.04
nitric oxide synthase 1	-2.30	1.19E-02	55.34	27.56
contactin 3	-2.31	6.78E-03	35.07	16.77
Unknown, ENSSSCG00000005398	-2.31	5.86E-03	78.55	32.13
BTB domain containing 11	-2.31	3.71E-04	3.13	1.38
zinc finger protein ZFPM2	-2.32	3.65E-02	3.35	1.34
Unknown, ENSSSCG00000012693	-2.33	9.32E-03	1.87	0.83
KIAA1324	-2.34	3.12E-03	56.42	26.89
Unknown, ENSSSCG00000031906	-2.35	2.52E-05	55.15	23.81
neuralized E3 ubiquitin protein ligase 1	-2.36	7.22E-07	12.67	5.51
vascular endothelial growth factor D	-2.37	1.02E-05	23.63	10.12
zinc finger protein 35	-2.38	1.53E-04	10.86	4.94
USH1 protein network component harmonin	-2.38	3.99E-02	5.13	1.94
transglutaminase 2	-2.38	2.35E-06	110.70	47.83
peroxisomal biogenesis factor 12	-2.40	1.23E-05	3.35	1.44
leucine rich repeat neuronal 1	-2.40	2.41E-03	2.61	1.11
ring finger protein 150	-2.40	1.11E-04	14.57	5.79
cytochrome b5 reductase 1	-2.41	3.23E-04	4.00	1.71
microsomal glutathione S-transferase 2	-2.41	1.39E-03	5.28	2.43
NPHS2, podocin	-2.41	2.57E-02	5.48	2.33
peptidyl arginine deiminase 2	-2.42	4.83E-02	5.88	2.74
RAN binding protein 17	-2.42	4.55E-04	109.28	42.34
keratin 14	-2.42	1.02E-05	10.33	4.39

zinc finger DHHC-type containing 2	-2.43	2.40E-03	15.63	7.55
ADAM metallopeptidase with thrombospondin type 1 motif 20	-2.44	2.49E-02	5.28	2.33
rho-related GTP-binding protein RhoV	-2.46	1.18E-02	2.39	1.00
relaxin/insulin like family peptide receptor 1	-2.47	4.48E-03	31.10	13.06
SPARC/osteonectin, cwcv and kazal like domains proteoglycan 2	-2.47	8.17E-04	27.58	13.88
fibroblast growth factor receptor 3	-2.47	2.81E-06	8.04	3.33
LHFPL tetraspan subfamily member 3	-2.48	3.51E-04	46.57	20.69
basic helix-loop-helix family member e41	-2.48	4.82E-02	5.01	1.53
glutamate ionotropic receptor kainate type subunit 1	-2.49	1.20E-05	12.27	4.84
chromosome 10 open reading frame 10	-2.52	1.54E-03	9.66	3.95
LanC like 3	-2.52	6.42E-03	5.64	2.29
tumor protein p53 inducible nuclear protein 1	-2.54	2.81E-06	164.04	65.73
Unknown, ENSSSCG00000037530	-2.54	1.48E-02	5.14	2.01
ADAM metallopeptidase with thrombospondin type 1 motif 18	-2.55	1.16E-02	34.82	16.02
V-set domain containing T-cell activation inhibitor 1	-2.55	2.01E-02	28.90	10.76
glycerol kinase	-2.55	1.45E-02	10.94	4.40
glycoprotein M6A	-2.56	7.80E-04	9.60	3.73
solute carrier family 7 member 2	-2.57	4.97E-08	10.45	4.18
collagen beta(1-O)galactosyltransferase 2	-2.57	1.76E-05	10.65	4.23
Sus scrofa collagen type III alpha 1 chain (COL3A1), mRNA.	-2.57	1.49E-05	1771.53	774.53
sphingomyelin phosphodiesterase acid like 3B	-2.59	5.64E-05	3.55	1.42
Sus scrofa S100 calcium binding protein A14 (S100A14), mRNA.	-2.61	1.38E-09	46.17	18.16
junctophilin 1	-2.62	3.22E-02	3.42	1.21
Rieske Fe-S domain containing	-2.63	5.18E-03	26.85	6.43
Sus scrofa complement C7 (C7), mRNA.	-2.64	2.04E-03	36.30	14.49
sosondowah ankyrin repeat domain family member A	-2.65	6.04E-03	10.60	4.06
transmembrane 4 L six family member 18	-2.66	9.78E-04	6.38	2.46
syndecan binding protein 2	-2.70	7.25E-06	9.70	4.06
dpy-19 like C-mannosyltransferase 1	-2.75	2.04E-04	60.81	23.10
Unknown, ENSSSCG00000035443	-2.78	2.93E-02	8.19	3.01
ATP binding cassette subfamily C member 11	-2.78	3.91E-02	0.61	0.22
Unknown, ENSSSCG00000032569	-2.82	7.36E-03	26.91	9.28
Unknown, ENSSSCG00000031037	-2.83	8.19E-03	12.51	4.51
S100 calcium binding protein A2	-2.85	3.96E-02	396.95	170.31
Unknown, ENSSSCG00000010703	-2.85	1.30E-06	77.46	29.43
Rho guanine nucleotide exchange factor 4	-2.87	2.73E-07	3.80	1.39
ankyrin repeat domain 34B	-2.93	5.61E-03	10.31	3.15
Unknown, ENSSSCG00000033750	-2.93	9.42E-05	6.43	2.27
Unknown, ENSSSCG00000010499	-2.94	1.26E-02	46.17	18.93

protein phosphatase 1 regulatory subunit 3D	-2.96	7.69E-03	12.20	4.76
embryonal Fyn-associated substrate	-2.97	2.65E-05	14.06	5.51
sarcoglycan gamma	-2.98	2.10E-02	3.05	1.22
type II iodothyronine deiodinase	-3.02	2.64E-04	23.57	7.67
SAM pointed domain containing ETS transcription factor	-3.05	3.56E-07	5.16	1.69
potassium voltage-gated channel subfamily C member 3	-3.08	1.75E-03	1.59	0.57
Unknown, ENSSSCG00000024669	-3.09	2.80E-07	43.09	14.07
adenosine deaminase domain containing 1	-3.11	1.17E-02	4.51	1.55
transmembrane protein 243	-3.14	6.59E-07	60.52	20.92
ATP binding cassette subfamily G member 1	-3.14	4.10E-09	10.80	3.79
phospholipid phosphatase 4	-3.17	2.58E-02	17.43	5.38
cytochrome P450 family 26 subfamily A member 1	-3.20	3.29E-02	10.49	3.48
teneurin transmembrane protein 1	-3.21	2.06E-02	5.05	0.82
lipase G, endothelial type	-3.24	7.67E-04	11.17	2.91
serine protease HTRA3 precursor	-3.28	1.86E-03	2.57	0.80
BCL2 associated athanogene 2	-3.29	1.97E-02	4.17	1.05
growth arrest and DNA damage-inducible protein GADD45 gamma	-3.32	5.01E-04	5.91	2.15
blood vessel epicardial substance	-3.33	2.83E-03	2.42	0.67
CD109 molecule	-3.38	7.04E-03	17.01	5.17
embigin	-3.48	4.32E-02	104.31	32.13
coiled-coil domain containing 3	-3.49	8.33E-05	83.91	22.52
Unknown, ENSSSCG00000036125	-3.50	2.10E-02	1.11	0.63
sodium voltage-gated channel alpha subunit 4	-3.52	1.88E-03	1.10	0.39
Unknown, ENSSSCG00000031550	-3.54	1.31E-03	41.21	10.00
putative monooxygenase p33MONOX	-3.55	1.31E-10	48.01	14.60
S100 calcium binding protein A6	-3.58	8.41E-06	98.08	29.39
integrin subunit beta 6	-3.58	5.34E-05	8.49	2.86
Unknown, ENSSSCG00000039147	-3.62	9.66E-08	124.29	35.00
transient receptor potential cation channel subfamily M member 5	-3.62	2.74E-03	0.92	0.26
ring finger protein 152	-3.65	9.27E-08	43.78	12.79
Unknown, ENSSSCG00000036728	-3.68	1.28E-02	3.95	1.09
Sus scrofa vanin 1 (VNN1), mRNA.	-3.68	3.34E-03	63.38	21.28
solute carrier family 6 member 2	-3.69	1.79E-04	3.85	1.07
Unknown, ENSSSCG00000021414	-3.70	1.26E-02	0.99	0.25
peptidoglycan recognition protein 4	-3.71	9.04E-03	1.38	0.40
CDC42 small effector 2	-3.74	2.35E-11	113.41	31.19
ST6 N-acetylgalactosaminide alpha-2,6-sialyltransferase 1	-3.75	5.33E-04	1.50	0.37
solute carrier family 23 member 1	-3.77	3.09E-06	28.49	7.36
glutathione S-transferase Mu 3-like	-3.81	1.18E-09	134.14	41.78

cAMP responsive element binding protein 3 like 4	-3.82	5.71E-07	5.75	1.47
C-C motif chemokine ligand 28	-3.83	2.33E-03	63.20	14.90
leucine rich repeat containing 66	-3.84	2.00E-02	1.70	0.34
phosphate cytidylyltransferase 1, choline, beta	-3.84	9.78E-03	1.09	0.30
neuropeptide S receptor 1	-3.86	1.04E-05	13.28	4.19
phospholipase A2 group III	-3.90	1.23E-02	0.91	0.24
Unknown, ENSSSCG00000038043	-3.92	7.72E-04	0.47	0.12
armadillo repeat containing 12	-3.93	5.82E-03	4.94	1.33
serum amyloid A-3 protein precursor	-3.94	3.38E-02	98.13	8.28
Unknown, ENSSSCG00000033649	-3.95	3.26E-02	0.41	0.12
melanophilin	-3.96	8.80E-06	8.75	2.61
acyloxyacyl hydrolase	-3.96	2.98E-04	7.48	2.16
chromosome 1 open reading frame 141	-3.99	2.45E-03	4.26	1.28
Protein S100-G Protein S100-G, minor isoform	-4.00	3.11E-02	15.47	2.09
transmembrane protein 139	-4.01	1.05E-02	5.92	1.52
Unknown, ENSSSCG00000032922	-4.03	4.49E-05	23.80	5.56
fibromodulin	-4.04	2.94E-08	13.16	3.10
Kell blood group, metallo-endopeptidase	-4.04	2.88E-02	3.85	0.63
Unknown, ENSSSCG00000017032	-4.06	2.48E-03	2.51	0.63
chordin like 1	-4.09	2.78E-08	96.90	22.04
Unknown, ENSSSCG00000010359	-4.14	2.33E-03	1.82	0.46
proline rich basic protein 1	-4.14	3.80E-04	2.56	0.61
Unknown, ENSSSCG00000011676	-4.16	8.74E-04	55.49	12.06
Unknown, ENSSSCG00000036177	-4.18	3.35E-02	4.80	1.17
marginal zone B and B1 cell specific protein	-4.19	6.07E-03	2.29	0.50
branched chain amino acid transaminase 1	-4.24	1.15E-04	97.57	35.20
cell adhesion molecule L1 like	-4.27	8.42E-04	5.14	1.04
fibronectin type III domain containing 1	-4.28	7.19E-11	21.86	5.15
Unknown, ENSSSCG00000032582	-4.32	1.78E-04	9.12	3.23
huntingtin associated protein 1	-4.43	2.01E-03	2.18	0.38
serpin family B member 11 (gene/pseudogene)	-4.46	1.34E-03	5.98	1.35
CD209 antigen	-4.51	1.02E-06	8.22	1.88
Sus scrofa coagulation factor V (F5), mRNA.	-4.52	3.15E-05	12.76	2.86
peroxisomal trans-2-enoyl-CoA reductase	-4.53	6.26E-08	31.69	6.74
Unknown, ENSSSCG00000004180	-4.54	1.02E-05	12.48	2.83
Unknown, ENSSSCG00000038475	-4.67	2.26E-06	13.80	3.05
ectonucleoside triphosphate diphosphohydrolase 3	-4.67	5.68E-10	20.33	5.24
Sus scrofa claudin 22 (CLDN22), mRNA.	-4.80	1.81E-03	4.60	1.03
glutamic--pyruvic transaminase 2	-4.84	4.75E-05	42.88	6.74

phosphoenolpyruvate carboxykinase 2, mitochondrial	-4.91	2.87E-04	12.37	2.72
neuromedin B	-4.98	9.54E-07	241.61	43.70
olfactory receptor family 10 subfamily G member 3	-5.07	2.46E-03	5.43	0.87
Unknown, ENSSSCG00000012032	-5.08	1.57E-02	6.42	2.02
4-hydroxyphenylpyruvate dioxygenase	-5.11	5.07E-04	2.55	0.59
interleukin 23 receptor	-5.20	4.08E-04	2.19	0.47
mucin 6, oligomeric mucus/gel-forming	-5.26	5.86E-03	1.02	0.11
Unknown, ENSSSCG00000036778	-5.30	3.43E-02	6.72	1.37
protein tyrosine phosphatase, non-receptor type 5	-5.34	4.69E-03	1.04	0.20
carboxylesterase 3 precursor	-5.45	2.93E-13	99.07	17.56
notum, palmitoleoyl-protein carboxylesterase	-5.64	2.23E-04	4.42	0.75
actin, beta like 2	-5.69	7.54E-03	7.26	1.13
Unknown, ENSSSCG00000023467	-5.69	1.62E-03	1.36	0.26
cytochrome P450 family 4 subfamily B member 1	-5.78	2.49E-04	1.32	0.22
copine 5	-5.90	5.34E-05	1.73	0.36
Unknown, ENSSSCG00000007899	-5.90	2.63E-02	2.20	0.29
Unknown, ENSSSCG00000005278	-5.90	2.52E-06	3.27	0.58
capping protein regulator and myosin 1 linker 3	-5.92	1.33E-02	1.05	0.18
Unknown, ENSSSCG00000020872	-6.05	1.40E-03	27.32	6.20
molybdenum cofactor sulfurase	-6.08	7.17E-10	40.01	7.28
POF1B, actin binding protein	-6.27	1.19E-02	5.57	0.64
Unknown, ENSSSCG00000037206	-6.39	1.97E-05	3.93	0.62
Unknown, ENSSSCG00000031475	-6.43	3.61E-05	16.56	2.28
Unknown, ENSSSCG00000030554	-6.45	1.42E-02	5.82	0.46
Unknown, ENSSSCG00000036224	-6.53	1.01E-08	5.55	1.34
arachidonate 15-lipoxygenase, type B	-6.59	2.56E-04	0.64	0.09
Unknown, ENSSSCG00000000983	-6.93	3.45E-06	3.36	0.40
leucine rich repeat LGI family member 2	-7.00	1.55E-05	13.48	2.96
Unknown, ENSSSCG00000013714	-7.01	9.74E-04	7.14	1.04
Dehydrogenase/reductase SDR family member 4	-7.08	8.92E-05	35.15	5.05
joining chain of multimeric IgA and IgM	-7.08	5.96E-11	81.45	22.48
gamma-aminobutyric acid type A receptor pi subunit	-7.14	1.31E-06	16.77	3.33
serine/threonine/tyrosine kinase 1	-7.41	4.95E-04	3.16	0.44
selectin L	-7.47	5.87E-06	136.79	20.15
Unknown, ENSSSCG00000038719	-7.82	5.11E-03	1.55	0.43
Sus scrofa annexin A8 (ANXA8), mRNA.	-7.88	1.09E-04	24.71	2.61
Unknown, ENSSSCG00000028567	-9.23	4.49E-05	5.02	0.79
hepatocyte nuclear factor 4 alpha	-10.40	5.64E-08	1.51	0.15
EPS8 like 3	-10.44	4.09E-04	0.89	0.07

Unknown, ENSSSCG00000033637	-10.80	1.76E-05	1.10	0.09
proenkephalin	-11.83	2.03E-08	2.60	0.23
synaptonemal complex protein 2	-12.52	1.09E-15	74.97	6.52
Unknown, ENSSSCG00000013369	-12.94	1.70E-02	9.93	0.48
Unknown, ENSSSCG00000039615	-13.86	1.89E-03	18.24	1.32
alkylglycerol monooxygenase	-14.79	8.55E-12	2.45	0.17
opsin 4	-15.44	4.89E-06	10.61	1.10
Sus scrofa salivary lipocalin (SAL1), mRNA.	-17.09	9.78E-04	553.35	49.05
fibrinogen gamma chain	-17.82	2.55E-06	22.43	1.31
aldo-keto reductase family 1 member B	-18.15	1.08E-05	86.35	4.94
Unknown, ENSSSCG00000038037	-18.56	7.15E-10	33.68	1.78
Sus scrofa opticin (OPTC), mRNA.	-19.01	7.39E-07	4.30	0.24
thioesterase superfamily member 5	-28.24	4.44E-15	12.14	0.50
dispatched RND transporter family member 3	-29.30	5.95E-05	2.04	0.06
Unknown, ENSSSCG00000039569	-36.58	2.64E-04	33.26	0.89
Unknown, ENSSSCG00000037293	-42.77	1.00E-09	11.57	0.21
Protein S100-A12	-81.23	3.84E-05	51.39	0.90
S100 calcium binding protein A9	-93.71	2.93E-13	241.10	2.80
matrix metallopeptidase 8	-176.74	1.55E-05	30.21	0.16
Unknown, ENSSSCG00000031087	-460.45	2.81E-06	28.05	0.00
Sus scrofa S100 calcium binding protein A8 (S100A8), mRNA.	-518.90	5.41E-07	657.40	0.79

Table S7: Top Endometrial Up-regulated Genes in Day 17 *CYP19A1*$^{-/-}$ verses *CYP19A1*$^{+/+}$.

Gene Name	FC	FDR	Day 17 *CYP19A1*+/+ CPM average	Day 17 *CYP19A1*-/- CPM average
Unknown, ENSSSCG00000015159	16.98	8.10E-03	0.20	3.16
alpha hemoglobin stabilizing protein	5.18	3.48E-02	0.52	2.59
transglutaminase 3	4.88	2.49E-02	0.19	0.88
Unknown, ENSSSCG00000014727	4.38	1.84E-02	11.67	55.37
5'-aminolevulinate synthase 2	3.91	2.96E-04	7.32	29.98
hemoglobin subunit beta	3.84	4.05E-03	486.27	1998.10
zinc finger homeobox 4	3.37	7.30E-03	0.70	2.17
Metalloreductase STEAP1	2.75	1.22E-03	11.01	31.16
Fatty acid-binding protein, heart	2.38	2.59E-02	5.77	14.08
Sus scrofa solute carrier family 3 member 1 (SLC3A1), mRNA.	2.29	2.49E-02	6.19	14.10
basic helix-loop-helix family member e40	2.28	1.84E-02	12.41	25.36

Table S8: Top Endometrial Down-regulated Genes in Day 17 *CYP19A1*$^{-/-}$ verses *CYP19A1*$^{+/+}$.

Gene Name	FC	FDR	Day 17 *CYP19A1*+/+ CPM average	Day 17 *CYP19A1*-/- CPM average
lipase G, endothelial type	-2.67	2.61E-03	7.71	2.91
estrogen sulfotransferase	-3.67	4.04E-05	18.23	5.03
chromosome 1 open reading frame 141	-4.72	5.45E-03	5.32	1.28
Unknown, ENSSSCG00000021414	-4.90	2.34E-02	1.31	0.25
calcium homeostasis modulator family member 5	-5.03	1.34E-06	18.96	6.76
calcium homeostasis modulator family member 6	-5.38	3.39E-03	3.79	1.62
interleukin 23 receptor	-6.54	5.94E-05	2.88	0.47
calcium dependent secretion activator	-10.62	2.69E-03	1.20	0.11
Unknown, ENSSSCG00000014746	-12.49	4.49E-02	2.38	0.17